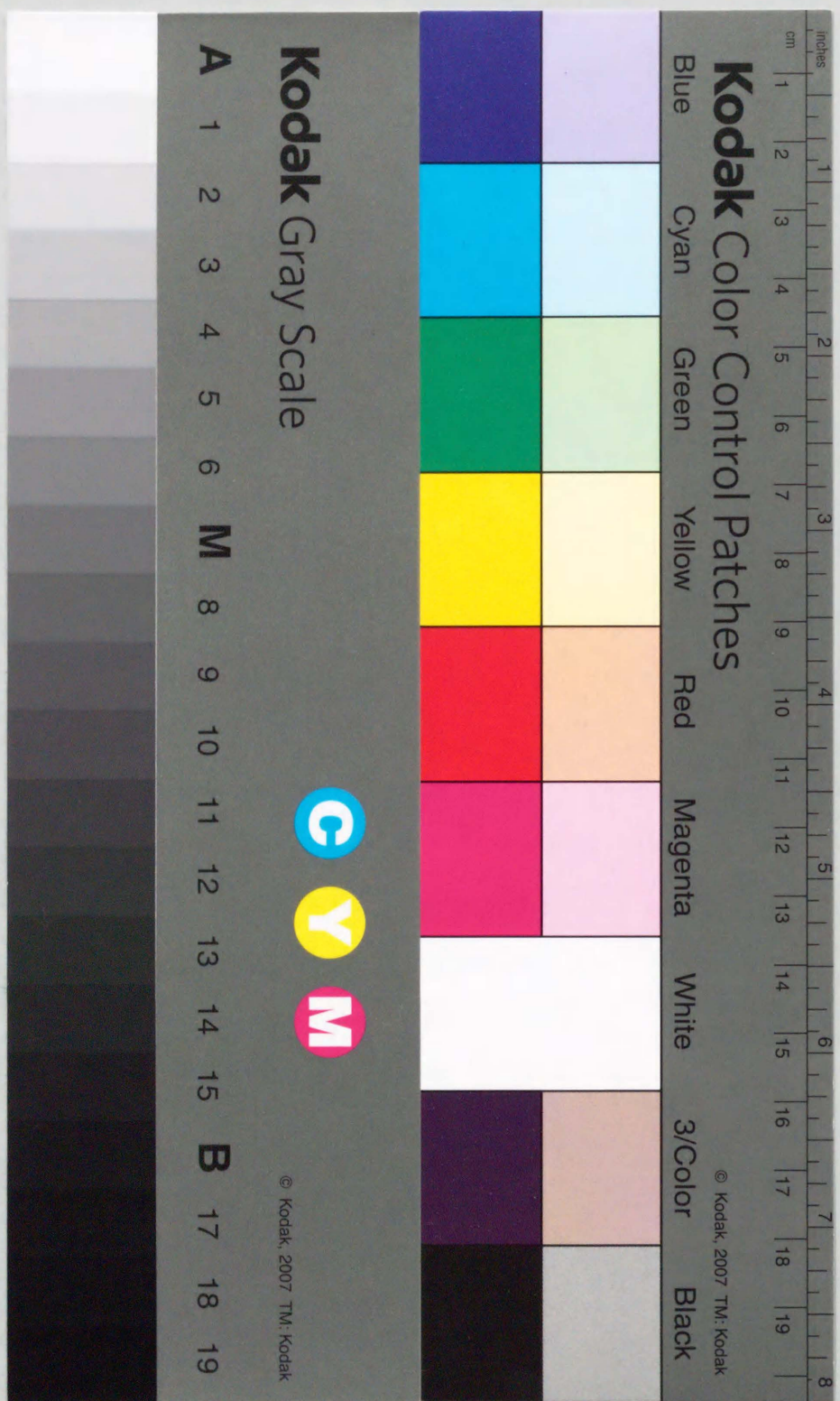


ELUCIDATION OF HYDRODESULFURIZATION  
MECHANISM ON Mo-BASED CATALYSTS BY  
<sup>35</sup>S RADIOISOTOPE TRACER METHOD

WEIHUA QIAN





①

**ELUCIDATION OF HYDRODESULFURIZATION  
MECHANISM ON Mo-BASED CATALYSTS BY  
<sup>35</sup>S RADIOISOTOPE TRACER METHOD**

**DIVISION OF CHEMICAL AND BIOLOGICAL SCIENCE AND  
TECHNOLOGY  
GRADUATE SCHOOL OF TECHNOLOGY  
TOKYO UNIVERSITY OF AGRICULTURE & TECHNOLOGY**

**WEIHUA QIAN**

**1995**



## TABLE OF CONTENTS

<b>1</b>	<b>HYDRODESULFURIZATION CATALYSIS</b>	
1.1	Introduction	1
1.2	Sulfur Compounds	4
1.3	Thermodynamics	4
1.4	Structure and Composition of Catalyst	7
1.4.1	Sulfided Mo/Al <sub>2</sub> O <sub>3</sub>	
1.4.2	Sulfided Co or Ni-Mo/Al <sub>2</sub> O <sub>3</sub>	
1.4.3	Roles of Co and Ni Promoters	
1.5	Reactivity, Reaction Networks and Kinetics	15
1.5.1	Reactivities	
1.5.2	Reaction Networks and Kinetics	
1.5.3	Binary and Multicomponent Mixture	
1.6	Support Effects on HDS Catalyst	29
1.7	On This Study	33
<b>2</b>	<b>HYDRODESULFURIZATION OF RADIOACTIVE <sup>35</sup>S-LABELED DIBENZOTHIOPHENE ON Mo/Al<sub>2</sub>O<sub>3</sub></b>	
2.1	Introduction	46
2.2	Experimental	48
2.2.1	Materials	
2.2.1	Apparatus and Procedure	
2.3	Results and Discussion	51
2.3.1	Hydrodesulfurization of <sup>35</sup> S-Labeled Dibenzothiophene	
2.3.2	Formation Rate Constant of <sup>35</sup> S-H <sub>2</sub> S and Amount of Labile Sulfur	
2.3.3	Amount of Sulfur on Sulfided Mo/Al <sub>2</sub> O <sub>3</sub>	



2.4	Conclusions	64
3	BEHAVIOR OF SULFUR ON <sup>35</sup> S-LABELED Mo/Al <sub>2</sub> O <sub>3</sub> IN HYDRODESULFURIZATION, HYDRODEOXYGENATION, AND HYDRODENITROGENATION	
3.1	Introduction	70
3.2	Experimental	71
3.2.1	Materials	
3.2.2	Apparatus and Procedure	
3.3	Results	72
3.3.1	Hydrodesulfurization Reaction	
3.3.2	Effect of Oxygen Compound	
3.3.3	Effect of Nitrogen Compounds	
3.4	Discussion	81
3.5	Conclusions	85
4	HYDRODESULFURIZATION OF RADIOACTIVE <sup>35</sup> S-LABELED DIBENZOTHIOPHENE ON Co-Mo/Al <sub>2</sub> O <sub>3</sub> , Ni-Mo/Al <sub>2</sub> O <sub>3</sub> , Co/Al <sub>2</sub> O <sub>3</sub> AND Ni/Al <sub>2</sub> O <sub>3</sub>	
4.1	Introduction	92
4.2	Experimental	93
4.2.1	Materials	
4.2.2	Apparatus and Procedure	
4.3	Results	94
4.3.1	Co-Mo/Al <sub>2</sub> O <sub>3</sub>	
4.3.2	Ni-Mo/Al <sub>2</sub> O <sub>3</sub>	
4.3.3	Mo/Al <sub>2</sub> O <sub>3</sub>	
4.3.4	Co/Al <sub>2</sub> O <sub>3</sub>	

4.3.5	Ni/Al <sub>2</sub> O <sub>3</sub>	
4.3.6	Formation Rate Constant of <sup>35</sup> S-H <sub>2</sub> S and Amount of Labile Sulfur	
4.4	Discussion	106
4.5	Conclusions	118
5	BEHAVIOR OF SULFUR ON <sup>35</sup> S-LABELED Co-Mo/Al <sub>2</sub> O <sub>3</sub> IN HYDRODESULFURIZATION OF SULFUR COMPOUNDS, AND IN A MIXED GAS OF H <sub>2</sub> S / H <sub>2</sub>	
5.1	Introduction	126
5.2	Experimental	126
5.2.1	Materials	
5.2.2	Apparatus and Procedure	
5.3	Results	128
5.3.1	Label of Labile Sulfur on Catalyst during HDS of <sup>35</sup> S-DBT	
5.3.2	Effect of Sulfur Compounds on Release Rate of <sup>35</sup> S-H <sub>2</sub> S	
5.3.3	Effect of Partial Pressure of H <sub>2</sub> S on Release Rate of <sup>35</sup> S-H <sub>2</sub> S	
5.3.4	Effect of Temperature on Release Rate of <sup>35</sup> S-H <sub>2</sub> S	
5.3.5	Release Rate Constant of <sup>35</sup> S-H <sub>2</sub> S	
5.4	Discussion	140
5.5	Conclusions	141
6	BEHAVIOR OF SULFUR ON <sup>35</sup> S-LABELED Co-Mo/Al <sub>2</sub> O <sub>3</sub> IN HYDRODESULFURIZATION OF 4-METHYLDIBENZOTHIOPHENE AND 4, 6-DIMETHYLDIBENZOTHIOPHENE	



6.1	Introduction	148
6.2	Experimental	149
6.2.1	Materials	
6.2.2	Apparatus and Procedure	
6.3	Results	151
6.3.1	Label of Labile Sulfur on Catalyst during HDS of $^{35}\text{S}$ -DBT	
6.3.2	Release of $^{35}\text{S}$ - $\text{H}_2\text{S}$ during HDS of 4-MDBT and 4, 6-DMDBT	
6.3.3	Release Rate of $^{35}\text{S}$ - $\text{H}_2\text{S}$ and Amount of Labile Sulfur	
6.4	Discussion	159
6.5	Conclusions	162
7	CONCLUSIONS	167
	PUBLICATIONS LIST	175
	ACKNOWLEDGMENTS	179

## Chapter One

### Hydrodesulfurization Catalysis



## Chapter One

# Hydrodesulfurization Catalysis

### 1.1 Introduction

Hydroprocessing catalysts based upon the transition metal sulfides have been widely used for over 70 years and molybdenum (Mo)-based catalysts still remain the main industrial catalysts in hydroprocessing of petroleum-based feedstocks (1). Original interest in these catalysts centered on their activity in the hydrogenation of coal liquids that contain considerable amounts of sulfur maintaining the transition metal in the sulfided state before the World War II. Cobalt (Co), nickel (Ni), Mo, tungsten (W) sulfides and their mixtures were recognized as the most active and least expensive of the transition metal sulfides (2). After the World War II, their major uses shifted to hydroprocessing of sulfur- and nitrogen-containing petroleum-based feedstocks with Co or Ni-promoted Mo and W catalysts usually supported on alumina. Today, the removal of sulfur, nitrogen, oxygen, and metals from fossil oil by reductive treatments in so-called hydroprocessing have been of importance with other large scale petroleum refining processes (cracking and reforming, etc.). Its application is growing to meet several needs, including the processing of heavier feeds, the production of high-performance lubricants, and cleanup of burning fuels to diminish air-polluting emissions of sulfur and nitrogen oxides that contribute to acid rain. Although alumina supported Mo-based catalysts, which were promoted with Co or Ni, were widely used in hydroprocessing, it is during the 1980-90s that a comparatively full comprehension of the location and the promotion of the promoter ions in



the hydrotreating catalysts was developed. In the past years new suggestions for the mechanisms of hydrodesulfurization (HDS), hydrodenitrogenation (HDN), hydrodeoxygenation (HDO), and hydrodemetalization (HDM) have also been put forward. In this paper we only concern with the HDS reaction, since the aim of this paper is only involved with the mechanism of HDS reaction and the limiting length of manuscript. For other hydrotreating work, one can refer recent articles on HDN (3, 4), HDO (5, 6), and HDM (7).

## 1.2 Sulfur Compounds

The sulfur compounds found in petroleum or synthetic oils generally fall into one of two types: heterocycles or nonheterocycles. The latter comprises of thiol or mercaptan. In this paper, we do not concern ourselves with HDS of later because they undergo HDS rapidly (1). Heterocycles mainly comprises of thiophene and its alkyl or phenyl substituents. A few were shown in Figure 1.1. Certainly, there are other heterocyclic sulfur compounds as sulfides. They also undergo HDS rapidly and there were few studies on HDS of sulfides (1).

## 1.3 Thermodynamics

The experimental conditions in hydrodesulfurization processes depend upon the boiling range and character of the feedstocks, the degree of desulfurization required and the catalyst employed. Industrial HDS is generally carried out at 300-425 °C and 10-200 atm (1, 8, 9). HDS of sulfur compounds is exothermic and essentially irreversible under the reaction conditions employed industrially. Representative values of the gas-phase-hydrodesulfurization equilibrium constants of several sulfur compounds,

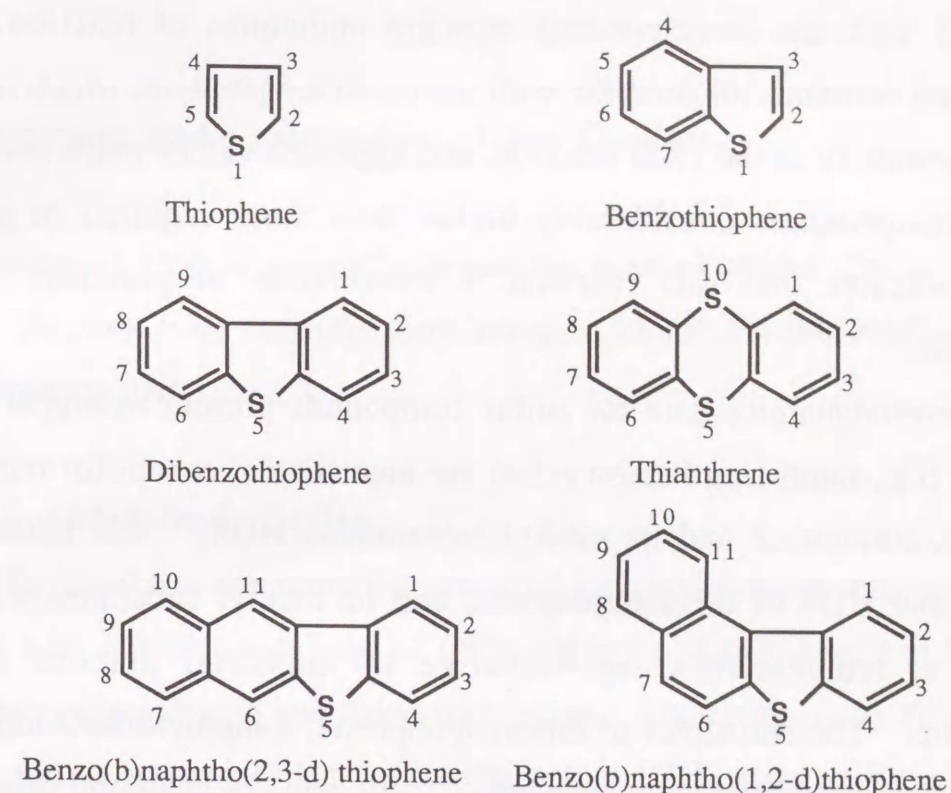


Figure 1.1. Structure of sulfur compounds.

Table 1.1. Equilibrium constants for HDS of selected sulfur compounds.

	log K		$\Delta H^\circ$ , kcal/mol of sulfur reactant
	227°C	427°C	
2-propanethiol + H <sub>2</sub>	6.05	4.45	-13
→ propane + H <sub>2</sub> S			
thiacyclohexane + 2H <sub>2</sub>	9.22	5.92	-27
→ n-pentane + H <sub>2</sub> S			
thiophene + 4H <sub>2</sub>	12.07	3.85	-68
→ n-butane + H <sub>2</sub> S			



including a mercaptan, a sulfide, and a heterocyclic compound, are listed in Table 1.1 with the corresponding standard enthalpies of reaction. The equilibrium constants all decrease with increased temperature, which indicates the exothermicity of the HDS reaction, and approach values much less than 1 only at temperatures considerably higher than those required in practice, which indicates that this reaction is irreversible in practical reaction conditions.

Thermodynamics data for sulfur compounds present in higher boiling fractions (i.e., multi-ring heterocycles) are unavailable, except for recent data for dibenzothiophene and its methyl substituents HDS. The latter results indicate that HDS of dibenzothiophene and its methyl substituents are also favored at temperature's representative of industrial practice and are exothermic. The enthalpies of dibenzothiophene, 4-methyldibenzothiophene, and 4, 6-dimethyldibenzothiophene are -12, -20, and -21 kcal/mol, respectively (10). Extrapolation of the latter results suggests that HDS of higher molecular weight sulfur compounds (e.g., benzonaphthothiophene) are also favored to temperature and are exothermic.

As being discussed subsequently, sulfur removal occurs with or without hydrogenation of the heterocyclic ring. The pathways involving prior hydrogenation of the ring is favored only at low temperature and at high pressures because hydrogenation of the sulfur-containing rings of sulfur compounds is equilibrium-limited at practical HDS temperatures. An example is reported by Weisser and Landa (11), in which the equilibrium constant for hydrogenation of thiophene to give tetrahydrothiophene is less than unity at temperatures above 350 °C. Thus, sulfur-removal pathways through hydrogenated sulfur intermediates may be inhibited at low pressures and high temperatures because of the low equilibrium concentrations of the latter species. It appears that new catalyst more active at low temperature must be

developed when extensive hydrogenation is also desired during the hydroprocessing.

#### 1.4 Structure and Composition of the Catalyst

Industrial HDS is generally carried out over a sulfided Co- or Ni-Mo/ $\gamma$ -Al<sub>2</sub>O<sub>3</sub>. Because both catalysts were based on Mo/Al<sub>2</sub>O<sub>3</sub>, Mo/Al<sub>2</sub>O<sub>3</sub> was also widely investigated.

##### 1.4.1 Sulfided Mo/ $\gamma$ -Al<sub>2</sub>O<sub>3</sub>

HDS catalysts are normally prepared by pore volume impregnation of alumina with aqueous solutions of (NH<sub>4</sub>)<sub>6</sub>Mo<sub>7</sub>O<sub>24</sub>, Co(NO<sub>3</sub>)<sub>2</sub>, and Ni(NO<sub>3</sub>)<sub>2</sub> with intermediate drying and calcination steps. The resulting oxide precursor of the catalyst is presulfided before the actual HDS reaction by a sulfiding procedure that may consist of reacting in a mixture of H<sub>2</sub>S and H<sub>2</sub> or thiophene and H<sub>2</sub>, or in a liquid feed of sulfur-containing molecules and H<sub>2</sub>. Today, most researchers agree that the resulting catalyst is (almost) completely sulfided, that is, MoO<sub>3</sub> is transformed into MoS<sub>2</sub> and the cobalt ions have passed from an oxide into a sulfide environment. During sulfiding as well as during actual HDS reaction, because the catalysts are highly reduced with H<sub>2</sub>S always present, thermodynamics predict that molybdenum should be in the MoS<sub>2</sub> form, cobalt in the Co<sub>9</sub>S<sub>8</sub>, and nickel in the Ni<sub>3</sub>S<sub>2</sub> or NiS form. Indeed, EXAFS studies of the Mo K-edge absorption spectra demonstrated that in sulfided Mo/Al<sub>2</sub>O<sub>3</sub> catalysts the average Mo ion has the same environment as an Mo ion in MoS<sub>2</sub> (12-15). The only difference was that in the catalyst the N(Mo-Mo) coordination number for the second shell of (Mo) neighbors surrounding each Mo ion was less than 6, which was found in pure MoS<sub>2</sub>. This indicates either that the size of MoS<sub>2</sub> particle slab on the alumina surface



is small, or that the long-range order in these particles is not perfect. Also temperature-programmed sulfidation studies have shown that the kinetics of sulfidation is fast enough to transform the majority of Mo and Co into the sulfide form (16).

MoS<sub>2</sub> belongs to a group of materials that crystallize with the layered structure, and it is found that each layer is composed of sheets of Mo atoms sandwiched between sheets of sulfur atoms. Within a given layer the bonding is mainly covalent, whereas between layers the bonding is mainly of the van der Waals type (17). Crystals grow in the form of platelets with large dimensions parallel to the basal sulfur planes and a small dimension perpendicular to the basal plane. Topsøe et al. claim that MoS<sub>2</sub> can be present

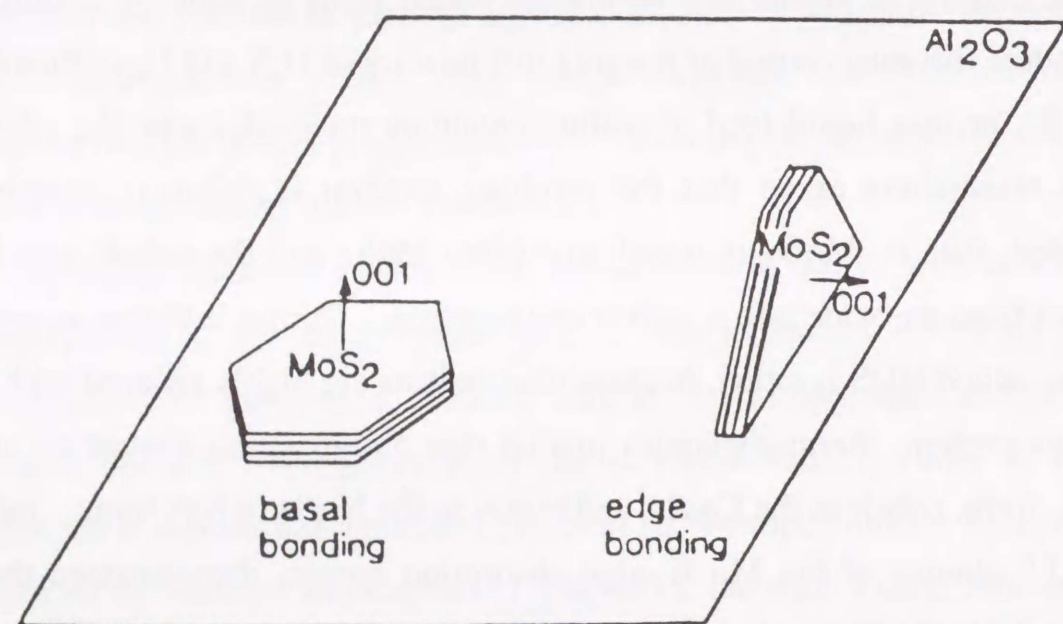


Figure 1.2. Orientation of small MoS<sub>2</sub> crystallites on the surface of Al<sub>2</sub>O<sub>3</sub>, suggesting that MoS<sub>2</sub> platelets are bonded to the alumina surface by Mo-O-Al bonds (Figure 1.2).

on industrial supports as very large patches of a wrinkle, one-slab-thick MoS<sub>2</sub> layer (18). In other studies three-dimensional-like structures were described. In a recent HRTRM model study of HDS catalysts, MoS<sub>2</sub> crystallites occurred in the form of platelets with among the ratio of a height-to-width of 0.4-0.7 (19). Some of these platelets were oriented at a nonzero angle to the surface,

Models of the active sites in Mo/Al<sub>2</sub>O<sub>3</sub> catalysts have usually been developed by consideration of the morphology of MoS<sub>2</sub>. On the basis of bond energy considerations, Voorhoeve had already assumed in 1971 that the anions in the basal planes of MoS<sub>2</sub> are more strongly bonded to the Mo cations than the anions at edges or corners (as in the layer lattice of TiCl<sub>3</sub>). Therefore catalysis most likely occurs at edges and corners, and not at basal planes (20). Experimental verification for this has been provided by a surface science study of the catalytic activity of an MoS<sub>2</sub> single crystal. Salmeron et al. showed that such a crystal, with a large ratio of basal plane over edge surface area, has a negligible activity for HDS of thiophene (21). However, sputtering of the basal plane and exposure of Mo ions increased the activity (22).

#### 1.4.2 Sulfided Co- or Ni-Mo/Al<sub>2</sub>O<sub>3</sub>

Many spectroscopic techniques are capable of detecting the presence of cobalt in one structure or another. Especially, the application of Mössbauer spectroscopy and EXAFS technique could quantitatively determine the simultaneous presence of different cobalt structures. In recent years, primarily due to the inverse Mössbauer studies by the Topsøe group and EXAFS research, a quantitative picture has emerged about the structure of cobalt in HDS catalysts (13, 23).

Cobalt can exist in several forms in a promoted Mo/Al<sub>2</sub>O<sub>3</sub> catalyst. In the oxide precursor form, cobalt ions interact strongly with the spinel type  $\gamma$ -Al<sub>2</sub>O<sub>3</sub> lattice and occupy octahedral sites just below Al<sub>2</sub>O<sub>3</sub> surface or



tetrahedral sites in the  $\text{Al}_2\text{O}_3$  bulk (24-26). At higher loading cobalt can also form  $\text{Co}_3\text{O}_4$  crystallites on the surface of the support. In the sulfide form, cobalt may be present in three forms, as  $\text{Co}_9\text{S}_8$  crystallites on the support, as cobalt ions adsorbed onto the surface of  $\text{MoS}_2$  crystallites, and in tetrahedral sites in the  $\text{Al}_2\text{O}_3$  lattice (23). Depending on the relative concentrations of cobalt and molybdenum (27) and on the pretreatment, a sulfided catalyst contains a relatively large amount either of  $\text{Co}_9\text{S}_8$  or of cobalt adsorbed on  $\text{MoS}_2$  (so-called Co-Mo-S phase). The structure of the catalyst in the sulfided state is predetermined by the structure of the oxide precursor. Therefore  $\text{Co}_3\text{O}_4$  was found to transform into  $\text{Co}_9\text{S}_8$ , cobalt ions in octahedral support sites transformed into cobalt adsorbed on  $\text{MoS}_2$  (Co-Mo-S phase), and cobalt ions in tetrahedral support sites remained in those positions (23).

By combining the Mössbauer studies with catalytic activity studies, Topsøe et al. established that the promoter effect of cobalt is related to the cobalt ions adsorbed on  $\text{MoS}_2$  (27). They have therefore confirmed suggestions made by Voorhoeve and Stuiver (20) and by Farragher and Cossee (28) that the promoter effect is not due to separate  $\text{Co}_9\text{S}_8$  crystallites but to cobalt ions in contact with  $\text{MoS}_2$ . Originally the occurrence of this adsorption state was somewhat confusing, since thermodynamically the most stable phase of cobalt under sulfide conditions is  $\text{Co}_9\text{S}_8$ . Furthermore, solid-state chemistry studies have shown that  $\text{CoMo}_2\text{S}_4$  is catalytic inactive (29) and that cobalt does not form ternary compounds with  $\text{MoS}_2$ , as it does with  $\text{NbS}_2$  and  $\text{TaS}_2$ . Nevertheless, it can adsorb on the surface of  $\text{MoS}_2$  crystallites. Farragher was the first to suggest that the cobalt is located at the edges of the  $\text{MoS}_2$  platelets. Proof for this suggestion was obtained by Chianelli et al. in scanning Auger studies of cobalt-promoted single crystals of  $\text{MoS}_2$ . An EXAFS study of the Co k-edge demonstrated that the cobalt ion in a sulfided Co-Mo/ $\text{Al}_2\text{O}_3$  catalyst surrounded by sulfur ions. However, no second shell

of neighboring ions can be determined, indicating that the cobalt ions are not present in a unique, well-ordered structure. Farragher suggested that the cobalt ions at the  $\text{MoS}_2$  edges are located between subsequent  $\text{MoS}_2$  layers, and he therefore called this a pseudointercalation structure, to differentiate it from real intercalation in which the cobalt ions would be randomly distributed between alternate  $\text{MoS}_2$  layers (28). Previously, intercalation proper had been suggested by Voorhoeve to be the structure of cobalt (20). On the other hand, Topsøe and Topsøe claimed that the cobalt ions are located at the edges of the molybdenum plane of an  $\text{MoS}_2$  layer, therefore extend the  $\text{MoS}_2$  layer (30). Convincing evidence for this model came from an infrared study on a series of sulfided Co-Mo/ $\text{Al}_2\text{O}_3$  catalysts, which NO was used as probe molecule. The IR spectrum of NO molecules adsorbed on cobalt ions can be distinguished from that of NO molecules on molybdenum ions. By increasing the cobalt loading at fixed molybdenum loading it was demonstrated that the spectrum of NO adsorbed on Co sites increased in intensity, while that of NO adsorbed on Mo sites decreased in intensity. If the cobalt ions had been in the location proposed by Farragher, the intensity of the NO on Co spectrum should have increased, but the intensity of the NO on Mo spectrum should be a stayed constant. Cobalt ion in the locations proposed by Topsøe and Topsøe, however, cover molybdenum ions and block adsorption of NO on these Mo ions. Therefore the observed behavior is according to the Co location proposed by Topsøe and Topsøe (30). A point that should be studied further is whether NO molecules actually chemisorb on the catalyst surface without disturbing its structure. If corrosive chemisorption were indeed to occur, the conclusions drawn from the IR adsorption study would need reinterpretation.

Either Farragher or Topsøe et al. describe the environment of the cobalt ions with octahedral or trigonal prismatic holes. On the basis of the solid-state



NMR work, Ledoux has recently suggested that the cobalt ions may indeed be situated in tetrahedral positions at the  $\text{MoS}_2$  edges (31).

Kasztelan et al. have quantitatively considered the solid-state structure of  $\text{MoS}_2$  and the edge location of the cobalt promoter by calculation the number of edge and corner Mo and Co sites as a function of  $\text{MoS}_2$  particle size (32). The geometry for a single  $\text{MoS}_2$  slab was considered. The reasonable fit between predictions and experimental results indicates that the assumptions underlying the model are not unrealistic.

In summary, the structure of a sulfided Co-Mo/ $\text{Al}_2\text{O}_3$  catalyst consists of small  $\text{MoS}_2$  crystallites that either lie with their basal planes parallel to the  $\text{Al}_2\text{O}_3$  surface or are edge-bonded to the  $\text{Al}_2\text{O}_3$  surface. The majority of the cobalt is present as cobalt ions adsorbed on the edges of the  $\text{MoS}_2$  crystallites and as  $\text{Co}_9\text{S}_8$  crystallites on the  $\text{Al}_2\text{O}_3$  surface. A high Co/Mo ratio and a high sulfidation temperature of the oxide precursor favor  $\text{Co}_9\text{S}_8$  formations, however, some cobalt is always present in tetrahedral sites in the  $\text{Al}_2\text{O}_3$  lattice. A schematic picture of the resulting structure is presented in Figure 1.3.

### 1.4.3 Role of the Cobalt or Nickel Promoter

There are four basic structural models that have been proposed to account for the results of HDS experiments.

#### (a) Monolayer Model

This model (33, 34) is based on the common belief that  $\text{MoO}_3$  a catalyst precursor, can be well dispersed as a monolayer on the  $\text{Al}_2\text{O}_3$  support (35) through dehydration of the surface. During sulfiding, sulfide ions replace the terminal oxide ions. Since the sulfur anion is larger than the oxygen anion, sulfur uptake in the monolayer configuration can occur only to a limited extent, corresponding to an S/Mo ratio of no more than unity (36). Massoth

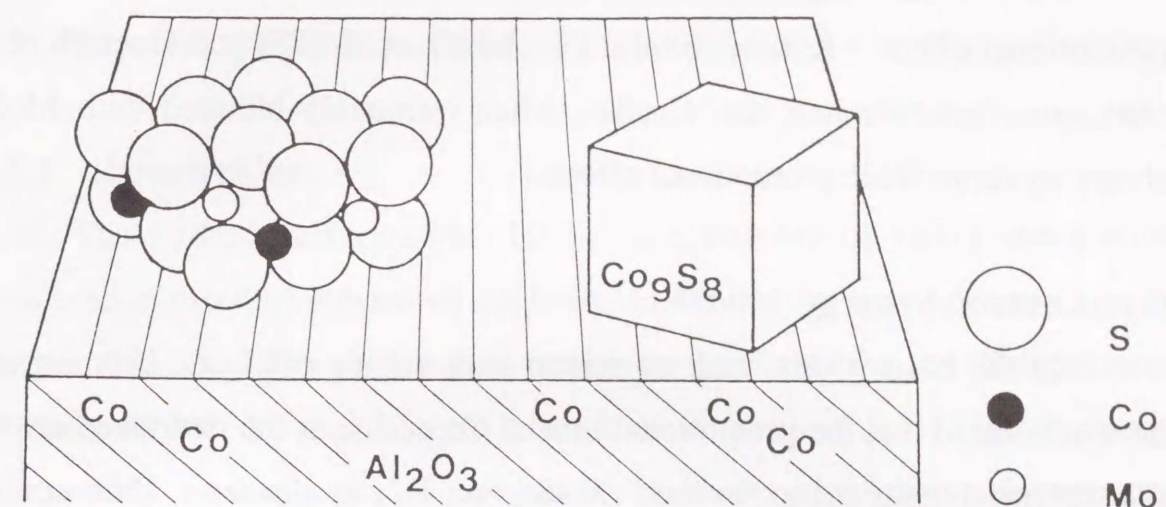


Figure 1.3 Structure of the different forms in which cobalt ions can be present in Co-promoted  $\text{MoS}_2/\text{Al}_2\text{O}_3$ .

(34), however, observed ratios as high as 2.75, which led him to propose a surface structure involving one-dimensional chains of  $\text{MoS}_2$ , instead of two-dimensional layers.

The difficulties of this model are that the role of promoter (such as Co or Ni) is uncertain, and that unsupported catalysts show catalytic behavior similar to the corresponding supported catalysts.

#### (b) Pseudointercalation Model

This model (20, 28) is based on the structure of bulk  $\text{MoS}_2$  that has a prismatic arrangement of S atoms around each Mo. The promoter Co or Ni is intercalated in the octahedral holes between S-Mo-S layers at the crystallite



edge. The active sites are thus believed to be exposed  $\text{Mo}^{3+}$  ions located at the sulfur-deficient edge sites.

It is not clear right now whether pseudointercalation is essential to the promotional effect. Karroua et al. (37), Zabala et al. (38) and Goetsch et al. (39) have demonstrated that  $\text{Co}_9\text{S}_8$ , when intimately blended with  $\text{MoS}_2$ , shows an appreciable promotional effect.

#### (c) Contact Synergy Model

On the basis of his work on mixed bulk sulfide catalysts, Delmon (40) have advocated that the promotional role of Co occurs at the interface between the thermodynamically favored  $\text{MoS}_2$  and  $\text{Co}_9\text{S}_8$  phases. This contact synergism between the two phases is explained by an electron transfer at the interface.

#### (d) "CoMoS" Phase model

The presence of an active phase, called "CoMoS" phase, in supported and unsupported CoMo catalysts has recently been identified by Topsøe and his co-workers (18 and the references therein) using Mössbauer spectroscopy. In alumina-supported catalysts it is suggested that the "CoMoS" phase is present as a single S-Mo-S sheet, with Co most likely present at molybdenum sites. In unsupported catalysts, the "CoMoS" phase likely consists of several layers with bulk  $\text{MoS}_2$ -like structures.

Summarizing, each of these models has its merits as far as HDS is concerned. While the details of the catalyst structures are still unclear, for high activity it seems important to have the promoter metals intimately associated with an  $\text{MoS}_2$ -like species. Several such models of the active phase(s) have recently been hypothesized by Yermakov et al. (69) and

Chianelli et al. (42). Models that are based on geometrical considerations have been proposed by Kasztelan et al. (32).

## 1.5 Reactivity, Reaction Networks and Kinetics

### 1.5.1 Reactivities

The hydrodesulfurization (HDS) of a number of sulfur compounds dissolved in n-cetane solvent on a Co-Mo/ $\text{Al}_2\text{O}_3$  catalyst have been reported by Nag et al. (43). The pseudo-first-order rate constants for the disappearance of each at 300 °C and 71 atm are given in Table 1.2. The three-ring compounds are 1 order of magnitude less reactive than the two-ring compounds, but the reactivity is similar for compounds having three or more rings.

The high-pressure reactivity data in Table 1.2 imply that dibenzothiophene is one of the compounds most representative of the unreactive sulfur

Table 1.2. Reactivities of several heterocyclic sulfur compounds.

Reactant	Pseudo-first-order Rate Constant, L/(s·g of catalyst)
thiophene	$1.38 \times 10^{-3}$
benzothiophene	$8.11 \times 10^{-4}$
dibenzothiophene	$6.11 \times 10^{-5}$
benzo (b) naphtho- (2, 3-d) thiophene	$1.61 \times 10^{-4}$
7, 8, 9, 10-tetrahydro- benzo (b) naphtho- (2, 3-d) thiophene	$7.78 \times 10^{-5}$



compounds in higher boiling fractions of fossil fuels. Because it is readily available commercially, it is a good model compound for characterizing the HDS chemistry of heterocyclic sulfur compounds.

The effect of methyl substituents on the reactivity of dibenzothiophene has also been investigated. Houalla et al. conducted the HDS reaction of methyl-substituted dibenzothiophene at 300°C and 102 atm with a flow reactor (44). Table 1.3 is described by pseudo-first-order kinetics. The methyl substituents in 2, 8-positions of dibenzothiophene hardly changed the reactivity and methyl groups in the 3 and 7 positions also had only a small effect on the reactivities. In contrast, methyl substituents at the 4-position reduced the reactivity by an order of magnitude, and methyl groups in the 4 and 6 positions reduced it somewhat more.

Recently, since the air pollution regulations become more strict, much attention has been focused on deep desulfurization of light oil. The developments of analytical techniques have enabled the analysis of poly-aromatic sulfur-containing compounds (PASC) such as alkylbenzothiophenes

Table 1.3. Reactivities of selected methyl-substituted dibenzothiophene.

Reactant	Pseudo-first-order Rate Constant, L/(g of catalyst·s)
dibenzothiophene	$7.38 \times 10^{-5}$
2,8-dimethyldibenzothiophene	$6.72 \times 10^{-5}$
3,7-dimethyldibenzothiophene	$3.53 \times 10^{-5}$
4,6-dimethyldibenzothiophene	$4.92 \times 10^{-6}$
4-methyldibenzothiophene	$6.64 \times 10^{-6}$

and alkylbenzothiophenes that are considered to be key compounds of the hydrodesulfurization of light oil (45-47). These methyl-substituted dibenzothiophenes are now recognized as the sulfur compounds that are most slowly converted in HDS of heavier fossil fuels. Kabe and co-workers reported the hydrodesulfurization of a middle distillate of Arabian light crude oil on a commercial Co-Mo/Al<sub>2</sub>O<sub>3</sub> at 350-390 °C (48). By the quantification of each sulfur-containing component in feed and products, they found that alkylbenzothiophenes was completely desulfurized at 350 °C independent of the presence of substituents and for dibenzothiophene and its alkyl-substituents, non-substituted dibenzothiophene was converted completely at 370 °C. In contrast, 6 % of 4-methyldibenzothiophene and 52 % of 4,6-dimethyldibenzothiophene were not converted even at 390 °C. Therefore, one of the challenges for future technology is to find catalysts and processes to desulfurize them. Compounds such as 4-methyldibenzothiophene are evidently the most appropriate model compounds for characterization of new catalysts and processes for heavy feeds.

The observation that the reactivity of the methyldibenzothiophenes substituted at positions  $\alpha$  (4 or 6) to the sulfur atom is only 1 order of magnitude smaller than those of the other substituted dibenzothiophenes indicate that there is not a significant steric effect and therefore suggests that adsorption of the sulfur compounds does not proceed on an end-on manner through the sulfur atom (33). If end-on adsorption predominated, the rate constant for HDS of 4,6-dimethyldibenzothiophene would be expected to be several orders of magnitude less than that for 4-methyldibenzothiophene. Kwart et al. (49) therefore proposed a multi-point adsorption model. They considered the adsorption of the sulfur compound through the sulfur atom or the bond between the carbon atoms that are in 4- and 3- or 6- and 5-positions relative to the sulfur atom. Consistent with this picture, Sauer et al. (50)



proposed reaction mechanisms for thiophene HDS on the basis of presumed analogies to molecular organometallic chemistry.

### 1.5.2 Reaction Networks and Kinetics

To gain a quantitative understanding of HDS kinetics, a common approach is to carry out HDS with representative model compounds. There have been two groups of studies among this line: those which establish the HDS kinetics and reaction pathways for a single sulfur-containing compound; and those which determine the interactions between HDS and other hydrotreating reactions such as hydrodeoxygenation (HDO), hydrodenitrogenation (HDN) and aromatic's hydrogenation. Experiments leading to the proposal of reaction networks have been carried out for thiophene, benzothiophene, dibenzothiophene and two isomers of benzonaphthothiophene.

#### (a) Thiophene.

Early thiophene HDS investigations, the great majority of which have been performed at atmospheric pressure have been reviewed (1, 8). Thiophene HDS evidently proceeds by two parallel pathways (Figure 1.4), although the reaction network is not completely understood, with results of different investigators being in less than full agreement. Rate equation from the low-pressure experiments indicates that thiophene inhibits its own HDS; in some investigations, hydrogen sulfide has been found to inhibit HDS. The possibility of inhibition by hydrogen is difficult to assess because only small ranges of hydrogen partial pressures have been used (8). Hydrogenation and hydrogenolysis are inferred to occur on two different kinds of sites since hydrogen sulfide affects rates of thiophene hydrogenolysis and olefin hydrogenation differently (1).

Table 1.4. Rate equations for thiophene hydrogenolysis and butene hydrogenation.

1. Thiophene hydrogenolysis on  $\sigma$  sites:

$$r_{T,\sigma} = \frac{k_{T,\sigma} K_{T,\sigma} K_{H_2,\sigma} P_T P_{H_2}}{[1 + (K_{H_2,\sigma} P_{H_2})^{1/2} + K_{T,\sigma} P_T + K_{H_2S,\sigma} P_{H_2S} / P_{H_2}]^3}$$

2. Butene hydrogenation on  $\tau$  sites:

$$r_{A,\tau} = \frac{k_{B,\tau} K_{B,\tau} K_{H_2,\tau} P_B P_{H_2}}{[1 + (K_{H_2,\tau} P_{H_2})^{1/2} + K_{A,\tau} P_A + K_{B,\tau} P_B]^2}$$

where the subscripts T, A, and B denote thiophene, butane, and butene, respectively.

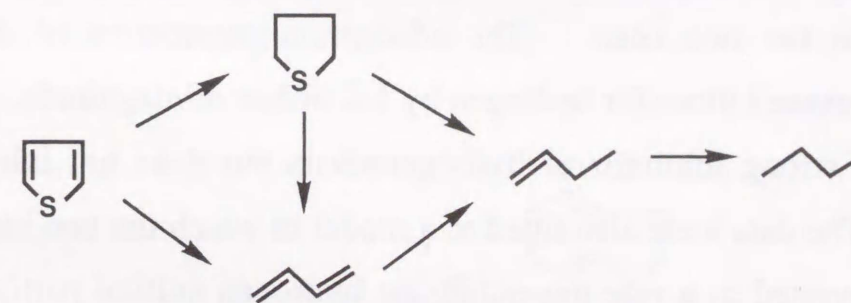


Figure 1.4. Thiophene reaction pathways.



In a thorough set of experiments characterizing HDS thiophene in the vapor phase (51), conditions were varied over a wide range. A reaction network was proposed in which thiophene hydrodesulfurized to give 1-butene and cis- and trans-butadiene, followed by hydrogenation of the butenes to give butane. Neither tetrahydrothiophene nor butadiene (which was proposed to be hydrogenated rapidly to give the three butenes) was detected. Two different kinds catalytic sites were assumed, one for thiophene hydrogenolysis and one for butene hydrogenation, according to results of low-pressure experiments (8). The data were correlated best by either of two sets of Langmuir-Hinshelwood rate equations, one based on a rate-determining surface reaction between adsorbed thiophene and molecularly adsorbed hydrogen and the other differing only in that hydrogen is assumed to be dissociatively adsorbed, which is a more realistic postulation. In each case, it was assumed that hydrogen sulfide was formed from reaction of gas-phase hydrogen with adsorbed sulfur by a Rideal-Eley mechanism. The rate equations based on the assumption of dissociatively adsorbed hydrogen is given in Table 1.4. The existence of two different kinds of sites was justified *a posteriori* by the large difference between adsorption equilibrium constants of hydrogen on the two sites. The adsorption parameters of the organic compounds exceed those for hydrogen by 1-2 orders of magnitude. Hydrogen sulfide is a strong inhibitor of hydrogenolysis but does not inhibit hydrogenation. The data were also fitted to a model in which the two kinds of sites are interconverted at a rate depending on hydrogen sulfide partial pressure, but the fit was not substantially better with this more complicated model.

**(b) Benzothiophene.**

Although benzothiophenes have long been recognized as major constituents of high boiling and residual petroleum fractions, little quantitative

Table 1.5. Rate equations for benzothiophene hydrogenolysis and hydrogenation.

1. Hydrogenolysis of benzothiophene on  $\sigma$  sites:

$$r_{D,\sigma} = \frac{k_{D,\sigma} K_{B,\sigma} K_{H_2,\sigma} P_D P_{H_2}}{[1 + (K_{H_2,\sigma} P_{H_2})^{1/2} + (K_{H_2S,\sigma} P_{H_2S} / P_{H_2}) + K_{B,\sigma} (P_B + P_D)]^3}$$

2. Hydrogenolysis of 1,2-dihydrobenzothiophene on  $\sigma$  sites:

$$r_{B,\sigma} = \frac{k_{B,\sigma} K_{B,\sigma} K_{H_2,\sigma} P_B P_{H_2}}{[1 + (K_{H_2,\sigma} P_{H_2})^{1/2} + (K_{H_2S,\sigma} P_{H_2S} / P_{H_2}) + K_{B,\sigma} (P_B + P_D)]^3}$$

3. Hydrogenation of benzothiophene on  $\tau$  sites:

$$r_{B,\tau} = \frac{k_{B,\tau} K_{B,\tau} (P_B P_{H_2} - P_D / K_1)}{[1 + K_{B,\tau} (P_B + P_D) + K_{E,\tau} P_E]^3}$$

where the subscripts B, D, E, and  $K_1$  denote benzothiophene, 1, 2-dihydrobenzothiophene, ethylbenzene, and the equilibrium constant for benzothiophene hydrogenation giving 1, 2-dihydrobenzothiophene, respectively.

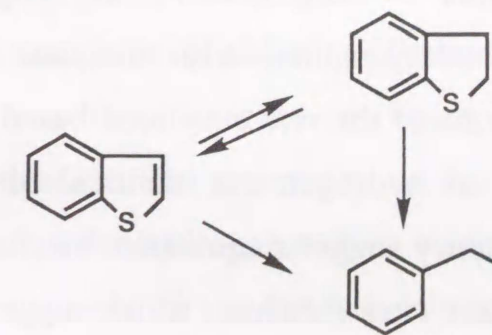


Figure 1.5. Reaction network for benzothiophene.



information is available concerning the behavior of this type of fused two-ring heterocyclic sulfur molecule under hydroprocessing conditions (8). The reported high-pressure experiments with liquid-phase reactants lead to contradictory conclusions regarding the network, whereas Daly reported that benzothiophene HDS gives ethyl benzene by either of two parallel pathways (52), Geneste et al. reported that ethyl benzene is formed from a dihydrobenzothiophene intermediate (53). The only rate constants reported were for benzothiophene disappearance.

A quantitative network has been reported for conversion of vapor-phase benzothiophene at higher pressures (54; Figure 1.5). Styrene was not detected and was assumed to be hydrogenated rapidly to give ethyl benzene after being formed from benzothiophene. As in the thiophene study reported by the same authors (51), two different types of catalytic sites were assumed: one for hydrogenolysis of benzothiophene and of 1, 2-dihydrobenzothiophene and one for hydrogenation of benzothiophene. A sequential design of experiments was used to minimize the number of data required for model discrimination and parameter estimation. A best-fit rate equation (Table 1.5) was based on a mechanism in which the surface reaction is the rate-limiting step on both types of sites, with dissociative adsorption of hydrogen and the rate-limiting step involving simultaneous addition of two hydrogen atoms. Hydrogenation on the hydrogenation sites is negligible. Hydrogen sulfide inhibits hydrogenolysis, but not hydrogenation, as for thiophene.

The functional forms of the rate equations based on the assumption of dissociative adsorption of hydrogen are identical for benzothiophene and thiophene. This consistency suggests equivalent mechanisms. Moreover, the adsorption parameters have similar values, which suggests that the parameters have a physical meaning in the context of Langmuir-Hishelwood models.

The effect of methyl substituents on benzothiophenes has been investigated by Geneste et al. (53) who observed that the conversion depends on the position and the number of methyl substituents, in the order:

Benzothiophene (1) > 2-methylbenzothiophene (0.4) > 3-methylbenzothiophene (0.2) > 2,3-dimethylbenzothiophene (0.1)

where the numbers in parentheses denote relative values of pseudo-first-order disappearance rate constants. The decrease in the rate is much less than expected from steric hindrance; the authors attributed the results to electronic effects, as a good correlation was obtained between the rate constant for hydrogenation and the first ionization potential.

#### (c) Dibenzothiophene.

Houalla et al. proposed a detailed network for dibenzothiophene HDS on the basis of data from two laboratory reactor types (55; Figure 1.6). Experiments were performed with dibenzothiophene and with its products as reactants, including 1, 2, 3, 4-tetrahydrodibenzothiophene, 1, 2, 3, 4, 5, 6-hexahydrodibenzothiophene, and biphenyl. Each of the hydrogenated dibenzothiophenes was rapidly converted to the other, and for purposes of a kinetics analysis, the two hydrodibenzothiophenes were lumped. Figure 1.6 indicates that dibenzothiophene conversion proceeds selectively through the path of least hydrogen consumption and that hydrogenation of biphenyl and cyclohexylbenzene is comparatively slow. However, the network shown is based on data from a flow reactor in which the hydrogen sulfide concentrations were low. The selectivity to the hydrogenated dibenzothiophene is higher when the hydrogen sulfide concentration is higher. The latter selectivity also depends on the catalyst composition, as Houalla et al. found that the yield of cyclohexylbenzene at a given conversion was about 3 times higher with Ni-Mo/Al<sub>2</sub>O<sub>3</sub> catalyst than with Co-Mo/Al<sub>2</sub>O<sub>3</sub> catalyst.



A similar network for dibenzothiophene hydrodesulfurization and hydrogenation was also reported (56) for Ni-Mo/Al<sub>2</sub>O<sub>3</sub> catalyst. The hydrogenolysis of dibenzothiophene to give biphenyl was only 2.5 times more rapid than its hydrogenation. The lower HDS selectivity (increased hydrogenation) in this network as shown in Figure 1.6 was attributed to the greater hydrogenation activity of the Ni-Mo/Al<sub>2</sub>O<sub>3</sub> catalyst in comparison with Co-Mo/Al<sub>2</sub>O<sub>3</sub>. However, a contribution of a higher hydrogen concentration in Bhide's experiments (it was approximately 50 % greater than that used by Houalla et al.) to the higher selectivity to hydrogenated dibenzothiophenes cannot be ruled out. The more rapid hydrogenation of dibenzothiophene suggests that the contribution of this pathway contributes more strongly at higher hydrogen concentrations, resulting in higher hydrogen consumption for HDS at high pressures.

The kinetics of dibenzothiophene disappearance was investigated by several authors (8, 57). Rate equations for dibenzothiophene disappearance were given, which associated with Langmuir-Hinshelwood mechanisms with hydrogen sulfide being an inhibitor. However, as Figure 1.6 shows, dibenzothiophene disappearance includes parallel hydrogenolysis and hydrogenation. In the work of Broderick and Gates (58), rate equations were given in Table 1.6 for each pathway. Experiments were carried out with differential conversion of liquid-phase reactants in a flow reactor at 275-325°C. The rates of hydrogenolysis and hydrogenation were taken as the respective rates of formation of biphenyl and of the lump consisting of cyclohexylbenzene and the two hydrogenated dibenzothiophenes. The rate equation for hydrogenolysis corresponds to a Langmuir-Hinshelwood mechanism whereby the rate-limiting step is a surface reaction between molecularly adsorbed hydrogen on one type of site and dibenzothiophene on another. Dibenzothiophene and hydrogen sulfide both inhibit hydrogenolysis,

Table 1.6. Rate equations for dibenzothiophene hydrogenolysis and hydrogenation.

1. Dibenzothiophene hydrogenolysis:

$$r = \frac{kK_{DT}K_{H_2}C_{DT}C_{H_2}}{(1 + K_{DT}C_{DT} + K_{H_2S}C_{H_2S})^2(1 + K_{H_2}C_{H_2})}$$

2. Dibenzothiophene hydrogenation:

$$r = \frac{k'K'_{DT}K'_{H_2}C_{DT}C_{H_2}}{1 + K'_{DT}C_{DT}}$$

where the subscript DT denotes dibenzothiophene.

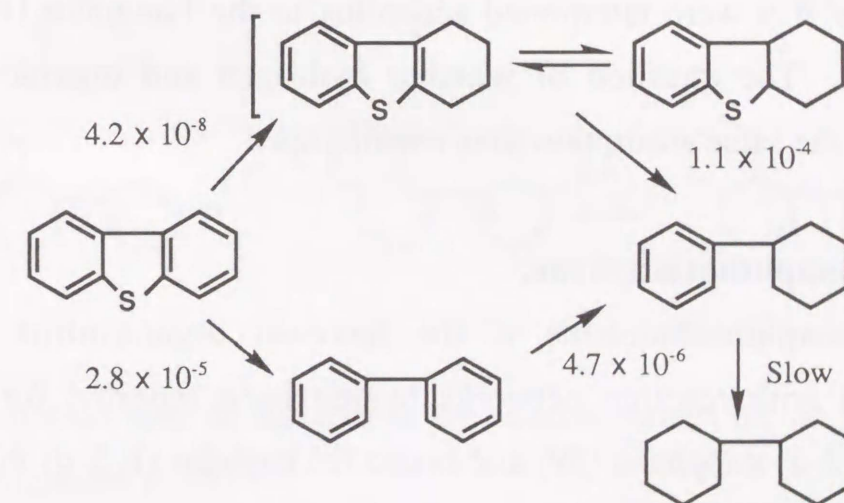


Figure 1.6. Reaction network for dibenzothiophene.

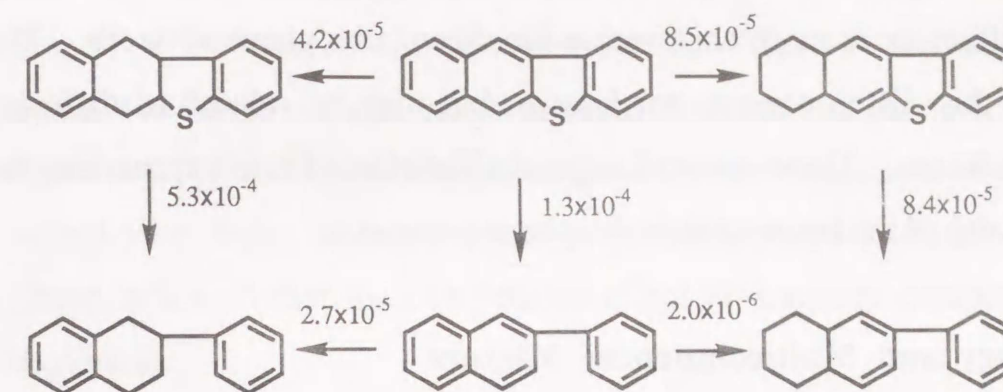


the latter more strongly, in agreement with the kinetics of thiophene and benzothiophene HDS. The adsorption parameter for hydrogen could not be estimated accurately as a function of temperature (as evidenced by the positive enthalpy of adsorption). Biphenyl is not an inhibitor. Exception of the dependence of the rate on hydrogen concentration, the equation is almost identical in form with equations for hydrogenolysis of thiophene and benzothiophene.

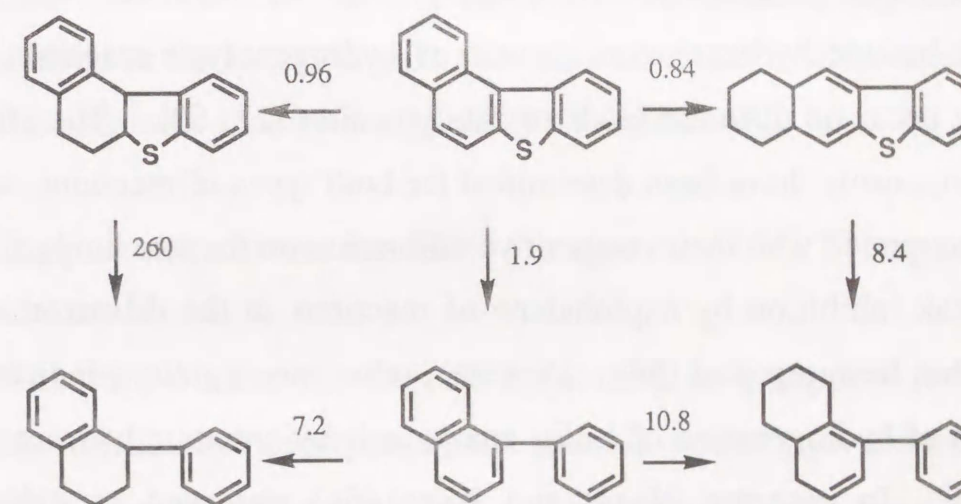
The difference in form between the dibenzothiophene hydrogenolysis rate equation and that for its hydrogenation is consistent with the notion that the two types of reactions take place on separate kinds of catalytic sites. As stated above, hydrogen sulfide does not inhibit hydrogenation. This agrees with results stated earlier for thiophene and benzothiophene. The difference in form between the dibenzothiophene hydrogenolysis equation and the thiophene and benzothiophene hydrogenolysis equations raises a question of the nature of the hydrogen adsorption. It does not seem plausible that hydrogen is molecularly adsorbed, as the equation for dibenzothiophene hydrogenolysis would imply if it were interpreted according to the Langmuir-Hinshelwood formalism. The question of whether hydrogen and organic molecules compete for the same adsorption sites remains open.

**(d) Benzonaphthothiophene.**

Benzonaphthothiophene is the heaviest organosulfur compound investigated with reaction networks having been reported for benzo (b) naphtho (2, 3-d) thiophene (59) and benzo (b) naphtho (1, 2-d) thiophene (8; Figure 1.7). In both networks, the rate of hydrogenation of the sulfur-containing reactant is comparable to that of its hydrogenolysis. For benzo (b) naphtho (2, 3-d) thiophene, the hydrogenolysis rate of the sulfur compound having a saturated ring adjacent to the sulfur atom is only about 4 times



(A) The numbers next to the arrows denote pseudo-first-order rate constants in L/(s-g of catalyst) at 300 °C.



(B) The numbers next to the arrows are relative values of the pseudo-first-order rate constants at 250 °C.

Figure 1.7. Reaction network for (A) benzo (b) naphtho (2, 3-d) thiophene and (B) benzo (b) naphtho (1, 2-d) thiophene.



greater than that of benzo (b) naphtho (1, 2-d) thiophene, the corresponding reactivity difference is more observed in the dibenzothiophene network. The reasons for this difference are not known, but may be related to differing reaction conditions. There are no Langmuir-Hinshelwood rate expressions for reactions in any of the benzonaphthothiophene networks.

### 1.5.3 Binary and Multicomponent Mixture

The structural similarity (e.g., aromaticity) of sulfur heterocycles to oxygen, nitrogen, and aromatic compounds suggest that all these types of compounds may interact with the catalytic sites in a more or less similar way. Conceivably, there exists strong competition among the various hydrotreating reactions and aromatic's hydrogenation. In processing of commercial feedstocks, such competitive effect surely plays an important role. HDS networks include hydrogenation as well as hydrogenolysis reactions, which evidently occur on different kinds of catalytic sites (58, 60). The effects of other components have been determined for both types of reactions, with the results interpreted with their competitive adsorption on the two kinds of sites.

Weak inhibition by naphthalene of reactions in the dibenzothiophene network has been reported (56). However, other investigations indicated that inhibition of hydrogenation of sulfur compounds by aromatic hydrocarbons is stronger. In contrast, Nagai and Kabe (61) observed in differential conversion experiments that addition of up to 2 wt% phenanthrene to a solution of 5 wt% dibenzothiophene decreased the yield of cyclohexylbenzene but not that of biphenyl. Phenanthrene was therefore assumed to adsorb solely on hydrogenation sites. Their assumption is consistent with results of Van Paradise et al. (54). They found that ethylbenzene is a strong inhibitor of benzothiophene hydrogenation. The value of the phenanthrene adsorption parameter estimated by Nagai and Kabe was equal to  $10 \text{ atm}^{-1}$  and comparable

to that obtained for thiophene HDS inhibition by La Vopa and Satterfield (62). Recently, Ishihara et al. reported that the effect of solvent under deep desulfurization conditions (concentration of dibenzothiophene = 0.1 wt%) was significant (63). The heat of adsorption of dibenzothiophene on Co-Mo/Al<sub>2</sub>O<sub>3</sub> would vary from 22 kcal/mol (in n-heptane) to 10 kcal/mol (in tetralin). These indicated that the competitive effect of aromatic compounds was not negligible.

Oxygen compounds mildly inhibit the reactions of sulfur compounds (6, 61, 64, 65). The poisoning of both hydrogenolysis and hydrogenation sites were inferred.

Basic organonitrogen compounds are the strongest among inhibitors of HDS (66) and therefore the most widely investigated, but only recently have quantitative inhibition effects been reported. Quinoline strongly inhibited all the reactions of the network. On the other hand, the inhibition effect of the nonbasic carbazole appears unexpectedly strong (62, 67).

### 1.6 Support Effects on the HDS Catalyst

The support that currently is most used as a support for industrial hydrodesulfurization catalysts is the gamma cubic type alumina. The interaction between Mo and alumina is known to influence the structure and activity of HDS catalyst based Mo (68-70). The strong interaction between Mo and alumina facilitates the formation of a monolayer rather than a multilayer Mo structure, resulting in higher dispersion of Mo on the support (68). The interaction between Mo and alumina may decrease the HDS activity because of the potential suppression of molybdate sulfidation (69). On the other hand, Mo sulfide that interacts strongly with alumina has a lower intrinsic activity as compared with weak interaction Mo sulfide (70). For Co-



and Ni-Mo/Al<sub>2</sub>O<sub>3</sub>, it was also recognized that alumina is not an inert carrier. The interaction between Mo and alumina is the results of a reaction between Mo anion and the basic (protonated) hydroxyl groups on the alumina surface during the catalyst preparation (71-72). The molybdate adsorption on the alumina surface might occur by the decomposition of the adsorbing molecules/ion and physisorption on coordinately unsaturated Al<sup>+3</sup> sites. (71, 72). On the other hand, the promoter ions, Co and Ni, can also react with the support and can occupy octahedral or tetrahedral sites in the external layers or even form CoAl<sub>2</sub>O<sub>4</sub> (NiAl<sub>2</sub>O<sub>4</sub>) depending on the conditions of preparation. The origin of the exclusive use of alumina can be ascribed to its outstanding textural and mechanical properties and its relatively low cost. One important factor is also the ability to regenerate catalytic activities after intensive use under hydrotreating conditions. Due to the necessity to develop hydrotreating catalysts with enhanced properties, other supports such as carbon, silica, zeolite, titania, etc. have been studied. In several cases, it was claimed that higher activities were obtained than those of alumina supported catalysts.

Active Co-Mo or Ni-Mo catalysts were prepared using carbon as support by Stevens and Edmonds (73), Duchet et al. (74), Bridgwater et al. (75), Topsøe et al. (23), Hoffmann et al. (76). Generally, the catalytic activities reported in these studies are greater than those of typical alumina-supported catalysts.

This high activity of the carbon-supported, mixed catalysts was explained by Topsøe et al. about the CoMoS model. Using Mössbauer emission spectroscopy, Topsøe et al. showed that the cobalt atoms are situated at MoS<sub>2</sub> crystallite edges in a so-called "CoMoS" structure and that this structure almost governs the HDS activity (9). These results were obtained for catalysts supported on either alumina or carbon, or even unsupported. Thus the support is not necessary for the creation of the mixed phases, but

nevertheless it may play an important role by enabling dispersed phases to be produced, which is particularly the case for carbon. Later on, Candia et al. reported that two types sulfiding temperature and type II at high sulfiding temperature (type II being more active than type I in HDS). The difference between type I and II were supposed to be the existence, in the first case, of remaining Mo-O-Al linkages, while type II CoMoS is fully sulfided, which means that the interaction between active phase and support is only of the van der Waals type. Topsøe's Mössbauer results suggested that type II CoMoS is the one that most resembles the carbon-supported CoMoS. According to these authors, the catalysts have different activities essentially because they contain slightly different active phases. To check the validity of this interpretation, van Veen et al. prepared fully sulfided CoMoS on carbon (77), alumina and silica using nitrilotriacetic acid to complex with both Co and Mo, so that the precursor support interaction should be the same for all supports. They concluded that, even when the active phase (CoMoS II) is invariant and its dispersion is invariant, the support influences its specific activity, the effect of carbon being positive in comparison to alumina and silica. Nevertheless, since the samples were not characterized by XPS or electron microscopy, it is difficult to know whether the morphology of the active phase, i.e., the crystallite dimensions and orientations, was similar.

The higher catalytic activity for Mo/C compared to Mo/Al<sub>2</sub>O<sub>3</sub> was also explained with differences in the structure of the sulfide phase present and in the interaction between this phase and the respective supports (78). A single slab monolayer strongly interacting with the support was assumed to be present on alumina, and small, three-dimensional particles essentially free of interaction on carbon. The net effect of the strong interaction with alumina is a merely optimal dispersion of the Mo sulfide phase and an electronic transfer



through the Mo-O-Al linkages. This electronic effect would explain the lower activity of alumina supported catalyst.

Carbon supports may also be used for preparing highly active Co or Ni catalysts (74, 79). In fact, it was shown that Co and Ni are even more active than (Co) or equally active (Ni) as the corresponding Mo-based catalysts when they are supported on carbon and much less active when supported on alumina. By comparing the EXAFS and XANES spectra of Co/C with those of pure  $\text{Co}_9\text{S}_8$  and  $\text{CoS}_2$ , it was shown by Bouwens et al. (80) that Co/C has a larger fraction of octahedral cobalt than  $\text{Co}_9\text{S}_8$ . Similarly, Topsøe et al. and van der Krann et al (81) showed by MES that for low Co concentration (<1%), the Co phases present in the carbon supported catalysts are different from  $\text{Co}_9\text{S}_8$ . Why this phase is formed on carbon instead of  $\text{Co}_9\text{S}_8$  as expected from thermodynamic considerations and why this phase is more active are still unanswered questions.

According to Prins and co-workers, the great advantage of a material as inert as carbon is the possibility that all transition metal compounds present in the precursor state will be quantitatively converted into their active sulfide form. This is why the same authors used this support for their thorough studies of the properties of transition metal sulfides (82) in HDS and HDN (83, 84). A similar approach was also used by Ledoux et al. with the same objective of comparing the catalytic properties of various sulfides (85).

An important drawback in the utilization of carbon materials for hydrotreating reaction is their extensive microporosity. For catalytic reactions involving large molecules the micropores are of little use, since the part of the transition metals will be deposited in these pores and be wasted. Most mesoporous carbons, on the other hand, have poor crushing strengths, low bulk density or too low a surface area.

Other kinds of supports such as silica-alumina,  $\text{TiO}_2$ ,  $\text{ZrO}_2$ , zeolites, clays, and natural minerals were also studied.

The inherent HDS and HDN capabilities of titania and zirconia supports have been also applied in ternary compounds and a  $\text{CoMo/TiO}_2\text{-ZrO}_2\text{-V}_2\text{O}_5$  catalysts was found to be twice as active as a commercial CoMo for HDS of heavy diesel and vacuum gas oil (86). It should be noted that the properties of such mixed oxides depend on the preparation procedure to a great extent. Moreover,  $\text{CoMo/TiO-ZrO}_2$ ,  $\text{CoMo/TiO}_2\text{-CeO}_2$  and  $\text{CoMo/TiO}_2\text{-MnO}_2$  catalysts present very high initial HDS activities (87).

The catalytic properties of molybdenum sulfide based catalysts supported on  $\text{SiO}_2\text{-Al}_2\text{O}_3$  depend on the amount of  $\text{SiO}_2$  and on the reaction, i.e., HDS, HYD, HC or HDN. Muralidhar et al. (88) found that HDS and HYD activities decrease with increase in  $\text{SiO}_2$  content from 10 to 75 %, while the activity for the hydrocracking of 2,4,4-trimethyl-1-pentene showed an opposite trend. These high hydrocracking activities have to be related to the properties of the proton acid supports and not to the properties of the sulfide phase. In the hydrotreatment of heavy feedstocks, it was observed that an increase of the HDS activity when 15%  $\text{SiO}_2\text{-Al}_2\text{O}_3$  was used as a support for NiMo catalyst comparing with the properties of the same active phase on alumina (89). However, a decrease was found at higher concentrations of silica, i.e., 25 %. The HDS activity decreased in both instances.

### 1.7 On This Study

The structures and reactivities of Mo-based catalysts have been widely investigated in hydrodesulfurization reaction and the active sites in catalysts have been discussed and many reaction mechanisms have been proposed in recent years. As indicated above, however, the structure of catalysts during



practical performance of HDS could not be clarified and problems concerning the behavior of sulfur species on the catalyst still remain to be solved. On the other hand, radioisotope tracer methods using radioactive  $^{35}\text{S}$  were believed to enable to clarify this problem because this method made it possible to understand more exactly how sulfur in sulfur compounds is translated to  $\text{H}_2\text{S}$  and how sulfur in the sulfided catalyst participates in the actual HDS reaction.

Sulfur has a radioisotope  $^{35}\text{S}$  with a half-life time of 87.5 days emitting soft  $\beta$ -radiation (167keV). It has not been extensively used to study HDS catalysts. Lukens et al. (90) have measured the accessible surface area of supported transition metal sulfides by isotope exchange with a labeled  $\text{H}_2\text{S}$  in liquid scintillation solution. Kalechits and co-workers (91, 92) have shown that in the hydrogenation of a mixture of benzene and  $^{35}\text{S}\text{-CS}_2$  on  $\text{WS}_2$  catalyst, the sulfur in the catalyst was exchanged with radioactive sulfur of the feedstocks. This labile sulfur would be a part of the nonstoichiometric sulfur of the catalyst that would be responsible for the acceleration of acid catalyzed reaction (isomerization and cracking). Gachet et al. (93) presulfided a commercial Co-Mo/ $\text{Al}_2\text{O}_3$  catalyst with the gas mixture of  $^{35}\text{S}\text{-H}_2\text{S}$  and  $\text{H}_2$ , then carried out the HDS of dibenzothiophene (DBT) at atmospheric pressure. They postulated that two types of sulfur appeared over the sulfided catalyst: labile sulfur and relatively fixed one. Gellman et al. (94) used radiotracer ( $^{35}\text{S}\text{-CS}_2$ ) labeling technique to measure removal rate of sulfur adsorbed on the Mo (100) surface in HDS of thiophene and postulated that the rate was fit with a first order kinetic equation. Isagulyants et al. (95) made an attempt to estimate quantitatively amount of sulfur held on the catalysts in the study where HDS of thiophene was conducted on a series of Co-Mo catalysts sulfided by  $^{35}\text{S}$  elements and  $^{35}\text{S}$ -thiophene, respectively. Their study pointed out that about 20-30 % of sulfur held on vacancy sites was exchangeable. Paal

and his group (96, 97) carried out hydrogenation reaction of cyclohexanol and HDS reaction of thiophene in a pulse microreactor over the  $\text{MoO}_3$ ,  $\text{CoMoO}_4$ ,  $\text{Mo}/\text{Al}_2\text{O}_3$  and  $\text{Mo}/\text{Al}_2\text{O}_3$  catalysts, which was promoted by Pd, Ir and Ru. In their study, the catalysts were sulfided by a gas mixture of  $^{35}\text{S}$  labeled  $\text{H}_2\text{S}$  and  $\text{H}_2$ . In these researches, however, all reactions were carried out at low pressure and over  $^{35}\text{S}$  labeled catalysts. So far, to our knowledge, the HDS reaction using  $^{35}\text{S}$  labeled sulfur compounds as model compound in the practical industrial operating conditions, i.e., at high pressure in flow fixed bed reactor, has not been studied yet.

The main objective of this work is to develop an understanding of the behavior of sulfur during the practical HDS condition and relation between labile sulfur and activity of catalyst using the radioactive  $^{35}\text{S}$  tracer. This thesis consists of five chapters. In *Chapter two*, first, the radioisotope tracer method was developed. A model sulfur compound to be considered more difficult for HDS,  $^{35}\text{S}$ -labeled dibenzothiophene was synthesized and HDS reaction of this model compound was carried on an  $\text{Mo}/\text{Al}_2\text{O}_3$  under the practical HDS condition. The radioactivities of unreacted  $^{35}\text{S}$ -dibenzothiophene and formed  $^{35}\text{S}\text{-H}_2\text{S}$  were monitored. The amount of labile sulfur on the working catalyst was determined. This method allows us to understand more exactly paths of the sulfur transfer from DBT to  $\text{H}_2\text{S}$  and the amount of sulfur in the catalyst participated in the actual HDS reaction. In *Chapter three*, labile sulfur on  $\text{Mo}/\text{Al}_2\text{O}_3$  was labeled by  $^{35}\text{S}$  during the reaction of  $^{35}\text{S}\text{-DBT}$ . Then, several sulfur compounds, e.g., thiophene, benzothiophene, or other heteroatom compounds, e.g., dibenzofuran, quinoline, were introducing to this catalyst. By tracing the radioactivity of  $^{35}\text{S}\text{-H}_2\text{S}$  releasing from the catalyst, we expect to gain the more information concerning the behavior of sulfur on the catalyst in hydrodesulfurization, hydrodeoxygenation and hydrodenitrogenation. In *Chapter four*, to



investigate the pronounced promotion of cobalt or nickel for Mo/Al<sub>2</sub>O<sub>3</sub>, the same method was applied to HDS of <sup>35</sup>S-DBT on Co-Mo/Al<sub>2</sub>O<sub>3</sub> and Ni-Mo/Al<sub>2</sub>O<sub>3</sub>. Compared the amount of labile sulfur in different catalysts, the promotion of cobalt and nickel were investigated. In *Chapter five*, a Co-Mo/Al<sub>2</sub>O<sub>3</sub> catalyst was labeled by <sup>35</sup>S during the reaction of <sup>35</sup>S-DBT. Then, several sulfur compounds and a mixed gas of H<sub>2</sub>S/H<sub>2</sub> were introduced to the catalyst. By estimating the release rate of <sup>35</sup>S-H<sub>2</sub>S from the catalyst, the exchange mechanism of sulfur on the catalyst with sulfur in the sulfur compounds was investigated. In *Chapter six*, the radioisotope tracer method was tried to investigate the reason that caused the difference of reactivity between DBT and methyl-substituted DBTs.

## Reference

1. Gates, B. C., Katzer, J. R., and Schuit, G. C. A., " *Chemistry of Catalytic Processes*", Chapter 5, McGraw-Hill, Inc., New York, 1979.
2. Donati, E. E., " *Advances in Catalysis and Related Subjects*", Vol. 8, p. 39, Academic Press, New York, 1956.
3. Satterfield, C. N., and Yang, S. H., *Ind. Eng. Chem. Proc. Des. Dev.*, **23**, 11 (1984).
4. Schulz, H., Schon, M., and Rahman, N. M., *Stud. Surf. Sci. Catal.*, **27**, 201 (1986).
5. Furimsky, E., *Catal. Rev.-Sci. Eng.*, **25**, 421 (1983).
6. Lee, C. L., and Ollis, D. F., *J. Catal.*, **87**, 325, 332 (1984).
7. Ware, R. A., and Wei, J., *J. Catal.*, **93**, 100, 122, 135 (1985).
8. Vrinat, M. L., *Appl. Catal.*, **6**, 137 (1983).
9. Speight, J. G., " *The Desulfurization of Heavy Oils and Residue*", Marcel Dekker, New York, 1981.
10. Kabe, T., Ishihara, A., and Zhang, Q., *Appl. Catal.*, **97**, L1 (1993)
11. Weisser, O., and Landa, S., " *Sulphide Catalysts, Their Properties and Applications*", Pergamon Press, Oxford, 1973.
12. Chiu, N.-S., Bauer, S. H., and Johnson, M. F. L., *J. Catal.*, **89**, 226 (1984); *ibid.*, **98**, 32 (1986).
13. Bouwens, S. M. A. M., Prins, R., de Beer, V. H. J., and Koningsberger, D. C., *J. Phys. Chem.*, **94**, 3711 (1990).
14. Bouwens, S. M. A. M., van Veen, J. A. R., Koningsberger, D. C., de Beer, V. H. J., and Prins, R., *J. Phys. Chem.*, **95**, 123 (1991).
15. Louwere, S. P. A., and Prins, R., *J. Catal.*, **133**, 1 (1992).
16. Arnoldy, P., van der Heijkant, J. A. M., de Bok, G. D., and Moulijn, J. A., *J. Catal.*, **92**, 35 (1985).



17. Williams, R.H., and Mcevoy, A. J., *J. Phys., D: Appl. Phys.*, **4**, 456 (1971).
18. Topsøe, H., and Clausen, B. S., *Catal. Rev. - Sci. Eng.*, **26**, 395 (1984).
19. Hayden, T. F., and Dumesic, J. A., *J. Catal.*, **103**, 366 (1987).
20. Voorhoeve, R. J. H., and Stuiver, J. C. M., *J. Catal.*, **23**, 234 (1971).
21. Salmeron, M., Somorjai, G. A., Wold, A., Chianelli, R. R., and Liang, K. S., *Chem. Phys. Lett.*, **90**, 105 (1982).
22. Farias, M., H., Gellman, A. J., Somorjai, G. A., Chianelli, R.R., and Liang, K. S., *Surf. Sci.*, **140**, 181 (1984).
23. Topsøe, H., Clausen, B., S., Topsøe, N. - Y., and Pedersen, E., *Ind. Eng. Chem. Fundam.*, **25**, 25 (1986).
24. Delannay, F., Haeussler, E., and Delmon, B., *J. Catal.*, **66**, 469 (1980).
25. Kasztrlan, S., Grimblot, J., and Bonnelle, J. P., *J. Phys. Chem.*, **91**, 1503 (1987).
26. Topsøe, H., and Clausen, B. S., *Appl. Catal.*, **25**, 273 (1986).
27. Wivel, C., Candia, R., Clausen, B. S., Mørup, S., and Topsøe, H., *J. Catal.*, **68**, 453 (1981).
28. Farragher, A. L., and Cossee, P., in *Proc. 5th Int. Congress Catalysis* (J. W. Hightower, Eds.), Palm Beach, North-Holland, Amsterdam, p. 1301, 1973
29. Hagenbach, G., Courty, Ph., and Delmon, B., *J. Catal.*, **23**, 295 (1971).
30. Topsøe, N.-Y., and Topsøe, H., *J. Catal.*, **84**, 386 (1983).
31. Ledoux, M. J., Michaux, O., Agostini, G., and Panissod, P., *J. Catal.*, **96**, 189 (1985).
32. Kasztelan, S., Toulhoat, H., Grimblot, J., and Bonnelle, J. P., *Appl. Catal.*, **13**, 127 (1984).
33. Lipsch, J. M. J. G., Schuit, G. C. A., *J. Catal.*, **15**, 179 (1969).
34. Massoth, F. E., *J. Catal.*, **36**, 164 (1975).
35. Massoth, F. E., *Adv. Catal.*, **27**, 265 (1978).

36. de Beer, V. H. J., van Sint Fiet, T. H. M., van der Steen, G. H. A. M., Zwaga, A. C., and Schuit, G. C. A., *J. Catal.*, **35**, 297 (1974).
37. Karroua, M., Matralis, H., Grange, P., and Delmon, B., *J. Catal.*, **139**, 371 (1993).
38. Zabala, J. M., Mainil, M., Grange, P., and Delmon, B., *React. Kinetic Catal. Lett.*, **3**, 285 (1975).
39. Goetsch, D. A., Carver, J. C., Seiver, R. L., and Sawyer, W. H., *8th North American Meeting of the Catalysis Society*, Philadelphia, May 1-4, 1983.
40. Delmon, B., *ACS. Div. Pet. Chem. Prepr.*, **22**, 503 (1977).
41. Yermakov, Y. I., Startsev, A. N., Burmistrov, V. A., Shumilo, O. N., and Bulgakov, N. N., *Appl. Catal.*, **18**, 33 (1985).
42. Chianelli, R. R., Pecoraro, T. A., Halbert, T. R., Pan, W. -H., and Stiefel, E. I., *J. Catal.*, **86**, 226 (1984).
43. Nag, N. K., Sapre, A. V., Broderick, D. H., and Gates, B. C., *J. Catal.*, **57**, 509 (1979).
44. Houalla, M., Broderick, D. H., Sapre, A. V., Nag, N.K., de Beer, V. H. J., Gates, B. C., and Kwart, H., *J. Catal.*, **61**, 523 (1980).
45. Skelton, R. J., Chang, H. C. K., and Lee, M. L., *Anal. Chem.*, **61**, 2292 (1989).
46. Bradley, C., and Schiller, D. J., *Anal. Chem.*, **58**(14), 3017 (1986).
47. Miki, Y., Sugimoto, Y., Yamadaya, S., and Oba, M., *Natl. Chem. Lab. Ind. Rep.*, **84** (12), 661 (1989).
48. Kabe, T., Ishihara, A., and Tajima, H., *Ind. Eng. Chem. Res.*, **31**, 1578 (1992).
49. Kwart, H., Schuit, G. C. A., and Gates, B. C., *J. Catal.*, **61**, 128 (1980).
50. Sauer, N. N., Markel, E. J., Schrader, G. L., and Angelici, R. J., *J. Catal.*, **117**, 295 (1989).



51. van Parijs, I. A., and Froment, G. F., *Ind. Eng. Chem. Prod. Res. Dev.*, **25**, 431 (1986).
52. Daly, F. P., *J. Catal.*, **51**, 221 (1978).
53. Geneste, P., Amblard, P., Bonnet, M., and Graffin, P., *J. Catal.*, **61**, 115 (1980).
54. van Parijs, I. A., Hosten, L. H., and Froment, G. F., *Ind. Eng. Chem. Prod. Res. Dev.*, **25**, 437 (1986).
55. Houalla, M., Nag, N. K., Sapre, A. V., Broderick, D. H., and Gates, B. C., *AIChE J.*, **24**, 1015 (1978).
56. Girgis, M. J., and Gates, B. C., *Ind. Eng. Chem. Res.*, **30**, 2021 (1991).
57. O'Brien, W. S., Chen, J. W., Nayak, R. V., and Carr, G. S., *Ind. Eng. Chem. Proc. Des. Dev.*, **25**, 221 (1986).
58. Broderick, D. H., and Gates, B. C., *AIChE J.*, **27**, 663 (1981).
59. Sapre, A. V., Broderick, D. H., Fraenkel, D., Gates, B. C., and Nag, N. K., *AIChE J.*, **26**, 690 (1980).
60. Satterfield, C. N., and Roberts, G. W., *AIChE J.*, **14**, 159 (1968).
61. Nagai, M., and Kabe, T., *J. Catal.*, **81**, 440 (1983).
62. LaVopa, V., and Satterfield, C. N., *J. Catal.*, **110**, 375 (1988).
63. Ishihara, A., Itoh, T., Hino, T., Nomura, M., Qi, P., and Kabe, T., *J. Catal.*, **140**, 184 (1993).
64. Odebunmi, E. O., and Ollis, D. F., *J. Catal.*, **80**, 65 (1983).
65. Krishnamurthy and Shah, Y. T., *Chem. Eng. Commun.*, **16**, 109 (1982).
66. Gutberlet, L. C., and Bertolacini, R. J., *Ind. Eng. Chem. Res. Dev.*, **23**, 246 (1983).
67. Nagai, M., Sato, T., and Aiba, A., *J. Catal.*, **97**, 52 (1986).
68. Massoth, F. E., in "Advances in Catalysis" (Eley, D. D., Pines, H., and Weisz, P. B., Eds.), Vol. **27**, p. 265. Academic Press, New York, 1978.

69. Scheffer, B., Arnoldy, P., and Moulijn, J. A., *J. Catal.*, **112**, 516 (1988).
70. Candia, R., Topsøe, H., and Clausen, B. S., in "Proceedings, 9th Iberoamerican Symposium on Catalysts", p.211, Lisbon, Portugal, 1984.
71. van Veen, J. A. R., Hendriks, P. A. J. M., Romes, E. J. G. M., and Andrea, R. R., *J. Phys. Chem.*, **94**, 5275 (1990).
72. Mensch, C. T. J., van Veen, J. A. R., van Wingerden, B., and van Dijk, M. P., *J. Phys. Chem.*, **92**, 4961 (1988).
73. Stevens, G. C., and Edmonds, T., in "Preparation of Catalysts II", (Delmon, B., Grange, P., Jacobs, P., and Poncelet, G., Eds.), Elsevier, Amsterdam, 1979, p.507.
74. Duchet, J. C., Van Oers, E. M., de Beer, V. H. J., and Prins, R., *J. Catal.*, **80**, 386 (1983).
75. Bridgewater, A. J., Burch, r., and Michell, P.C. H., *Appl. Catal.*, **4**, 267 (1982).
76. Hoffman, C. Breysse, M., Leclercq, C., and Frety, R., in "Actas 10° Simposio Ibero-Americano de Catalisis (Merida)", (U. L. A., Eds.), Vol. **1**, p.380 (1986).
77. van Veen, J. A. R., Gerkena, E., van der Kraan, A. M., and Knoester, A., *J. Chem. Soc., Chem. Commun.*, 1684 (1987).
78. Vissers, J. P. R., Scheffer, B., de Beer, V. H. J., Moulijn, J. A., And Prins, R., *J. Catal.*, **105**, 277 (1987).
79. de Beer, V. H. J., Duchet, J. C., and Prins, R., *J. Catal.*, **72**, 369 (1981).
80. Bouwens, S. M. A. M., Koningsberger, D. C., de Beer, V. H. J., and Prins, R., *Catal. Lett.*, **1**, 55 (1988).
81. Van der Kraam, A. M., Craye, M. V. J., Gerkema, E., Ramselaar, W. L. T. M., and de Beer, V. H. J., *Hyperfine Int.* **46**, 567 (1989).



82. Vissers, J. P. R., Groot, C. K., van Oers, E. M., de Beer, V. H. J., and Prins, R., *Bull. Soc. Chim. Belg.*, **93**, 813 (1984).
83. Eijsbouts, S., Sudhakar, C., de Beer, V. H. J., and Prins., R., *J. Catal.*, **127**, 605 (1991).
84. Eijsbouts, S., de Beer, V. H. J., and Prins., R., *J. Catal.*, **127**, 619 (1991).
85. Ledoux, M. J., Michaux, O., and Agostini, G., *J. Catal.*, **102**, 430 (1986).
86. Wang, I., and Chang, R. C., *J. Catal.*, **117**, 266 (1989).
87. Daly, F. P., *J. Catal.*, **116**, 600 (1989).
88. Muralidhar, G., Massoth, F. E., and Shabtai, J., *J. Catal.*, **85**, 44 (1984).
89. Breysse, M., Portefaix, J. L., and Vrinat, M., *Catal. Today*, **10**, 489 (1991).
90. Lukens, H. R., Meisenheimer, J. R. G., and Wilson, J. N., *J. Phys. Chem.*, **66**, 469 (1962).
91. Pavlova, K. A., Panteleeva, B. D., Deryagina, E. N., and Kalechits, I. V., *Kinet. Katal.*, **6**, 3, 493 (1965).
92. Kalechits, I. V., and Deryagina, E. N., *Kinet. Katal.*, **8**, 3, 604 (1969).
93. Gachet, C. G., Dhainaut, E., de Mourgues, L., Candy, J. P. and Fouilloux, P., *Bull. Soc. Chim. Belg.*, **90** (12), 1279 (1981).
94. Gellman, A. J., Bussell, M. E., and Somorjai, G. A., *J. Catal.*, **107**, 103 (1987).
95. Isagulyants, G. V., Greish, A. A., and Kogan, V. M., "Symposium of International Catalyst Annual Conference in Canada", p. 35, 1988.
96. Dobrovolszky, M., Tetenyi, P., and Paal, Z., *Chem. Eng. Commun.*, **83**, 1 (1989).
97. Dobrovolszky, M., Paal, Z., and Tetenyi, P., *Catal. Today*, **9**, 113 (1991).

## Chapter Two

### Hydrodesulfurization of Radioactive $^{35}\text{S}$ -Labeled Dibenzothiophene on $\text{Mo}/\text{Al}_2\text{O}_3$



Chapter Two  
**Hydrodesulfurization of Radioactive  $^{35}\text{S}$ -Labeled  
Dibenzothiophene on  $\text{Mo}/\text{Al}_2\text{O}_3$**

**Abstract**

To estimate the behavior of sulfur on a hydrodesulfurization catalyst,  $^{35}\text{S}$ -labeled dibenzothiophene ( $^{35}\text{S}$ -DBT) was hydrodesulfurized on a sulfided  $\text{Mo}/\text{Al}_2\text{O}_3$  in a fixed-bed pressurized flow reactor. After the hydrodesulfurization (HDS) reaction of  $^{32}\text{S}$ -DBT reached the steady state, the reactant solution of  $^{35}\text{S}$ -DBT was substituted for that of  $^{32}\text{S}$ -DBT with the same concentration of DBT. In this period, the radioactivities of unreacted  $^{35}\text{S}$ -DBT and formed  $^{35}\text{S}$ - $\text{H}_2\text{S}$  was monitored. The radioactivity of unreacted  $^{35}\text{S}$ -DBT reached the steady state immediately, while more time was needed for that of formed  $^{35}\text{S}$ - $\text{H}_2\text{S}$  to reach the steady state. This shows that the sulfur in dibenzothiophene was not directly released as hydrogen sulfide but initially accommodated on the catalyst. After the radioactivity of formed  $^{35}\text{S}$ - $\text{H}_2\text{S}$  reached the steady state, the reactant solution of  $^{32}\text{S}$ -DBT was substituted for that of  $^{35}\text{S}$ -DBT with the same concentration of DBT again. The behavior of sulfur on the catalyst was quantified from the formation rates of  $^{35}\text{S}$ - $\text{H}_2\text{S}$  in an increase or decrease periods of radioactivity. It was found that the amount of labile sulfur, which could be calculated from the maximum amount of  $^{35}\text{S}$  accommodated on the catalyst, increased with increasing the reaction temperature and DBT concentration. In addition, it was suggested that the total sulfur on the sulfided catalyst under practical HDS reaction conditions existed as  $\text{MoS}_{1.92}$ .



## 2.1 Introduction

The structures and reactivities of sulfided Mo/Al<sub>2</sub>O<sub>3</sub> catalyst have been widely investigated in hydrodesulfurization reaction (HDS), because Mo sulfide supported on alumina is the most basic form of HDS catalysts (1, 2). It has been believed that MoS<sub>2</sub>-like phase is present on alumina surface in sulfided molybdena-alumina catalysts. For example, it was shown by means of EXAFS that molybdenum atoms in the sulfided catalysts are present in MoS<sub>2</sub>-like structures and that these are ordered in very small domains (3-5). Hayden and Dumesic in TEM study of HDS catalysts reported that MoS<sub>2</sub> crystallites were created on thin films of alumina (6). Further, the amount of sulfur on sulfided molybdena-alumina catalyst has been directly measured by means of several methods. Arnoldy et al. showed by temperature-programmed sulfiding of Mo/Al<sub>2</sub>O<sub>3</sub> catalysts that sulfiding of a 4.5 atoms-Mo/nm<sup>2</sup> catalyst can be completed at ca. 500 K, up to an S/Mo ratio of 1.9 (7). Kabe et al. also reported that, by the thermogravimetric analysis of sulfiding processes, total sulfur present in sulfided Mo/Al<sub>2</sub>O<sub>3</sub> corresponded to MoO<sub>1.5</sub>S<sub>1.5</sub> (8).

On the other hand, the active sites in sulfided Mo/Al<sub>2</sub>O<sub>3</sub> catalysts have been discussed and many reaction mechanisms have been proposed in recent years (2, 9, 10). When it was assumed that the anions in the basal planes of MoS<sub>2</sub> are more strongly bonded to the Mo cations than the anions at edges or corners, sulfur vacancy would be created at edges and corners rather than at basal planes (11). Therefore, the catalytic activity of HDS was expected to be much higher at edges and corners. This assumption has been experimentally verified by surface science studies of the catalytic activity of an MoS<sub>2</sub> single crystal (12, 13). As described in *Chapter 1*, when the HDS reaction begins with the adsorption of thiophenes to the sulfur vacancy, two mechanisms have

been proposed: One is the one-point (end-on) mechanism where the reactant thiophene molecule is assumed to adsorb upright on the surface (14). The other is the side-on mechanism where the adsorption of thiophene takes place through "multipoint" adsorption (15). Recently, it was shown in kinetic study of HDS of methyl-substituted dibenzothiophenes (DBTs) that DBTs are adsorbed on the catalyst through the  $\pi$ -electrons of their aromatic rings rather than unshared electrons of their sulfur (16). Despite these extensive studies, the nature of active sites and the behavior of surface sulfur species have not been clarified unambiguously.

To elucidate the behavior of sulfur species on HDS catalysts, radioisotopic tracer methods using <sup>35</sup>S have been developed. Gachet et al. (17) presulfided a commercial Co-Mo/Al<sub>2</sub>O<sub>3</sub> catalyst with the gas mixture of <sup>35</sup>S-H<sub>2</sub>S and H<sub>2</sub>, then carried out the HDS of dibenzothiophene (DBT) at atmospheric pressure. They postulated that two types of sulfur appeared over the sulfided catalyst: labile sulfur and relatively fixed one. Campbell et al. (18) found that an MoS<sub>2</sub> catalyst picks up radioactive <sup>35</sup>S from <sup>35</sup>S-H<sub>2</sub>S during its contact with the catalyst in the study where hydrogenation of 1,3-butadiene was carried out in a vacuum system over the molybdenum disulfides catalyst. Dobrovolszky et al. (19, 20) carried out the hydrogenation reaction of cyclohexanol and HDS reaction of thiophene over the MoO<sub>3</sub>, CoMoO<sub>4</sub>, Mo/Al<sub>2</sub>O<sub>3</sub> and Pd, Ir or Ru-Mo/Al<sub>2</sub>O<sub>3</sub> catalysts sulfided by a gas mixture of <sup>35</sup>S-labeled H<sub>2</sub>S and H<sub>2</sub> in a pulse microreactor. Isagulyants et al. (21) made an attempt to estimate quantitatively the amount of sulfur held on Co-Mo catalysts sulfided by <sup>35</sup>S elements and <sup>35</sup>S-thiophene. These studies pointed out that about 20-30 wt% of the sulfur of the catalyst were exchangeable. Gellman et al. (22) used radiotracer (<sup>35</sup>S-CS<sub>2</sub>) labeling technique to measure the removal rate of sulfur adsorbed on the Mo (100) surface in HDS of thiophene and reported that the rate was fit with a first order kinetic equation. The use



of  $^{35}\text{S}$  was believed to enable to clarify the behavior of sulfur in catalysts. In these experiments, however, all reactions were carried out over  $^{35}\text{S}$ -labeled catalysts at low pressure. As far as we know, the HDS reaction using  $^{35}\text{S}$  labeled sulfur compounds as model compound in the practical industrial operation conditions, e.g., at high pressure in flow fixed bed reactor, has not been studied yet.

In this chapter, we have conducted the HDS reaction of  $^{35}\text{S}$ -labeled dibenzothiophene ( $^{35}\text{S}$ -DBT) to trace the behavior of  $^{35}\text{S}$  on catalysts at practical conditions of HDS. After the hydrodesulfurization of dibenzothiophene ( $^{32}\text{S}$ -DBT) reached the steady state at high pressure and prevailing temperature, the reactant solution of  $^{35}\text{S}$ -DBT was substituted for that of  $^{32}\text{S}$ -DBT under the same conditions. The radioactivities of unreacted  $^{35}\text{S}$ -DBT and formed  $^{35}\text{S}$ - $\text{H}_2\text{S}$  were monitored with the reaction time. After the radioactivity of formed  $^{35}\text{S}$ - $\text{H}_2\text{S}$  reached the steady state, the reactant solution was changed again to  $^{32}\text{S}$ -DBT under the same conditions. The amount of labile sulfur on the working catalyst was determined from an increase and a decrease in the rates of formed  $^{35}\text{S}$ - $\text{H}_2\text{S}$ . This method allows us to understand more exactly paths of the sulfur transfer from DBT to  $\text{H}_2\text{S}$  and the amount of sulfur in the catalyst participated in the actual HDS reaction.

## 2.2 Experimental

### 2.2.1 Materials

Decalin (Kishida Chemicals, commercial GR grade) was further purified by passing column (i.d. 20 mm, 30 cm) containing activated alumina (0.063-0.200 mm).  $^{35}\text{S}$ -labeled dibenzothiophene ( $^{35}\text{S}$ -DBT) was synthesized by the following method: To obtain  $^{35}\text{S}$  labeled sulfur, the commercial toluene solution of  $^{35}\text{S}$  (total radioactivity: 1.5 mCi, Amersham, Co. Ltd.) was mixed

sufficiently with 8.7 g sulfur ( $^{32}\text{S}$ ), then the toluene in mixture was evaporated at room temperature, and the sulfur mixture was dried for 24 hours in vacuo until the toluene was entirely removed. Using this  $^{35}\text{S}$ -labeled sulfur, DBT was synthesized according to the method developed by Gilman and Jocoby (23). After the crude DBT was recrystallized by ethanol, colorless needle crystallites (purity more than 99.9%) were obtained. Dibenzothiophene ( $^{32}\text{S}$ -DBT) was synthesized by the similar method except without radioactive  $^{35}\text{S}$ . Hydrogen (99.99 %) was obtained from Tohei Chemicals. Hydrogen sulfide in hydrogen ( $\text{H}_2\text{S}$  5.0%) was obtained from Takachio Chemicals.  $\text{Mo}/\text{Al}_2\text{O}_3$  catalyst ( $\text{MoO}_3$ : 12.5 wt%) was prepared by following steps:  $\gamma\text{-Al}_2\text{O}_3$  (Specific Surface 260  $\text{m}^2/\text{g}$ , Pore Volume 0.79  $\text{cm}^3/\text{g}$ ) was impregnated with aqueous ammonium heptamolybdate solution ( $(\text{NH}_4)_6\text{Mo}_7\text{O}_{24}\cdot 4\text{H}_2\text{O}$ ) by the usual impregnation technique. Then, impregnated catalysts were dried at 120  $^\circ\text{C}$  for 8 h and calcined at 450  $^\circ\text{C}$  for 24 h in air and were crushed and screened to 20 to 35 mesh granules.

### 2.2.2 Apparatus and Procedure

The reactor was a i.d.-8 mm stainless-steel tube packed with 1.0 g of catalyst particles diluted with quartz sand (30-50mesh) to 3.5  $\text{cm}^3$  bed volume and 7 cm bed height. The single charge was used throughout the entire series of experiments. After calcined at 450  $^\circ\text{C}$  in air overnight, the catalyst was presulfided with a mixture of 5 %  $\text{H}_2\text{S}$  in  $\text{H}_2$  flowing at 30 liters/h at atmospheric pressure and 400  $^\circ\text{C}$  for 3h. After the presulfidation, the reactor was cooled in  $\text{H}_2\text{S}/\text{H}_2$  to the reaction temperature and was pressurized with hydrogen. Then, the decalin solution containing DBT was supplied to the reactor by a high-pressure liquid pump (Kyowa Seimitsu KHD-16).

Typical reaction conditions were  $\text{H}_2$  flow rate 25 liters/h, WHSV 28  $\text{h}^{-1}$ , reaction pressure 10-50  $\text{kg}/\text{cm}^2$ , concentrations of DBT in decalin 0.5-3 wt%,



and reaction temperature 300-360 °C. The liquid product was collected from a gas-liquid separator. The produced H<sub>2</sub>S was absorbed by bubbled through a commercial basic scintillator solution (Carbosorb, Packard Co. Ltd.). For each run, the liquid products and absorbed H<sub>2</sub>S solution samples were collected every 15 min. The components of liquid products were analyzed by gas chromatography with an FID detector (Hitachi 163, Hitachi Co. Ltd.) using a commercial capillary column (G-column 250). Radioactivities of the unreacted <sup>35</sup>S-DBT in liquid product and the formed <sup>35</sup>S-H<sub>2</sub>S in the absorbed solution were measured by a liquid scintillation counter (LSC-1000, Aloka, Co. Ltd.), after adding proper scintillation solvent to each fraction. For the liquid scintillation counting, the procedures were available (24).

Typical operation procedures were as follows: (a) A decalin solution of 1 wt% <sup>32</sup>S-DBT was pumped into the reactor until the conversion of DBT became constant (ca. 3h). (b) After that, the decalin solution of 1 wt% <sup>35</sup>S-DBT was substituted for that of <sup>32</sup>S-DBT. The reaction with <sup>35</sup>S-DBT was performed until the amount of <sup>35</sup>S-H<sub>2</sub>S released from the exit of the reactor became constant. (c) The reactant solution was returned again to the decalin solution of 1 wt% <sup>32</sup>S-DBT. This reaction with <sup>32</sup>S-DBT was continued for 4-5 h.

In order to estimate the actual amount of sulfur on the sulfided Mo/Al<sub>2</sub>O<sub>3</sub> catalyst under practical reaction conditions, another experiment was carried out. After the catalyst was calcined at 450 °C for 24 h in air, the reaction was performed following the operation procedure: (a) The reaction system was pressurized with H<sub>2</sub> to 50 kg/cm<sup>2</sup> and heated to 360 °C. (b) The decalin solution of 1 wt% <sup>35</sup>S-DBT was pumped into the reactor and reacted for ca. 6 h at 360 °C and 50 kg/cm<sup>2</sup>. (c) After that, the solution of 1 wt% <sup>32</sup>S-DBT was substituted for that of <sup>35</sup>S-DBT and reacted for ca. 4 h. The amount of sulfur on the catalyst was determined from the balance of radioactivity.

## 2.3 Results and Discussion

### 2.3.1 Hydrodesulfurization of <sup>35</sup>S-Labeled Dibenzothiophene

The changes in radioactivity of unreacted <sup>35</sup>S-DBT and produced <sup>35</sup>S-H<sub>2</sub>S with the reaction time during the hydrodesulfurization (HDS) reaction at 360°C, 1.0 wt% of DBT, and 25 kg/cm<sup>2</sup> are shown in Figure 2.1. During the reaction period (ca. 11 h), the conversion of DBT was held almost constant at ca. 37 %. Major products were biphenyl (BP) and cyclohexylbenzene (CHB). After the decalin solution of <sup>32</sup>S-DBT was replaced by that of <sup>35</sup>S-DBT (2160 dpm/ml), the radioactivity of unreacted <sup>35</sup>S-DBT in liquid products increased and reached a steady state (1340 dpm/ml) immediately. The conversion (38.1%) calculated from the radioactivity of the steady state was in good agreement with the conversion (37.5%) estimated from GC analysis (Table 2.1). In the case of produced <sup>35</sup>S-H<sub>2</sub>S, however, about 155 min was needed to reach the steady state in released radioactivity. When the solution of <sup>35</sup>S-DBT was replaced with that of <sup>32</sup>S-DBT at 400 min, the radioactivity of unreacted <sup>35</sup>S-DBT also decreased immediately from the steady state (1340 dpm/ml) to normal state (25 dpm/ml), but the time delay for produced <sup>35</sup>S-H<sub>2</sub>S from its steady state (820 dpm/ml) to normal state (40 dpm/ml) was about 155 min.

To investigate the time delay, we conducted another similar reaction under the same conditions except for pressure (10 kg/cm<sup>2</sup>). When biphenyl (0.5 wt%) was added into the reactant solution of <sup>35</sup>S-DBT (DBT = 1.0 wt%), the changes in radioactivity of unreacted <sup>35</sup>S-DBT and produced <sup>35</sup>S-H<sub>2</sub>S were shown in Figure 2.2. The changes in the concentration of produced BP and CHB with the reaction time were also plotted. With the increase in radioactivity of unreacted <sup>35</sup>S-DBT, the concentration of BP increased and reached a steady state immediately. This indicates that BP did not delay but eluted immediately in the same manner as DBT. Therefore, the time delay



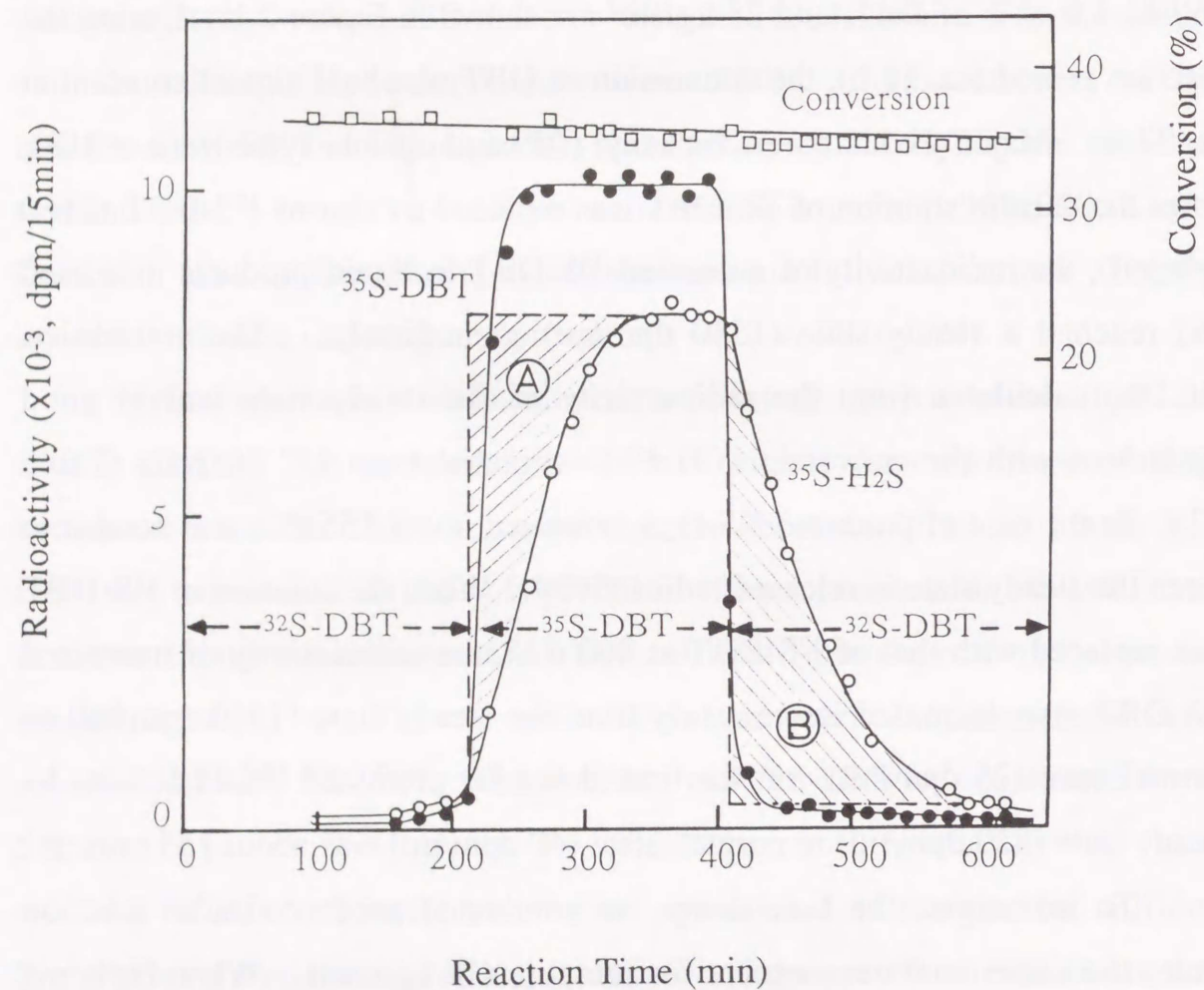


Figure 2.1. Operation procedure in hydrodesulfurization of  $^{35}\text{S-DBT}$ .  
 $\text{Mo/Al}_2\text{O}_3$ , Temperature  $360^\circ\text{C}$ , Pressure  $25\text{ kg/cm}^2$ .

●:  $^{35}\text{S-DBT}$ , ○:  $^{35}\text{S-H}_2\text{S}$ , □: Conversion.

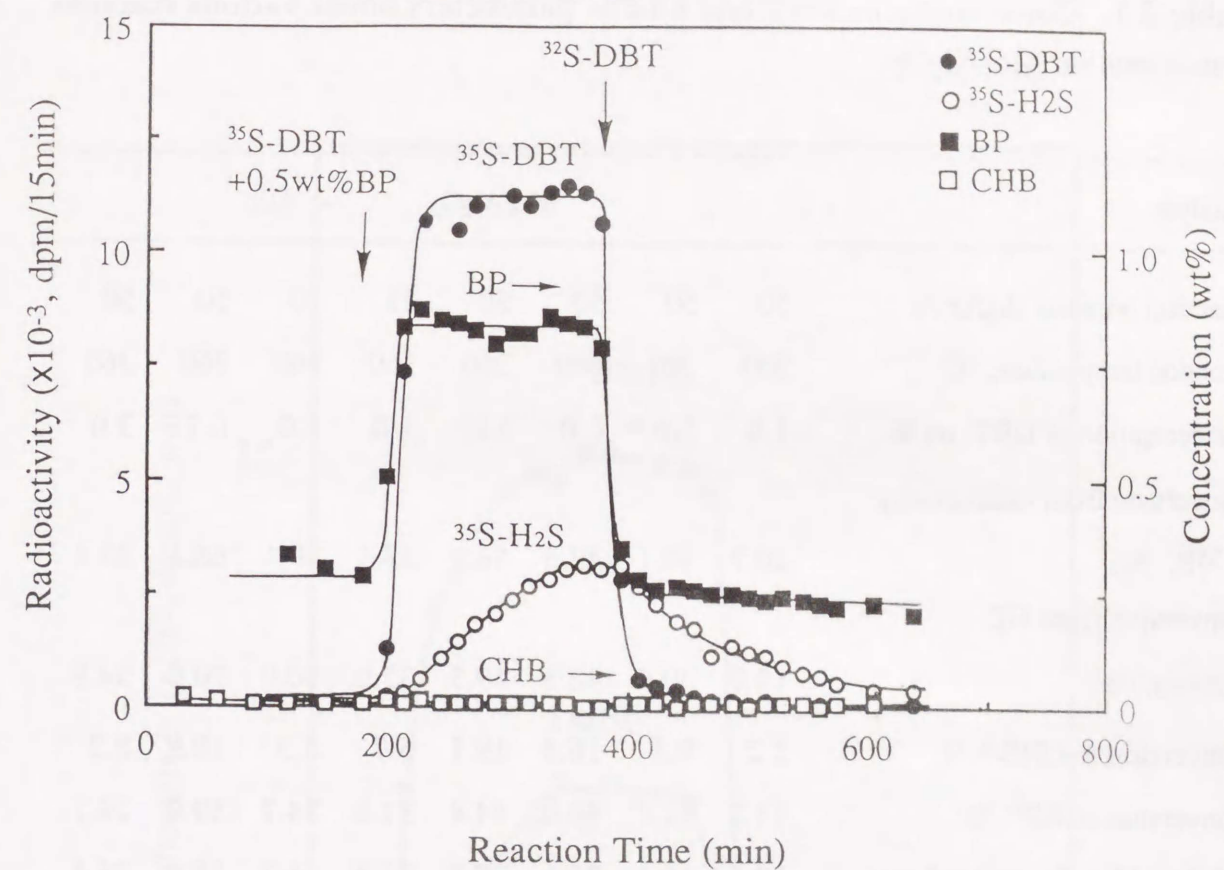


Figure 2.2. Changes in radioactivities of unreacted  $^{35}\text{S-DBT}$  and formed  $^{35}\text{S-H}_2\text{S}$  with reaction time and concentrations of produced biphenyl (BP) and cyclohexylbenzene (CHB) with reaction time.

$\text{Mo/Al}_2\text{O}_3$ ,  $360^\circ\text{C}$ ,  $10\text{ kg/cm}^2$ , DBT 1 wt%, BP 0.5 wt%.

for  $^{35}\text{S-H}_2\text{S}$  could not be due to the reaction system. From these results, it could be suggested that the sulfur in DBT is not directly released as  $\text{H}_2\text{S}$  but accommodated on the catalyst.

Figure 2.3 shows the effect of DBT concentrations on radioactivity of formed  $^{35}\text{S-H}_2\text{S}$ . The time delay to reach the steady state of the radioactivity



Table 2.1. Conversions of DBT and kinetic parameters under various reaction conditions on Mo/Al<sub>2</sub>O<sub>3</sub>.

Catalyst	Mo/Al <sub>2</sub> O <sub>3</sub>							
Reaction pressure (kg/cm <sup>2</sup> )	50	50	50	50	25	10	50	50
Reaction temperature, °C	300	320	340	360	360	360	360	360
Concentration of DBT, wt %	1.0	1.0	1.0	1.0	1.0	1.0	0.5	3.0
Conversion from radioactivity of <sup>35</sup> S, (%)	20.7	33.1	43.5	56.9	38.1	29.1	66.1	33.4
Conversion from GC analysis, (%)	19.0	30.9	42.3	59.3	37.5	30.0	70.0	34.8
Conversion to CHB <sup>a</sup> , %	5.2	9.3	16.4	19.1	5.7	5.3	10.9	8.2
Conversion to BP <sup>b</sup> , %	13.7	21.6	40.0	44.4	31.8	24.7	59.0	26.7
Labile sulfur, S <sub>0</sub> , mg/g of cat.	10.5	15.1	20.6	25.3	21.4	14.2	18.6	35.5
S <sub>0</sub> /S <sub>Total</sub> <sup>c</sup> , %	18.9	27.1	37.0	45.4	38.4	25.5	33.4	63.7
Release rate constant of <sup>35</sup> S-H <sub>2</sub> S, k, ×10 <sup>-2</sup> , min <sup>-1</sup>	1.44	1.66	1.68	1.84	1.43	1.08	1.54	2.40
S <sub>0</sub> × k, mg/min.g.cat.	0.151	0.250	0.346	0.467	0.306	0.153	0.286	0.852
Rate of DBT HDS, mg/min.g.cat.	0.155	0.252	0.346	0.467	0.306	0.245	0.270	0.851

<sup>a</sup> CHB = cyclohexylbenzene. <sup>b</sup> BP = biphenyl. <sup>c</sup> S<sub>Total</sub> is defined as amount of sulfur when Mo atoms in the catalyst existed as MoS<sub>2</sub>.

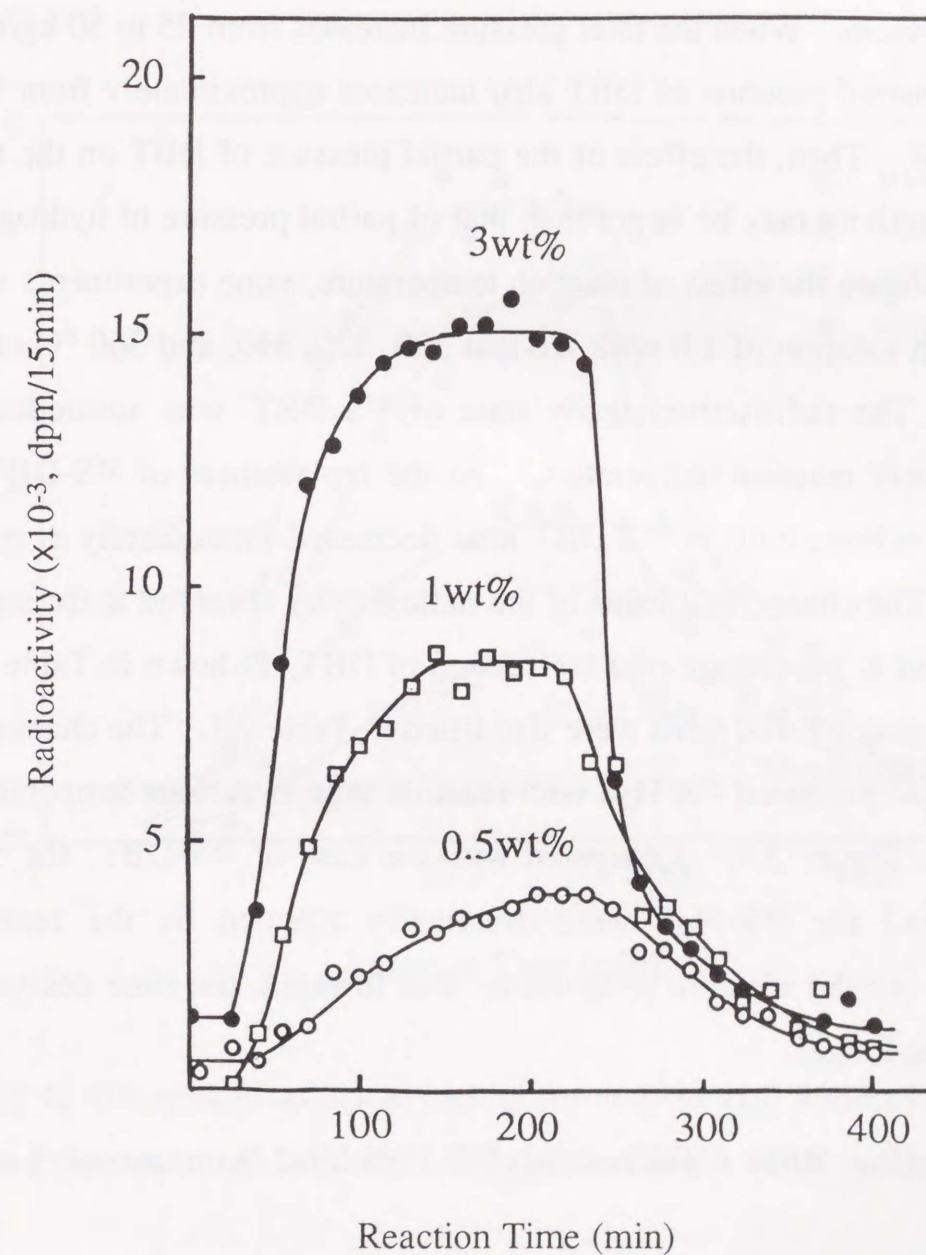


Figure 2.3. Changes in radioactivities of formed <sup>35</sup>S-H<sub>2</sub>S with reaction time for various DBT concentrations. Mo/Al<sub>2</sub>O<sub>3</sub>, 50 kg/cm<sup>2</sup>, 360 °C.



increased with a decrease in the concentration of DBT. Comparing with the results at 25 and 50 kg/cm<sup>2</sup> in Figures 1 and 3, the total pressure affects the changes in radioactivity of formed <sup>35</sup>S-H<sub>2</sub>S. Apparently, it seems that the time delay to reach the radioactive steady state of formed <sup>35</sup>S-H<sub>2</sub>S decreased with an increase in pressure. When the total pressure increases from 25 to 50 kg/cm<sup>2</sup>, however, the partial pressure of DBT also increases approximately from 0.03 to 0.06 kg/cm<sup>2</sup>. Then, the effect of the partial pressure of DBT on the time delay of radioactivity may be larger than that of partial pressure of hydrogen.

To investigate the effect of reaction temperature, same experiments were conducted with solution of 1.0 wt% DBT at 300, 320, 340, and 360 °C under 50 kg/cm<sup>2</sup>. The radioactive steady state of <sup>35</sup>S-DBT was immediately achieved at every reaction temperature. At the replacement of <sup>35</sup>S-DBT to <sup>32</sup>S-DBT, the radioactivity of <sup>35</sup>S-DBT also decreased immediately at every temperature. The change in a value of the radioactivity observed at the steady state correspond to the change of a conversion of DBT as shown in Table 2.1. The conversions to BP and CHB were also listed in Table 2.1. The changes in radioactivities of produced <sup>35</sup>S-H<sub>2</sub>S with reaction time at various temperatures were shown in Figure 2.4. Compared with the case of <sup>35</sup>S-DBT, the time delays observed for <sup>35</sup>S-H<sub>2</sub>S were drastically affected by the reaction temperature. As the reaction temperature was lowered, the time delays for <sup>35</sup>S-H<sub>2</sub>S became longer.

### 2.3.2 Formation Rate Constant of <sup>35</sup>S-H<sub>2</sub>S and Amount of Labile Sulfur.

The first-order plot of the radioactivity of produced <sup>35</sup>S-H<sub>2</sub>S in the decreasing period (Figure 2.1) was shown in Figure 2.5, and it indicated a good linear relationship. Then, this line can be revealed as a function of time:

$$\ln y = \ln z - kt \quad (2.1)$$

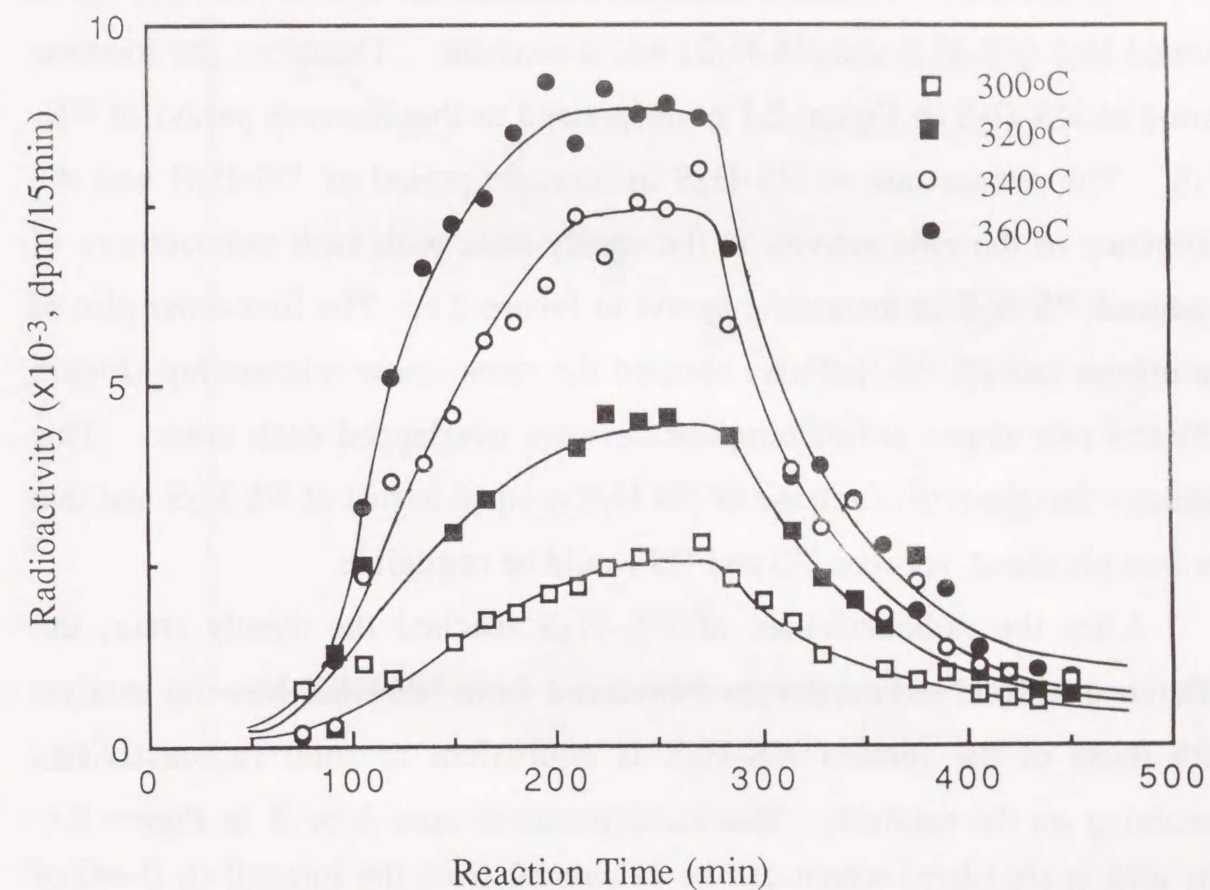


Figure 2.4. Changes in radioactivities of formed <sup>35</sup>S-H<sub>2</sub>S with reaction time at various temperature. Mo/Al<sub>2</sub>O<sub>3</sub>, 50 kg/cm<sup>2</sup>, DBT 1 wt%.



where  $y$  represents the formed rate of  $^{35}\text{S-H}_2\text{S}$  (dpm/min),  $z$  the formed rate of  $^{35}\text{S-H}_2\text{S}$  at steady state (dpm/min),  $k$  the rate constant of the release of  $^{35}\text{S-H}_2\text{S}$  ( $\text{min}^{-1}$ ),  $t$  reaction time (min). The rate constants under various conditions are also listed in Table 2.1. The activation energy of the release of  $^{35}\text{S-H}_2\text{S}$  calculated from Arrhenius plot of the rate constants was 4.2 kcal/mol.

Because the conversion was almost a constant always the total amount of formed  $\text{H}_2\text{S}$  ( $^{32}\text{S-H}_2\text{S}$  and  $^{35}\text{S-H}_2\text{S}$ ) was a constant. Therefore, the increase period of  $^{35}\text{S-H}_2\text{S}$  in Figure 2.1 corresponded to the decrease period of  $^{32}\text{S-H}_2\text{S}$ . The release rate of  $^{32}\text{S-H}_2\text{S}$  in increase period of  $^{35}\text{S-H}_2\text{S}$  was the difference of the radioactivity at the steady state with each radioactivity of produced  $^{35}\text{S-H}_2\text{S}$  in increasing period in Figure 2.1. The first-order plot of the release rate of  $^{32}\text{S-H}_2\text{S}$  also showed the same linear relationship (Figure 2.5) and two slopes at this temperature were overlapped each other. This indicates that the rate of release of  $^{35}\text{S-H}_2\text{S}$  is equal to that of  $^{32}\text{S-H}_2\text{S}$  and that the isotopic effect between  $^{35}\text{S}$  and  $^{32}\text{S}$  would be negligible.

After the radioactivities of  $^{35}\text{S-H}_2\text{S}$  reached the steady state, the difference of total radioactivities introduced from  $^{35}\text{S-DBT}$  into the catalyst with those of the formed  $^{35}\text{S-H}_2\text{S}$  is equivalent to total radioactivities remaining on the catalyst. This corresponds to area A or B in Figure 2.1. The area is  $z/k$  (dpm) which can be calculated from the integral ( $t: 0-\infty$ ) of equation 2.1. Since all  $^{35}\text{S}$  on the catalyst was originated from the desulfurization of  $^{35}\text{S-DBT}$  and the isotope effect between  $^{35}\text{S}$  and  $^{32}\text{S}$  was thought to be negligible, the concentration of  $^{35}\text{S}$  in sulfur introduced to the catalyst at the steady state should be equal to the concentration of  $^{35}\text{S}$  in sulfur of  $^{35}\text{S-DBT}$ . The concentration of  $^{35}\text{S}$  in sulfur of  $^{35}\text{S-DBT}$  could be defined as  $^{35}\text{S}_{\text{DBT}}/S_{\text{DBT}}$  (dpm/g), where  $^{35}\text{S}_{\text{DBT}}$  is radioactivities in 1 mol of DBT (dpm/mol) and  $S_{\text{DBT}}$  is the amount of sulfur in 1 mol DBT (g/mol). According to this, the amount of the sulfur incorporated into the catalyst, i.e.,

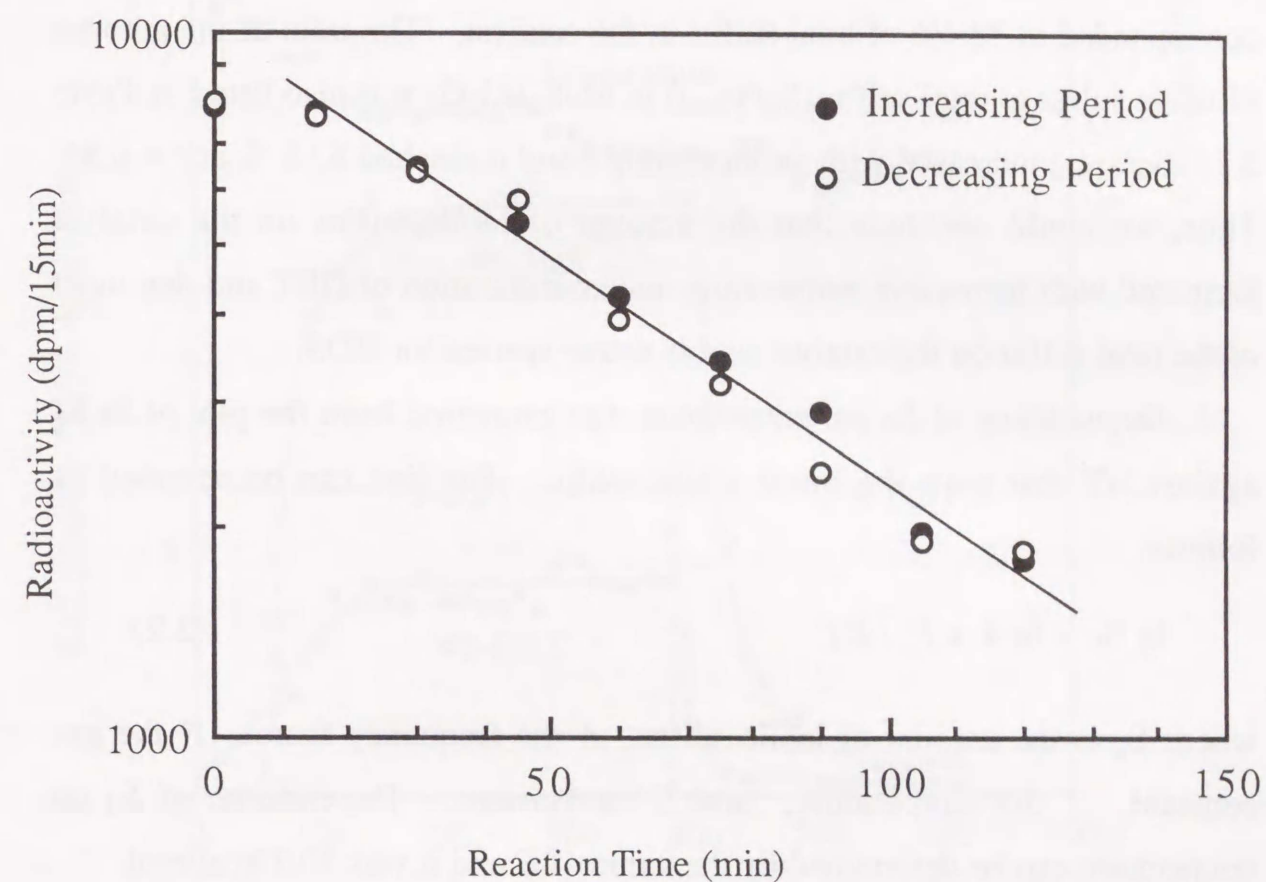


Figure 2.5. First order plots of the release rate of  $^{35}\text{S-H}_2\text{S}$ .  
Mo/Al<sub>2</sub>O<sub>3</sub>, 360 °C, 25 kg/cm<sup>2</sup>.



labile sulfur on the catalyst ( $S_0$ ) can be presented by  $(z/k)/(^{35}\text{S}_{\text{DBT}}/S_{\text{DBT}})$ . These are also listed in Table 2.1. If the sulfur on the catalyst was assumed to exist in  $\text{MoS}_2$  under the reaction condition (25), the total amount of sulfur on the catalyst is 55.7 mg of sulfur/g of catalyst. At 25 kg/cm<sup>2</sup> and 360 °C the amount of labile sulfur was 21.4 mg of sulfur/g of catalyst which corresponded to 38.4% of total sulfur in the catalyst. The ratio of the amount of labile sulfur to total sulfur ( $S_0/S_{\text{Total}}$ ) in  $\text{MoS}_2/\text{Al}_2\text{O}_3$  was also listed in Table 2.1.  $S_0/S_{\text{Total}}$  increased with an increasing  $r$  and it reached 63.8 % at  $r = 0.85$ . Thus, we could conclude that the amount of labile sulfur on the catalyst increased with increasing temperature and concentration of DBT and that most of the total sulfur on the catalyst acts as active species for HDS.

Dependence of  $S_0$  on temperature was estimated from the plot of  $\ln S_0$  against  $1/T$  that gave the linear relationship. The line can be revealed as follows:

$$\ln S_0 = \ln A + E / RT \quad (2.2)$$

where  $S_0$  is the amount of labile sulfur,  $A$  the frequency factor,  $R$  the gas constant,  $T$  the temperature, and  $E$  a constant. Dependence of  $S_0$  on temperature can be determined by the value of  $E$  and it was 10.7 kcal/mol.

The product between the rate constant of the release of  $^{35}\text{S}\text{-H}_2\text{S}$  and the amount of labile sulfur at each temperature ( $S_{0k}$ ) represents the apparent rate of the release of  $\text{H}_2\text{S}$  which was nearly equal to the apparent rate of DBT HDS ( $r$ ) as shown in Table 2.1. Although the former was determined from the kinetic calculation of  $^{35}\text{S}$  transfer and the latter was calculated from the conversion of DBT, both values should be the same because the conversion of 1 mol of DBT forms 1 mol of  $\text{H}_2\text{S}$  in HDS. The agreement confirms the validity of our remarks.

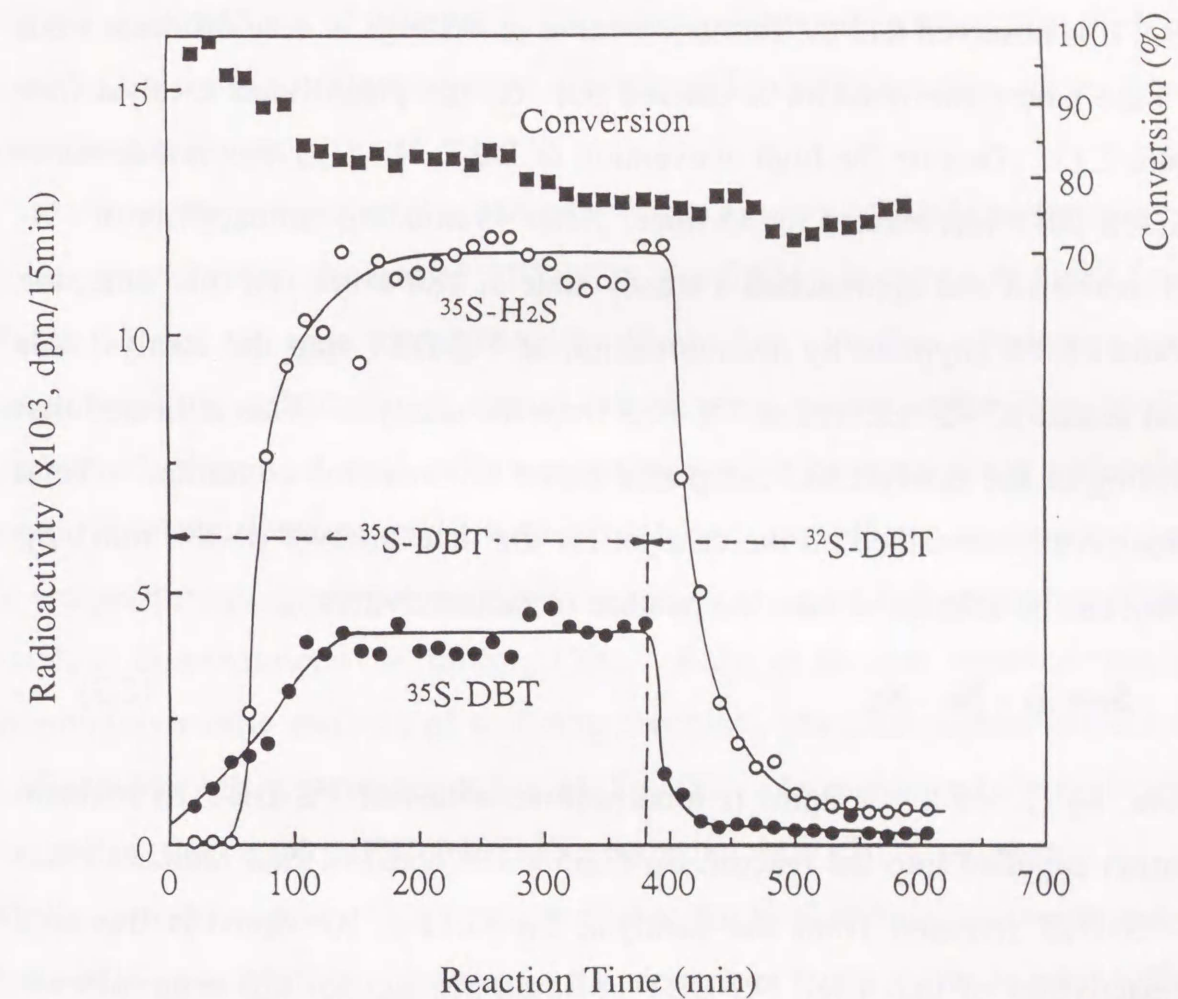


Figure 2.6. Changes in the conversion of DBT and radioactivities of unreacted  $^{35}\text{S}\text{-DBT}$  and formed  $^{35}\text{S}\text{-H}_2\text{S}$  with reaction time on an oxidized  $\text{Mo}/\text{Al}_2\text{O}_3$  calcined at 450 °C in air for 24 h.



### 2.3.3 Amount of Sulfur on Sulfided Mo/Al<sub>2</sub>O<sub>3</sub>

To determine the sulfided state of the catalyst, HDS of <sup>35</sup>S-DBT was directly performed on MoO<sub>3</sub>/Al<sub>2</sub>O<sub>3</sub> without the presulfidation. Figure 2.6 shows the changes in radioactivities of unreacted <sup>35</sup>S-DBT and produced <sup>35</sup>S-H<sub>2</sub>S. It is observed that the formation curve of <sup>35</sup>S-H<sub>2</sub>S is very different from the case where the reaction is carried out on the presulfided catalyst (see Figure 2.1). Despite the high conversion of DBT, <sup>35</sup>S-H<sub>2</sub>S was not detected until <sup>35</sup>S-DBT was reacted for 45 min. After 45 min, the radioactivity of <sup>35</sup>S-H<sub>2</sub>S increased and approached a steady state at 180 min. At this state, the amount of <sup>35</sup>S supplied by decomposition of <sup>35</sup>S-DBT into the catalyst was equal to that of <sup>35</sup>S released as <sup>35</sup>S-H<sub>2</sub>S from the catalyst. This indicated that sulfiding of the catalyst had completed under this reaction condition. Total radioactivities remained on the catalyst for the time interval (0-180 min), S<sub>R</sub> (dpm), can be calculated from the balance of radioactivities:

$$S_R = S_T - S_H - S_D \quad (2.3)$$

where, S<sub>T</sub> (1.746 × 10<sup>5</sup> dpm) is total radioactivities of <sup>35</sup>S-DBT in reactant solution supplied into the reactor, S<sub>H</sub> (7.35 × 10<sup>4</sup> dpm) is total radioactivities of <sup>35</sup>S-H<sub>2</sub>S released from the catalyst, S<sub>D</sub> (3.11 × 10<sup>4</sup> dpm) is the total radioactivities of unreacted <sup>35</sup>S-DBT in liquid product for this time interval. As mentioned above, the concentration of <sup>35</sup>S in sulfur of <sup>35</sup>S-DBT could be defined as <sup>35</sup>S<sub>DBT</sub>/S<sub>DBT</sub> (dpm/g), where <sup>35</sup>S<sub>DBT</sub> is radioactivities in 1 mol of DBT (dpm/mol) and S<sub>DBT</sub> is the amount of sulfur in 1 mol DBT (g/mol). According to this, the amount of total sulfur in sulfided catalyst can be presented by S<sub>R</sub>/(<sup>35</sup>S<sub>DBT</sub>/S<sub>DBT</sub>) (= 7.00 × 10<sup>4</sup> × 7.65 × 10<sup>-7</sup> = 0.0536 g of sulfur/g of catalyst = 1.92 mol of sulfur/mol of Mo). From this calculation, it can be concluded that Mo on the catalyst exists as MoS<sub>1.92</sub>. On the other hand, when <sup>35</sup>S-DBT was replaced by <sup>32</sup>S-DBT, the radioactivities of <sup>35</sup>S-DBT

immediately decreased and that of <sup>35</sup>S-H<sub>2</sub>S decreased more slowly (see Figure 2.6). According to the method mentioned in section 2.3.2, the amount of labile sulfur on the sulfided catalyst can be calculated from the first-order plot of the radioactivities of <sup>35</sup>S-H<sub>2</sub>S released in this decreasing period and it is 0.0280 g of sulfur/g of catalyst. This also indicates that more than 50% of total sulfur on the sulfided catalyst participated in HDS reaction under these reaction conditions.

From the present results, the ratio of the amount of labile sulfur to total sulfur was 63.8% at the rate of DBT HDS (*r* = 0.85). It can be deduced from Table 2.1 that the ratio increases with values of *r*. Further, although it was assumed in this calculation that total sulfurs were present in the form MoS<sub>2</sub>, the actual amount of total sulfurs may be smaller because anion vacancies would be always present on the working catalyst. Scheffer et al. reported that in temperature-programmed sulfiding of Mo/Al<sub>2</sub>O<sub>3</sub>, total sulfurs present in the catalyst corresponded to MoS<sub>1.8</sub> (29). Kabe et al. also reported that in thermogravimetric analysis of sulfiding processes, the total sulfurs present in sulfided Mo/Al<sub>2</sub>O<sub>3</sub> corresponded to MoS<sub>1.5</sub> (8). As mentioned above, it was suggested that total sulfur present in sulfided Mo/Al<sub>2</sub>O<sub>3</sub> corresponded to MoS<sub>1.92</sub> in this work. If it is assumed that the total sulfurs is present in the form MoS<sub>1.8</sub> or MoS<sub>1.92</sub>, the ratio of the amount of labile sulfur to total sulfur is 70.6 or 66.5% at *r* = 0.85, respectively. Therefore, it can be concluded that a significant amount of sulfur on sulfided Mo/Al<sub>2</sub>O<sub>3</sub> is labile if the rate of DBT HDS is sufficiently fast. It has been reported that Mo in a sulfided Mo/Al<sub>2</sub>O<sub>3</sub> catalyst is present mainly as single slab MoS<sub>2</sub> structures (26-28), where the coordination mode of Mo is tetrahedral. Even if Mo has such structures, however, all sulfurs are not in the same environment because there are some interactions between alumina and MoS<sub>2</sub>. The sulfurs present between Mo atoms and alumina may be different from others. The difference



in the environment of sulfur may generate the change in the amount of labile sulfur with reaction conditions.

## 2.4 Conclusions

Hydrodesulfurization reaction of  $^{35}\text{S}$ -labeled dibenzothiophene ( $^{35}\text{S}$ -DBT) was carried out on a sulfided  $\text{Mo}/\text{Al}_2\text{O}_3$  in a fixed-bed pressurized flow reactor and the following conclusions were obtained: The sulfur in dibenzothiophene was not directly released as hydrogen sulfide but initially accommodated on the catalyst. The incorporation of sulfur in DBT into the catalyst generated  $\text{H}_2\text{S}$ . The amount of labile sulfur increased with the reaction temperature and DBT concentration. This fact suggested that most of sulfurs were labile when the rate of DBT HDS was sufficiently fast. In addition, total sulfur present in sulfided  $\text{Mo}/\text{Al}_2\text{O}_3$  corresponded to  $\text{MoS}_{1.92}$  under the reaction conditions.

## References

1. Chianelli, R. R., *Catal. Rev.-Sci. Eng.*, **26** (3 & 4) 361 (1984).
2. Prince, R., de Beer, V. H. J., and Somorjai, G. A., *Catal. Rev.-Sci. Eng.*, **31** (1 & 2), 1 (1989).
3. Clausen, B. S., Topsoe, H., Candia, R., Villadsen, J., Lengeler, B., Als-Nielsen, J., and Christensen, F., *J. Phys. Chem.*, **85**, 3868 (1981).
4. Parham, T. G., and Merrill, R. P., *J. Catal.*, **85**, 295 (1984).
5. Chiu, N-S., Bauer, S. H., and Johnson, M. F. L., *J. Catal.*, **98**, 32 (1986).
6. Hayden, T. F., and Dumesic, J. A., *J. Catal.*, **103**, 366 (1987).
7. Arnoldy, P., van den Heijkant, J. A. M., de Bok, G. D., and Moulijn, J. A., *J. Catal.*, **92**, 35 (1985).
8. Kabe, T., Yamadaya, S., Oba, M., Miki, Y., *Int. Chem. Eng.*, **12**, 366 (1972).
9. Girgis, M.J., and Gates, B. C., *Ind. Eng. Chem. Res.*, **30**, 2021 (1991).
10. Nagai, M., and Kabe, T., *J. Catal.*, **81**, 440 (1983).
11. Voorhoeve, R. J. H., and Stuijver, J. C. M., *J. Catal.*, **23**, 228 (1971).
12. Salmeron, M., Somorjai, G. A., Wold, A., Chianelli, R. R., and Liang, K. S., *Chem. Phys. Lett.*, **90**, 105 (1982).
13. Farias, M. H., Gellman, A. J., Somorjai, G. A., Chianelli, R. R., and Liang, K. S., *Surf. Sci.*, **140**, 181 (1984).
14. Lipsch, J. M. J. G., and Schuit, G. C. A., *J. Catal.*, **15**, 179 (1969).
15. Kwart, H., Schuit, G. C. A., and Gates, B. C., *J. Catal.*, **61**, 128 (1980).
16. Kabe, T., Ishihara, A., and Zheng, Q., *Appl. Catal.*, **97**, L1 (1993).
17. Gachet, C. G., Dhainaut, E., de Mourgues, L., Candy, J. P., and Fouillous, P., *Bull. Soc. Chim. Belg.*, **90**, 1279 (1981).



18. Campbell, K. C., Mirza, M. L., Thomson, S. J., and Webb, G., *J. Chem. Soc. Faraday Trans. I*, **80**, 1689 (1984).
19. Dobrovolszky, M., Tetenyi, P., and Paal, Z., *Chem. Eng. Commun.*, **83**, 1 (1989).
20. Dobrovolszky, M., Paal, Z., and Tetenyi, P., *Catal. Today*, **9**, 113 (1991).
21. Isagulyants, G. V., Greish, A. A., and Kogan, V. M., *Proc. 9th Internal Congr. Catal.*, (Phillips, M. J., and Ternay, M., Eds.), Calgary, **1**, 35 (1988).
22. Gellman, A. J., Bussell, M. E., and Somorjai, G. A., *J. Catal.*, **107**, 103 (1987).
23. Gilman, H., and Jacoby, A. L., *J. Org. Chem.*, **4**, 108 (1939).
24. a) Kobayashi, Y., and Maudsley, D. V., *Biological Applications of Liquid Scintillation Counting*, Academic Press, New York (1974). b) Horrocks, D. L., *Applications of Liquid Scintillation Counting*, Academic Press, New York (1974). c) Crook, M., and Johnson P., *Liquid Scintillation Counting*, Vol. 4, Heyden and Son, London (1977).
25. de Beer, V. H. J., van Sint Fiet, T. H. M., van der Steen, G. H. A. M., Zwaga, A. C., and Schuit, G. C. A., *J. Catal.*, **35**, 297 (1974).
26. Topsoe, N.-Y., *J. Catal.*, **64**, 235 (1980).
27. Grimblot, J. G., Dufresne, P., Gengembre, L., and Bonelle, J. P., *Bull. Soc. Chim. Belg.*, **90**, 1261 (1981).
28. Pollack, S. S., Sanders, J. V., and Tischer, R. E., *Appl. Catal.*, **8**, 383 (1983).
29. Scheffer, B., de Jonge, J. C. M., Arnoldy, P., and Moulijn, J. A., *Bull. Soc. Chim. Belg.*, **93**, 751 (1984).

### Chapter Three

## Behavior of Sulfur on $^{35}\text{S}$ -Labeled $\text{Mo}/\text{Al}_2\text{O}_3$ in Hydrodesulfurization, Hydrodeoxygenation, and Hydrodenitrogenation



Chapter Three  
**Behavior of Sulfur on  $^{35}\text{S}$ -Labeled  $\text{Mo}/\text{Al}_2\text{O}_3$  in  
Hydrodesulfurization, Hydrodeoxygenation, and  
Hydrodenitrogenation**

**Abstract**

To investigate the behavior of sulfur during the hydrodesulfurization (HDS),  $^{35}\text{S}$ -labeled dibenzothiophene ( $^{35}\text{S}$ -DBT) was reacted on a sulfided  $\text{Mo}/\text{Al}_2\text{O}_3$ . It was found that  $^{35}\text{S}$  in  $^{35}\text{S}$ -DBT was accommodated on the catalyst and the concentration of  $^{35}\text{S}$  on the catalyst reached a steady state under a fixed reaction condition.  $^{35}\text{S}$  accommodated on the catalyst cannot be removed without the incorporation of sulfur from HDS of sulfur compounds such as DBT, benzothiophene, thiophene, and thiophenol. The removal rate of  $^{35}\text{S}$  from the catalyst depended upon the rate of HDS of these compounds, that is, the rate of sulfur incorporated into the catalyst. It was suggested that  $\text{H}_2\text{S}$  is formed from some portion of sulfur on the surface of the catalyst other than from that in the sulfur compounds. On the other hand, when hydrodenitrogenation (HDN) and hydrodeoxygenation (HDO) reactions were carried out on the catalyst containing  $^{35}\text{S}$ , only some portion of  $^{35}\text{S}$  could be replaced by oxygen atoms and released as  $^{35}\text{S}$ - $\text{H}_2\text{S}$ ; in contrast to this,  $^{35}\text{S}$  was hardly replaced by nitrogen atoms. This indicates that  $\text{H}_2\text{S}$  formation from the labile sulfur occurs only in hydrogenolysis but not in hydrogenation.



### 3.1 Introduction

Although a number of attempts have been made to elucidate the mechanism of hydrodesulfurization (HDS) (1-8), there are few examples that enable us to determine the behavior of sulfur in desulfurization catalyst. Recently, some researchers used  $^{35}\text{S}$  as a tracer of HDS to dissolve this problem (9-14). However, they did not determine the behavior of sulfur on sulfided catalyst under the operating condition of HDS reaction because  $^{35}\text{S}$  was only used under low pressure or vacuum conditions. In *Chapter 2*, we have reported the first example of HDS of  $^{35}\text{S}$ -labeled DBT on sulfided  $\text{Mo}/\text{Al}_2\text{O}_3$  under the operating condition of HDS, which has achieved the determination of labile sulfur on the catalyst (15). It was found that the amount of labile sulfur on sulfided  $\text{Mo}/\text{Al}_2\text{O}_3$  increased with an increase in temperature and the initial concentration of DBT. Furthermore, we found that all the Mo atoms on the catalyst existed as  $\text{MoS}_{1.92}$ . However, it was not yet clear whether sulfur on the catalyst can be released by the adsorption of DBT or by the incorporation of sulfur of DBT.

Regarding with the adsorption of molecules onto  $\text{Mo}/\text{Al}_2\text{O}_3$  catalysts, aromatics and unsaturated hydrocarbons could strongly adsorbed on the catalyst to inhibit the reaction. We have already reported that aromatics retarded HDS of DBT (16). It has been reported that sulfur, oxygen and nitrogen compounds can adsorb more strongly on the catalyst than hydrocarbons in hydrodesulfurization (HDS), hydrodenitrogenation (HDN) and hydrodeoxygenation (HDO) (17, 18). In the course of our study, we are interested in the reactivities of sulfided catalysts with aromatic compounds containing nitrogen and oxygen as well as sulfur-containing compounds. In this chapter, we have investigated the hydroprocessing of dibenzothiophene (DBT), benzothiophene (BT), thiophene (T), thiophenol (TP), dibenzofuran

(DBF), carbazole (CBL) and quinoline (QNL) on  $^{35}\text{S}$ -labeled  $\text{Mo}/\text{Al}_2\text{O}_3$  by tracing the changes in the radioactivity of  $^{35}\text{S}$ . We expect to have more information concerning the behavior of sulfur on a sulfided molybdenum catalyst. When these compounds containing heteroatoms are hydrogenolyzed on the sulfided catalyst, the heteroatoms will be incorporated into the catalyst and, as a result,  $^{35}\text{S}$  may be released as  $^{35}\text{S}\text{-H}_2\text{S}$ . If  $^{35}\text{S}$  on the catalyst cannot be released with the introduction of the compound containing heteroatoms, the effect of their adsorption on the catalyst may be estimated based on the behavior of the sulfur remaining on the catalyst.

### 3.2 Experimental

#### 3.2.1 Materials

Benzothiophene, thiophene, thiophenol, dibenzofuran, carbazole, quinoline and decalin were obtained from Kishida Co. Ltd.  $^{32}\text{S}$ -DBT was synthesized according to the method reported by Gilmon (19).  $^{35}\text{S}$ -labeled dibenzothiophene was obtained from the process described in *Chapter 2*.

$\text{Mo}/\text{Al}_2\text{O}_3$  catalyst containing 12.5 wt%  $\text{MoO}_3$  was prepared by conventional impregnation technique with the use of ammonium heptamolybdate. Before the reaction, the catalyst was presulfided with 5 vol%  $\text{H}_2\text{S}/\text{H}_2$  gas mixture by heating to 200 °C at a rate of 5 °C/min and then to 400 °C at a rate of 2 °C/min, and maintained at 400 °C for 3 h.

#### 3.2.2 Apparatus and Procedure

The reactions were carried out with a fixed-bed flow reactor at 50 kg/cm<sup>2</sup>, 360 °C and WHSV 28 h<sup>-1</sup>. Products were analyzed by a gas chromatography with an FID detector. The radioactivities of formed  $^{35}\text{S}\text{-H}_2\text{S}$  and unreacted  $^{35}\text{S}$ -DBT were measured by a liquid scintillation counter.



Typical two operation procedures were following:

Operation procedure 1: (a) A decalin solution of 1 wt%  $^{32}\text{S}$ -DBT was pumped into the reactor until the conversion of DBT became constant (about 3h). (b) After that, a decalin solution of 1 wt%  $^{35}\text{S}$ -DBT was substituted for that of 1 wt%  $^{32}\text{S}$ -DBT. The reaction with  $^{35}\text{S}$ -DBT was performed until the amount of  $^{35}\text{S}$ - $\text{H}_2\text{S}$  released from the exit of the reactor became constant. (c) Then, the reactant solution was substituted again with the decalin solution of 1 wt%  $^{32}\text{S}$ -DBT and was reacted for 4-5 h.

Operation procedure 2: Operation steps (a) and (b) in this procedure were the same as them in the operation procedure 1. (c) The reactant solution of  $^{35}\text{S}$ -DBT was replaced by decalin. The reaction was continued for ca. 4 h. (d) After that, the decalin solution of 1 wt%  $^{32}\text{S}$ -DBT or other heteroatom compound was substituted for decalin and was reacted for about 4-5 h.

### 3.3 Results

#### 3.3.1 HDS Reaction

When a solution of 1 wt% DBT was reacted according to the operation procedure 1 at 360 °C and 50 kg/cm<sup>2</sup>, the changes in radioactivities of unreacted  $^{35}\text{S}$ -DBT and produced  $^{35}\text{S}$ - $\text{H}_2\text{S}$  with the reaction time is shown in Figure 3.1. It is observed that the radioactivity of unreacted  $^{35}\text{S}$ -DBT in the liquid product increases and approaches a steady state immediately. In the case of produced  $^{35}\text{S}$ - $\text{H}_2\text{S}$ , however, about 130 min was needed to approach a steady state in radioactivities of produced  $^{35}\text{S}$ - $\text{H}_2\text{S}$ . When the solution of  $^{35}\text{S}$ -DBT was replaced with that of  $^{32}\text{S}$ -DBT at ca. 410 min, the radioactivities of unreacted  $^{35}\text{S}$ -DBT also decreased immediately from the steady state to normal state. However the time delay for produced  $^{35}\text{S}$ - $\text{H}_2\text{S}$  from its steady state to normal state was about 130 min. Moreover, the same HDS reactions were

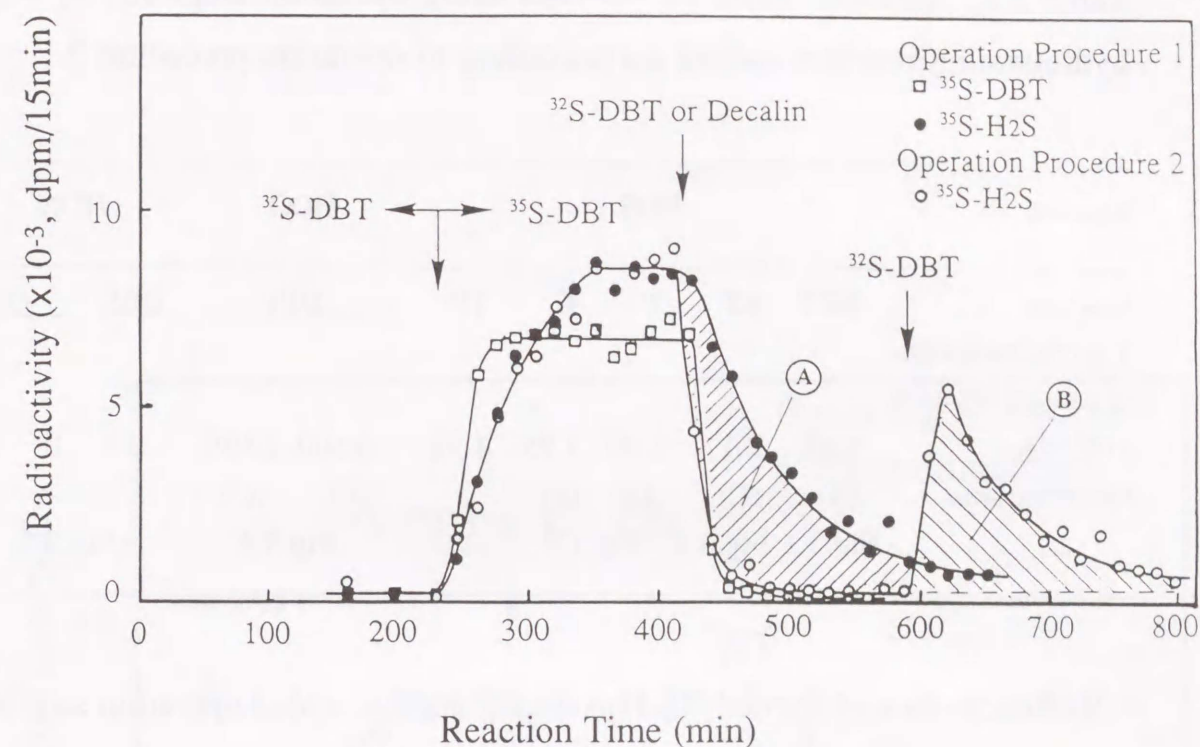


Figure 3.1. Change in radioactivities of unreacted  $^{35}\text{S}$ -DBT and formed  $^{35}\text{S}$ - $\text{H}_2\text{S}$  with reaction time. Mo/ $\text{Al}_2\text{O}_3$ , 360 °C, 50 kg/cm<sup>2</sup>, DBT 1wt%.

carried out at 360 °C and 50 kg/cm<sup>2</sup> when the length of the catalytic bed was changed from 7 cm to 3 cm, no effect on the time delay for  $^{35}\text{S}$ - $\text{H}_2\text{S}$  elution was found. It indicated that the time delay did not correspond to the adsorption /desorption of  $\text{H}_2\text{S}$  along the bed. As mentioned in previous paper (15), these results indicate that the sulfur in DBT is not directly released as hydrogen sulfide but accommodates on the catalyst and the changes in radioactivities of formed  $^{35}\text{S}$ - $\text{H}_2\text{S}$  during the decreasing period can be also revealed as a exponential function for time.

Instead of the replacement of the  $^{35}\text{S}$ -DBT solution to the  $^{32}\text{S}$ -DBT solution, the  $^{35}\text{S}$ -DBT solution was replaced by decalin solvent (operation procedure 2). The change in radioactivities of formed  $^{35}\text{S}$ - $\text{H}_2\text{S}$  with the



Table 3.1. Radioactivities of  $^{35}\text{S}\text{-H}_2\text{S}$  during operation steps (d) in various hydrotreating reaction carried out according to operation procedure 2.

Reaction	HDS					HDO		HDN		
	DBT	BT	T	T	TP	DBF	CBL	QNL		
Total radioactivities of formed $^{35}\text{S}\text{-H}_2\text{S}$ $\times 10^3$ , dpm	1.92	2.11	2.07	1.95	1.92	0.500	1.50 <sup>a</sup>	0	0	1.09 <sup>a</sup>
Reference area	(B)	(C)	(D)	(E)	—	(F)	(G)			(H)
	Fig.3.1	Fig.3.2	Fig.3.3	—	—	Fig.3.4	—	—	—	Fig.3.5

<sup>a</sup> Radioactivities of formed  $^{35}\text{S}\text{-H}_2\text{S}$  during another added operation step (e) (see text). <sup>b</sup> Area A in Figure 3.1 is  $1.92 \times 10^3$  dpm.

reaction time is also shown in Figure 3.1. It is observed that a portion of  $^{35}\text{S}$ , which is represented with the shaded area A in Figure 3.1, remained on the catalyst when only decalin solvent was substituted for the reactant solution of  $^{35}\text{S}\text{-DBT}$ . Even though when the catalyst was reduced in an atmosphere of high pressure of hydrogen for ca. 3 h,  $^{35}\text{S}\text{-H}_2\text{S}$  was hardly produced. This indicates that the sulfur accommodated on the catalyst was not eluted without the supply of sulfur by HDS of DBT. That is,  $^{35}\text{S}$  remaining on the catalyst did not adsorb as  $^{35}\text{S}\text{-H}_2\text{S}$  on the catalyst but was exchanged with the labile sulfur on the catalyst. When the reactant solution was replaced with  $^{32}\text{S}\text{-DBT}$  at ca. 590 min, this portion of  $^{35}\text{S}$  can be released again as  $^{35}\text{S}\text{-H}_2\text{S}$  as shown in Figure 3.1. Almost all  $^{35}\text{S}$  on the catalyst could be replaced by  $^{32}\text{S}$  derived from HDS of  $^{32}\text{S}\text{-DBT}$ . This can be verified by a fact that the shaded area B is approximately equal to the shaded area A as shown in Table 3.1.

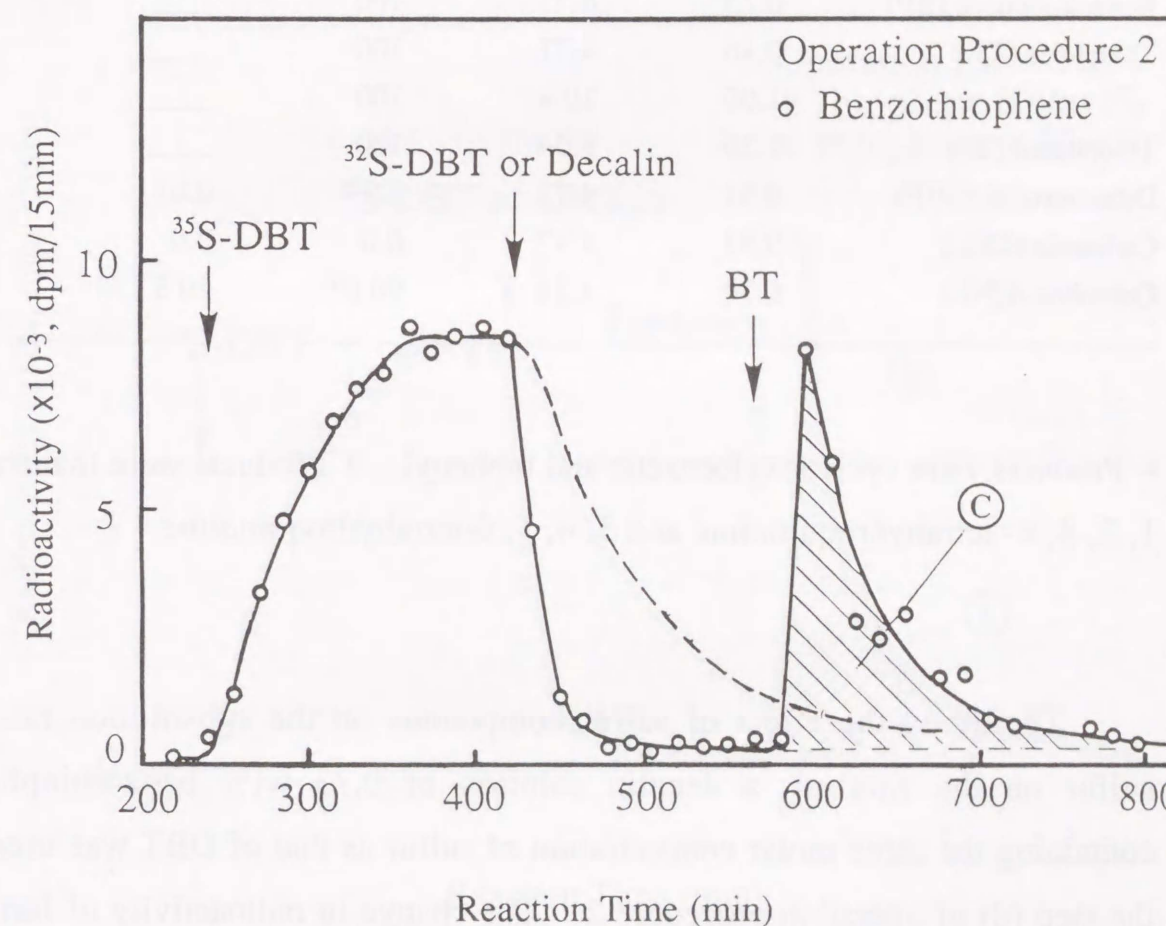


Figure 3.2. Change in radioactivities of formed  $^{35}\text{S}\text{-H}_2\text{S}$  with reaction time.  $\text{Mo}/\text{Al}_2\text{O}_3$ ,  $360^\circ\text{C}$ ,  $50 \text{ kg}/\text{cm}^2$ , BT 0.73 wt%.



Table 3.2. Conversions and pseudo-first-order rate constants of the hydrogenation reaction for various heteroatom compounds.

Compounds	Concentration in decalin		Conversion %	Rate Constant $\times 10^6$ , L/s.g.catalyst
	wt %	$\times 10^2$ , mol/L		
Dibenzothiophene (DBT)	1.0	4.77	59.3	8.0
Benzothiophene (BP)	0.73	4.77	100	—
Thiophene (T)	0.46	4.77	100	—
	1.00	10.4	100	—
Thiophenol (TP)	1.20	9.54	100	—
Dibenzofuran (DBF)	0.91	4.77	7.3 <sup>a</sup>	0.67
Carbazole (CRL)	0.91	4.77	0.0	0.0
Quinoline (QNL)	0.70	4.78	90.0 <sup>b</sup>	20.5

<sup>a</sup> Products were cyclohexylbenzene and biphenyl. <sup>b</sup> Products were mainly 1, 2, 3, 4- tetrahydroquinoline and 3, 4, 5, 6-tetrahydroquinoline.

To survey the effect of sulfur compounds on the substitution rate of sulfur on the catalyst, a decalin solution of 0.73 wt% benzothiophene containing the same molar concentration of sulfur as that of DBT was used in the step (d) of operation procedure 2. The change in radioactivity of formed  $^{35}\text{S-H}_2\text{S}$  with reaction time is shown in Figure 3.2. It can be observed that the formation curve of  $^{35}\text{S-H}_2\text{S}$  is the same as the case of  $^{32}\text{S-DBT}$ , until the operation step (c) during the reaction according to operation procedure 2. However, when the reactant solution was changed from decalin to the decalin solution of benzothiophene in operation step (d),  $^{35}\text{S-H}_2\text{S}$  formation rate, i.e., the rate for which  $^{35}\text{S}$  on the catalyst was replaced by  $^{32}\text{S}$  in benzothiophene, was more rapid than that in the case of  $^{32}\text{S-DBT}$ . This could be attributed as

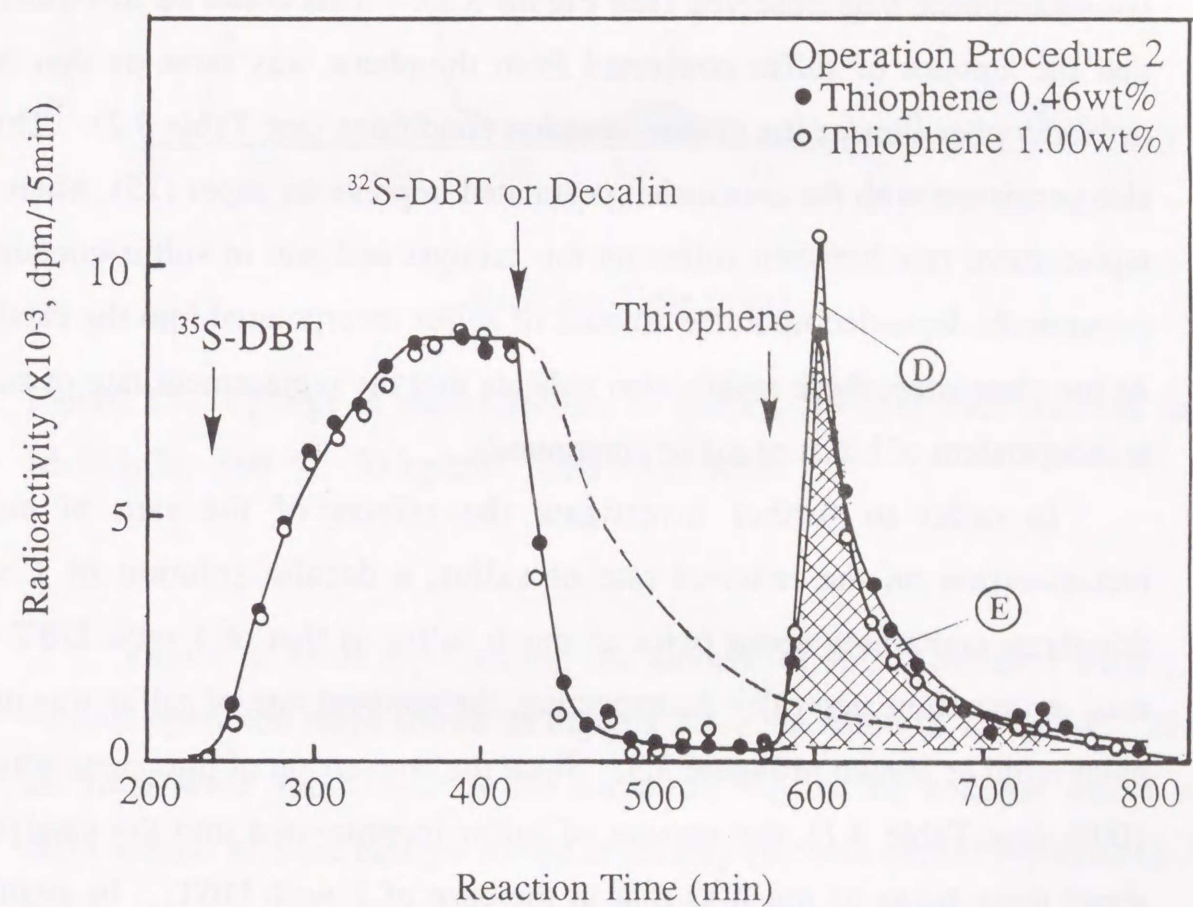


Figure 3.3. Change in radioactivities of formed  $^{35}\text{S-H}_2\text{S}$  with reaction time. Mo/Al<sub>2</sub>O<sub>3</sub>, 360 °C, 50 kg/cm<sup>2</sup>, T: 0.46 wt% and 1.00 wt%.



the increase of  $^{32}\text{S}$  incorporated from benzothiophene into the catalyst since HDS rate of benzothiophene was more rapid (conversion = 100%) than that of DBT (conversion = 59.3 %; see Table 3.2).

When a decalin solution of 0.46 wt% thiophene containing the same sulfur molar concentration as the solution of DBT was used to conduct the same reaction, the same formation curve of  $^{35}\text{S}\text{-H}_2\text{S}$  as the case of benzothiophene was observed (see Figure 3.3). This could be attributed as that the amount of sulfur converted from thiophene was same as that from benzothiophene under the present reaction conditions (see Table 3.2). This is also consistent with the conclusion postulated in previous paper (15), where the replacement rate between sulfur on the catalyst and one in sulfur-containing compounds depended upon the amount of sulfur incorporated into the catalyst. At the same time, these results also indicate that the replacement rate of sulfur is independent of kinds of sulfur compounds.

In order to further investigate the effects of the rate of sulfur incorporation on the removal rate of sulfur, a decalin solution of 1 wt% thiophene containing about twice as much sulfur as that of 1 wt% DBT was used in operation step (d). As expecting, the removal rate of sulfur was much more rapid as shown in Figure 3.3. Since the conversion of thiophene was yet 100% (see Table 3.1), the amount of sulfur incorporated into the catalyst is about three times as much as that in the case of 1 wt% DBT. In addition, when a decalin solution of 1 wt% thiophenol, containing twice as much sulfur as that of 1 wt% DBT was used, a formation curve of  $^{35}\text{S}\text{-H}_2\text{S}$  similar to the case of 1 wt% thiophene was obtained, because the conversion of thiophenol was also 100% and the rate of  $^{32}\text{S}$  incorporation was similar to that of 1 wt% thiophene (see Table 3.1). This further indicates that the removal rate of sulfur is independent of the kinds of sulfur compounds and depends only upon the rate of sulfur incorporated into the catalyst.

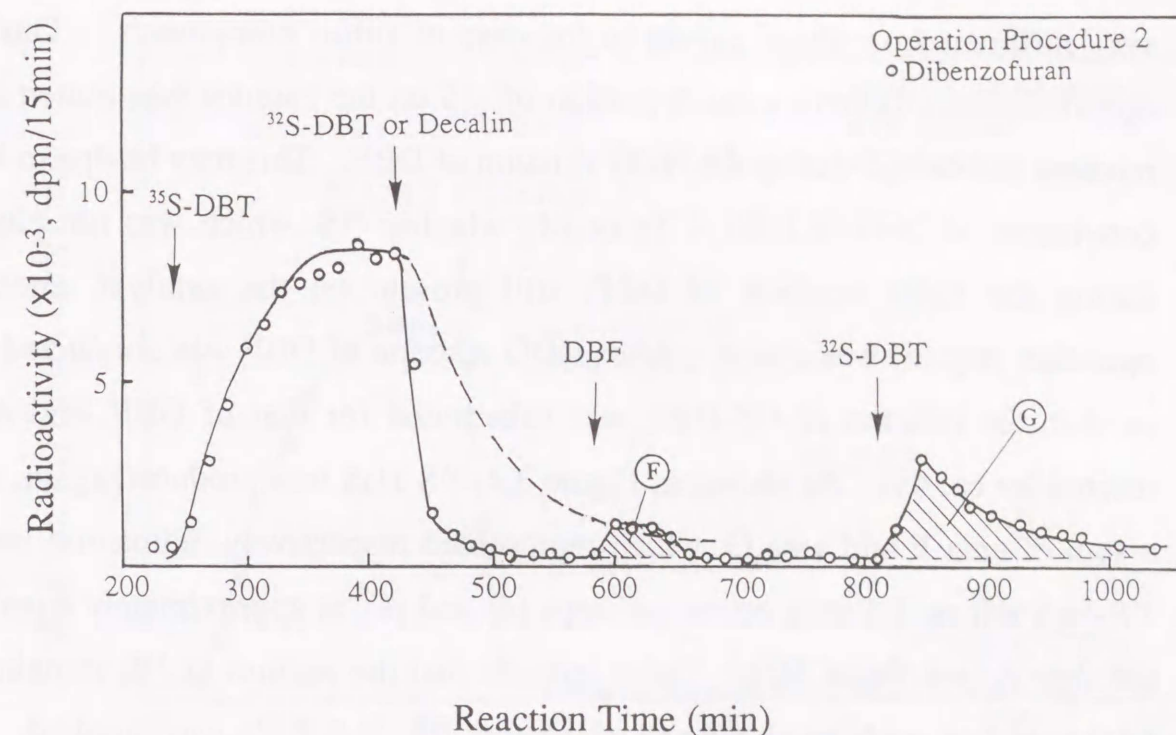


Figure 3.4. Change in radioactivities of formed  $^{35}\text{S}\text{-H}_2\text{S}$  with reaction time.  $\text{Mo}/\text{Al}_2\text{O}_3$ , 360 °C, 50 kg/cm<sup>2</sup>, DBF: 0.91 wt%.

Values of areas representing the amount of sulfur released during the various operation steps shown in Figures 3.1-3 are listed in Table 3.1. Since all areas were approximately the same, all  $^{35}\text{S}$  on the catalyst which was incorporated into the catalyst in operation step (b), was almost replaced by  $^{32}\text{S}$  during the operation step (d), although the replacement rates of sulfur were different from each other.

### 3.3.2 Effect of Oxygen Compound

Figure 3.4 shows the changes in radioactivities of formed  $^{35}\text{S}\text{-H}_2\text{S}$  when a solution of dibenzofuran (DBF) was used in the operation step (d) of operation procedure 2. As reported by Lavopa et al. (20), the major products were BP and CHB. It can be observed that the formation curve of  $^{35}\text{S}\text{-H}_2\text{S}$  is



very different from those curves in the case of sulfur compounds. During operation step (d), only a small portion of  $^{35}\text{S}$  on the catalyst was eluted and released as  $^{35}\text{S}-\text{H}_2\text{S}$  during the HDO reaction of DBF. This may be due to low conversion of DBF (7.3 %). To certify whether  $^{35}\text{S}$ , which was not eluted during the HDO reaction of DBF, still present on the catalyst, another operation step (e) was added. After HDO reaction of DBF was conducted for ca. 4 h, the solution of  $^{32}\text{S}-\text{DBT}$  was substituted for that of DBF, and then reacted for ca. 4 h. As shown in Figure 3.4,  $^{35}\text{S}-\text{H}_2\text{S}$  was produced again, and a sum of area F and area G, which represented respectively radioactivities of  $^{35}\text{S}-\text{H}_2\text{S}$  released during operation steps (d) and (e), is approximately equal to the area A (see Table 3.1). These indicate that the portion of  $^{35}\text{S}$  remaining on the catalyst could be eluted and released as  $^{35}\text{S}-\text{H}_2\text{S}$  if  $^{32}\text{S}$  was supplied.

### 3.3.3 Effect of Nitrogen Compounds

When a decalin solution of a nonbasic nitrogen-containing compound (carbazole) was used in operation step (d) of operation procedure 2, it can be observed that  $^{35}\text{S}-\text{H}_2\text{S}$  was scarcely detected during the operation step (d) (see Figure 3.5). This is because the conversion of carbazole is nearly zero. As reported by Behinds (18), when a decalin solution of quinoline was used in operation steps (d) of operation procedure 2, quinoline was hydrogenated rapidly to produce 1, 2, 3, 4 - tetrahydroquinoline and 5, 6, 7, 8-tetrahydroquinoline but HDN of quinoline to give hydrocarbons occurred hardly (see Table 3.2). At the same time, radioactivities of  $^{35}\text{S}-\text{H}_2\text{S}$  could hardly be detected (see Figure 3.5). After HDN reaction of quinoline was conducted for ca. 4 h, the operation steps (e) was also added, namely, the solution of  $^{32}\text{S}-\text{DBT}$  was substituted for that of quinoline, and reacted for ca. 4 h. Although  $^{35}\text{S}-\text{H}_2\text{S}$  was produced again as shown in Figure 3.5, the total radioactivities of released  $^{35}\text{S}-\text{H}_2\text{S}$  (area H in Figure 3.5) were smaller than total radioactivities

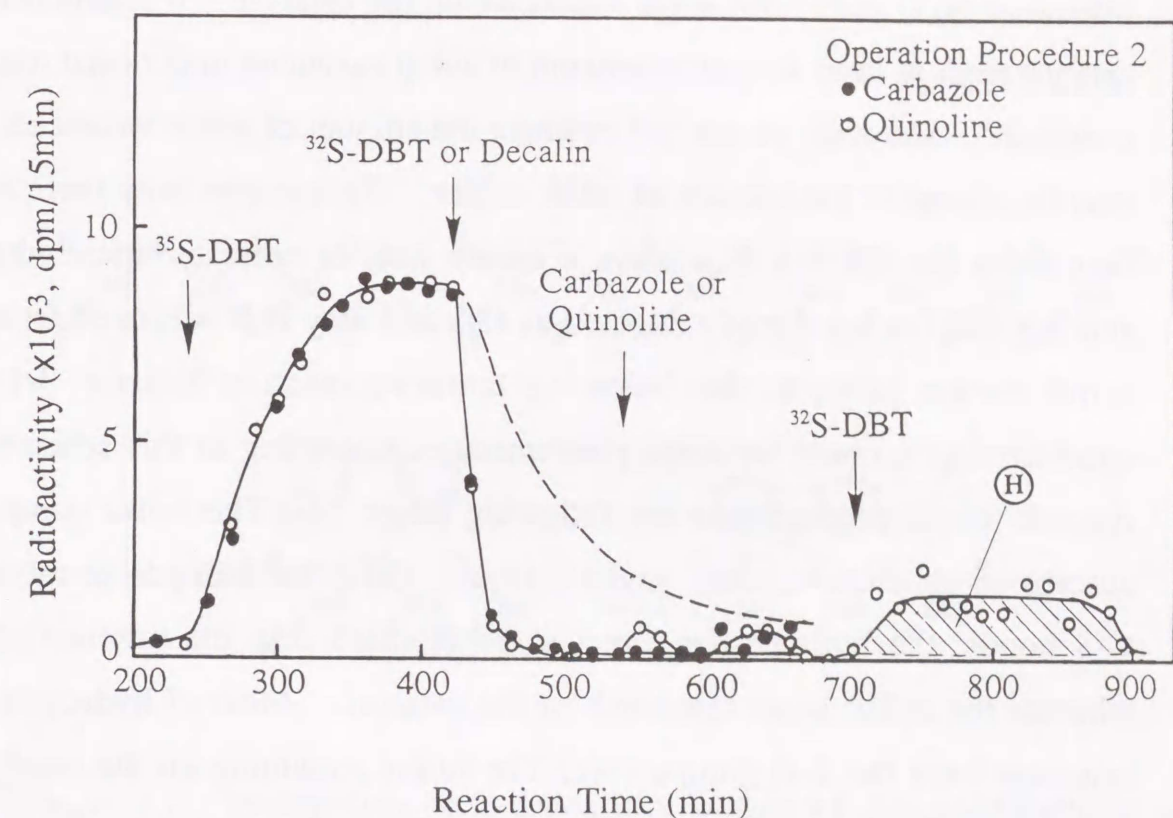


Figure 3.5. Change in radioactivities of formed  $^{35}\text{S}-\text{H}_2\text{S}$  with reaction time.  $\text{Mo}/\text{Al}_2\text{O}_3$ ,  $360^\circ\text{C}$ ,  $50\text{ kg}/\text{cm}^2$ , CBL: 0.91 wt%, QNL: 0.70 wt%.

of  $^{35}\text{S}$  remained on the catalyst (area A, see Table 3.1). This may be due to a fact that the catalyst was poisoned by quinoline since the reactivity of DBT HDS decreased from 59.3 % to 33.3 %. This makes it possible for a portion of  $^{35}\text{S}$  to be still held on the catalyst because the amount of labile sulfur on the catalyst decreased with decrease in the HDS rate (15).

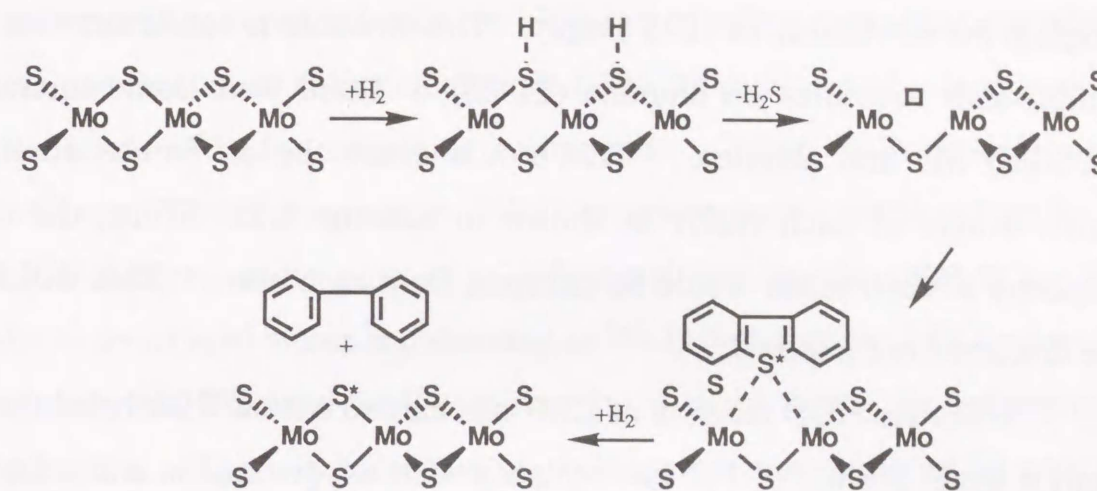
### 3.4 Discussion

As shown in Figure 3.1,  $\text{H}_2\text{S}$  was not formed in the absence of DBT while the incorporation of sulfur in DBT onto catalyst generated  $\text{H}_2\text{S}$ . The

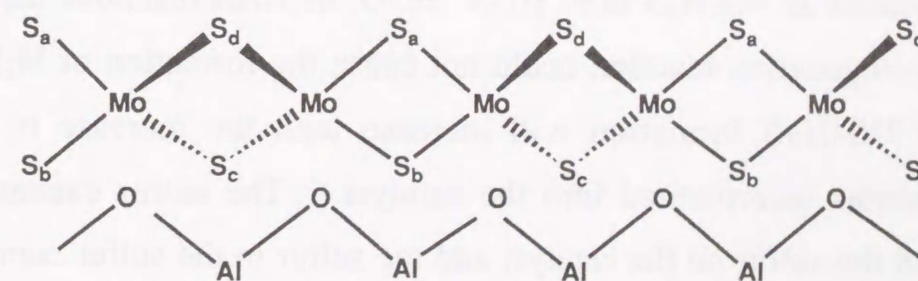


release of  $H_2S$  could form anion vacancies on the catalyst. It seems that the catalyst tends to keep a constant amount of anion vacancies under each reaction condition. Although we can not estimate the amount of anion vacancies, this may be related to the amount of labile sulfur. To interpret why there is the time delay for  $^{35}S-H_2S$  to achieve a steady state of radioactivities, why the sulfur in DBT is not directly released as  $H_2S$  and why  $H_2S$  is formed from the sulfur on the catalyst, the following tentative reaction Scheme 3.1 was considered to account for these phenomena. According to this scheme, the reaction would proceed with the following steps: (a) The sulfur compound adsorbs on an anion vacancy on the catalyst. (b) After the hydrogenolysis of C-S bonds, the hydrocarbon species are released into the gaseous phase, whereas the sulfur atom remained on the catalyst. (c) Most of hydrogen may originate from the S-H groups. (d) The sulfur remaining on the catalyst is hydrogenated and forms a new S-H group. (e) At the same time, the release of hydrogen sulfide generates a new anion vacancy. Therefore, a shift of active sites on the catalyst surface would occur.

For this mechanism of HDS, only after the sulfur in DBT was incorporated into the catalyst was the sulfur on the catalyst surface released as  $H_2S$ . When an anion vacancy was occupied by sulfur removed from DBT, a new anion vacancy appeared on the catalyst surface. At that time, a probability of sulfur being released as  $H_2S$  for all labile sulfur may be the same. Therefore, after  $^{32}S$ -DBT was substituted for  $^{35}S$ -DBT in operation procedure 1 (see Figure 3.1), the decreasing curve of formed  $^{35}S-H_2S$  can be revealed as an exponential function of time. In contrast to this, after the solution of  $^{35}S$ -DBT was substituted for that of  $^{32}S$ -DBT, the increasing curve of formed  $^{35}S-H_2S$  can be revealed as logarithmic function for time. According to this mechanism, the product of HDS-biphenyl would eluted immediately in the same manner as DBT. It was consistent with the results in *Chapter 2*.



Scheme 3.1. Mechanism of hydrodesulfurization of dibenzothiophene on sulfided  $Mo/Al_2O_3$ .  $S^*$ :  $^{35}S$ ,  $\square$ : Anion vacancy.



Scheme 3.2. Tetrahedral structure of  $MoS_2$  phase on alumina.  
Mobile capacity of sulfur:  $S_a > S_c (S_d) > S_b$ .



In *Chapter 2*, we found that the amount of labile sulfur on the sulfided catalyst changes depending on the reaction conditions. In the present paper, the structure of the active species shown in Scheme 3.2 was used in order to explain the mechanism of HDS simply. This structure is consistent with MoS<sub>2</sub> single-slab structures on alumina (21-23). There were some interactions between Mo and alumina. This would cause the difference among the environment of each sulfur as shown in Scheme 3.2. Thus, the mobile capacity of each sulfur would be different from each other. This will further be discussed in *Chapter 4*.

When the HDO reaction of DBF was carried out on <sup>35</sup>S-labeled catalyst, only a small portion of <sup>35</sup>S was replaced with oxygen atoms and released as <sup>35</sup>S-H<sub>2</sub>S (see Figure 3.4) because of the low conversion of HDO of DBF. In addition, for the case of HDN of quinoline, although the hydrogenation rate of quinoline was very quick, the HDN reaction of quinoline hardly occurred (see Table 3.2). Thus, <sup>35</sup>S was scarcely replaced by nitrogen compounds (see Figure 3.5). On the contrary, for the HDS reaction of sulfur compounds such as thiophene which can be desulfurized more easily than DBT, <sup>35</sup>S remaining on the catalyst was replaced at a more rapid rate than that in the case of DBT. These results indicated that <sup>35</sup>S remaining on the catalyst could not be removed and released as <sup>35</sup>S-H<sub>2</sub>S until HDN, HDO, or HDS reactions has proceeded. The hydrogenation reaction could not cause the formation of H<sub>2</sub>S. And the rate of <sup>35</sup>S-H<sub>2</sub>S formation will increase with the increase in the rate of heteroatoms incorporated into the catalyst. The sulfur exchange reaction between the sulfur on the catalyst and the sulfur in the sulfur compounds may not be a rate-determining step for HDS reaction but a fast reaction. This is consistent with the result that the formation rate of H<sub>2</sub>S from the catalyst depended only upon the rate of sulfur incorporation into the catalyst and the kind of sulfur compound was irrelevant.

### 3.5 Conclusions

In this chapter, the conclusions were obtained: The removal rate of <sup>35</sup>S from the catalyst depended upon the HDS rate of sulfur-containing compounds, that is, the amount of sulfur incorporated into the catalyst and was independent of the kinds of sulfur-containing compounds. When hydrodenitrogenation (HDN) and hydrodeoxygenation (HDO) reactions were carried out on the <sup>35</sup>S-labeled catalyst, some portion of <sup>35</sup>S remaining on the catalyst could be replaced by oxygen atoms and released as <sup>35</sup>S-H<sub>2</sub>S during the HDO reaction, in contrast to this, <sup>35</sup>S were hardly replaced by N atoms during the hydrogenation of quinoline. These indicate that the hydrogenation reaction could not cause the formation of H<sub>2</sub>S from the labile sulfur. Only when hydrogenolysis reaction proceeded, the labile sulfur was substituted to heteroatoms and released as H<sub>2</sub>S.



## Reference

1. Lipsch, J. G., and Schuit, G. C. A., *J. Catal.*, **15**, 179 (1969).
2. Schuit, G. C. A., and Gates, B. C. *AIChE J.*, **19**, 3, 417 (1973).
3. Massoth, F. E., in "Advances in Catalysis" (Eley, D. D., Pines, H., and Weisz, P. B., Eds.), Academic Press, N. Y., **27**, p. 265 (1978).
4. Delmon, B., "Proceedings, Climax 3rd International Conference on Chemistry and Uses of Molybdenum" (Barry, H. F., and Mitchell, P. C. H., Eds.), Climax Molybdenum Co., Ann Arbor, Michigan, p. 73 (1979).
5. Voorhoeve, R. J. H., and Stuiver, J. C. M., *J. Catal.*, **23**, 228 (1971).
6. Farragher, A. L., and Cossee, P., in "Proceedings, 5th International Congress on Catalysis", Palm Beach, 1972 (Hightower, J. W., Eds.), North-Holland, Amsterdam, p. 1301 (1973).
7. Ratnasamy, P., and Sivasanker, S., *Catal. Rev. Sci. Eng.*, **22**, 401 (1980).
8. Topsøe, H., Clausen, B. S., Candia, R., Wivel, C., and Mørup, S., *J. Catal.*, **68**, 433 (1981).
9. Gachet, C. G., Dhainaut, E., de Mourgues, L., Candy, J. P., and Fouillous, P., *Bull. Soc. Chim. Belg.*, **90**, 1279 (1981).
10. Campbell, K. C., Mirza, M. L., Thomson, S. J., and Webb, G., *J. Chem. Soc. Faraday Trans. I*, **80**, 1689 (1984).
11. Dobrovolszky, M., Tetenyi, P., and Paal, Z., *Chem. Eng. Commun.*, **83**, 1 (1989).
12. Dobrovolszky, M., Paal, Z., and Tetenyi, P., *Catal. Today*, **9**, 113 (1991).
13. Isagulyants, G. V., Greish, A. A., and Kogan, V. M., "Proc. 9th International Congress on Catalysis", (Phillips, M. J., and Ternay, M., Eds.), Calgary, **1**, 35 (1988).
14. Gellman, A. J., Bussell, M. E., and Somorjai, G. A. *J. Catal.*, **107**, 103 (1987).
15. Kabe, T., Qian, W., Ishihara, A., and Ogawa, S., *J. Phy. Chem.*, **98**, 907 (1994).
16. Ishihara, A., Itoh, T., Hino, T., Qi, P., and Kabe, T., *J. Catal.*, **140**, 184 (1993).
17. Girgis, M. J., and Gates, B. C., *Ind. Eng. Chem. Res.*, **30**, 2021 (1991).
18. Behinde, M. V., *Ph. D. Dissertation*, University of Delaware, Newark, 1979.
19. Gilmon, H., and Jacoby, A. L., *J. Org. Chem.*, **4**, 108 (1939).
20. Lavopa, V., and Scatterfield, C. N., *Energy & Fuels*, **1**, 323 (1987).
21. Topsøe, N.-Y., *J. Catal.*, **64**, 235 (1980).
22. Grimblot, J. G., Dufresne, P., Gengembre, L., and Bonelle, J. P., *Bull. Soc. Chim. Belg.*, **90**, 1261 (1981).
23. Pollack, S. S., Sanders, J. V., and Tischer, R. E., *Appl. Catal.*, **8**, 383 (1983).



Faint, illegible text visible through the paper from the reverse side of the page.

**Chapter Four**

**Hydrodesulfurization of Radioactive  $^{35}\text{S}$ -Labeled  
Dibenzothiophene on Co-Mo/ $\text{Al}_2\text{O}_3$ , Ni-Mo/ $\text{Al}_2\text{O}_3$ ,  
Co/ $\text{Al}_2\text{O}_3$ , and Ni/ $\text{Al}_2\text{O}_3$**



Chapter Four  
**Hydrodesulfurization of Radioactive  $^{35}\text{S}$ -Labeled  
Dibenzothiophene on Co-Mo/ $\text{Al}_2\text{O}_3$ , Ni-Mo/ $\text{Al}_2\text{O}_3$ ,  
Co/ $\text{Al}_2\text{O}_3$ , and Ni/ $\text{Al}_2\text{O}_3$**

**Abstract**

The radioisotope tracer method has been used to get quantitatively new insight into the behavior of sulfur on the sulfided Co-Mo/ $\text{Al}_2\text{O}_3$ , Ni-Mo/ $\text{Al}_2\text{O}_3$ , Co/ $\text{Al}_2\text{O}_3$ , and Ni-Mo/ $\text{Al}_2\text{O}_3$ . The apparent activation energies of HDS reaction for DBT for all catalysts were  $20 \pm 1$  kcal/mol. The formation rate constants of  $^{35}\text{S}$ - $\text{H}_2\text{S}$  were determined and the amounts of labile sulfur on the sulfided catalysts were estimated by tracing the changes in radioactivities of the unreacted  $^{35}\text{S}$ -DBT and the formed  $^{35}\text{S}$ - $\text{H}_2\text{S}$  during the HDS reaction of  $^{35}\text{S}$ -labeled dibenzothiophene ( $^{35}\text{S}$ -DBT). It was deduced that the maximum value of labile sulfur related to HDS reaction was ca. 75% of total sulfur in the sulfided Mo/ $\text{Al}_2\text{O}_3$ . Compared with the amounts of labile sulfur in the sulfided Co-Mo/ $\text{Al}_2\text{O}_3$ , Mo/ $\text{Al}_2\text{O}_3$  and Co/ $\text{Al}_2\text{O}_3$ , it was determined that the amounts of labile sulfur were 19.9, 9.1 and 2.0 mg of sulfur/g of catalyst at  $260^\circ\text{C}$  for three catalysts, respectively. Thus, it was suggested that the sulfur in the form of  $\text{Co}_9\text{S}_8$  on the sulfided Co-Mo/ $\text{Al}_2\text{O}_3$  was nonlabile and that the sulfur attached to both Mo and Co atom was more labile and related to HDS reaction. The similar result was also obtained for Ni-Mo/ $\text{Al}_2\text{O}_3$  and Ni/ $\text{Al}_2\text{O}_3$ . Therefore, the promotion of Co and Ni for Mo-based catalyst were attributed to that they made the sulfur bonded to both Mo and Co or Ni in  $\text{MoS}_2$  phase more labile.



## 4.1 Introduction

Mo-based catalysts used in HDS of petroleum feedstocks and recently in the deep HDS catalysts of light oil have yet been extensively studied (1-4). However, the catalysts' structures have been ambiguous. Recent studies showed that the sulfides in sulfided Mo-based catalysts were present in the form of MoS<sub>2</sub>-like phase (5, 6) and that CoMoS and NiMoS-like phase existed in sulfided Co or Ni-Mo/Al<sub>2</sub>O<sub>3</sub> (7, 8). Moreover extensive studies on the sulfided Mo-based catalysts have indicate that the HDS activity is related to the presence of sulfur vacancies on the MoS<sub>2</sub> structure (9-11). The addition of Co or Ni leads to a large increase in the activity that can be attributed to the promoter decorating the edges of MoS<sub>2</sub> with so-called CoMoS or NiMoS type structures (12, 13). However, there is another fact indicating that the formation of a special association between Mo and promoters is not the only reason for synergy. Delmon and co-worker (14-17) have shown that catalysts containing little or no CoMoS or NiMoS phase were quite active and sometimes had a more stable activity. To reconcile different results concerning the surface structure of the Mo-based catalysts and the mechanism of HDS, to use <sup>35</sup>S-radioisotope as a tracer provided a clue to this exploration because the sulfur played the most important role in the HDS reaction (18).

On the other hand, dibenzothiophenes are sulfur-containing compounds very difficult to desulfurize even under deep HDS conditions (4). In *Chapter 2*, we discussed that HDS reaction of <sup>35</sup>S-labeled dibenzothiophene (<sup>35</sup>S-DBT) on sulfided Mo/Al<sub>2</sub>O<sub>3</sub>. It was found that the sulfur on the catalyst during HDS reaction was labile and the amount of labile sulfur increased with temperature and the initial concentration of dibenzothiophene and that the sulfur in dibenzothiophene was not directly released as H<sub>2</sub>S but initially accommodated on the catalyst (19, 20). In this chapter, we would discuss the

behavior of sulfur in commercial Co- and Ni-Mo/Al<sub>2</sub>O<sub>3</sub> catalysts. We have conducted HDS reaction of <sup>35</sup>S-labeled dibenzothiophene on sulfided Co-Mo/Al<sub>2</sub>O<sub>3</sub> and Ni-Mo/Al<sub>2</sub>O<sub>3</sub> catalysts under practical conditions of HDS. To elucidate the role of labile sulfur in the HDS reaction and the promotion effect of Co and Ni in sulfided Co- and Ni-Mo/Al<sub>2</sub>O<sub>3</sub>, Mo/Al<sub>2</sub>O<sub>3</sub>, Co/Al<sub>2</sub>O<sub>3</sub>, and Ni/Al<sub>2</sub>O<sub>3</sub> were also used as compared catalysts. The mobile capacity of sulfur on the catalyst was estimated from the formation rates of <sup>35</sup>S-H<sub>2</sub>S in an increase and a decrease in radioactivity. We expected to understand more exactly how the promoter Co or Ni enhanced the reactivity of Mo/Al<sub>2</sub>O<sub>3</sub> and how sulfur in the sulfided catalyst participated in the actual HDS reaction.

## 4.2 Experimental

### 4.2.1 Materials.

<sup>32</sup>S-DBT and <sup>35</sup>S labeled dibenzothiophene were synthesized according to the method reported in *Chapter 2*. Decalin was a commercial GR grade. Commercial Co-Mo/Al<sub>2</sub>O<sub>3</sub> (Ketjen fine 124, MoO<sub>3</sub>: 12.3 wt%, CoO: 3.8 wt%, Surface Area: 274 m<sup>2</sup>/g) and Ni-Mo/Al<sub>2</sub>O<sub>3</sub> (Ketjen fine 153, MoO<sub>3</sub>: 15.3 wt%, NiO: 2.9 wt%, Surface Area: 197 m<sup>2</sup>/g) were used in this work. Mo/Al<sub>2</sub>O<sub>3</sub> (MoO<sub>3</sub> 16.0 wt%), Co/Al<sub>2</sub>O<sub>3</sub> (CoO 4.0 wt%), and Ni/Al<sub>2</sub>O<sub>3</sub> (NiO 3.0 wt%) were prepared by the conventional impregnation technique using aqueous solution of ammonium molybdenate ((NH<sub>4</sub>)<sub>6</sub>Mo<sub>7</sub>O<sub>24</sub>·4H<sub>2</sub>O), cobalt nitrate (Co(NO<sub>3</sub>)<sub>2</sub>·6H<sub>2</sub>O), and nickel nitrate (Ni(NO<sub>3</sub>)<sub>2</sub>·6H<sub>2</sub>O), respectively. After the impregnation, the samples were dried at 120°C for 10 h and calcined at 450°C for 24 h in air.

### 4.2.2 Apparatus and Procedure

The detail of a used apparatus was described in *Chapter 2*. The HDS reaction was carried out with a pressurized flow reactor, and the typical



reaction conditions were as follows: catalyst 1 g (20-35 mesh), total pressures 25-50 kg/cm<sup>2</sup>, reaction temperature 210-400 °C, flow rate of hydrogen 25 liters/h, WHSV 28-56 h<sup>-1</sup>, concentration of DBT in decalin 1.0-3.0 wt%. The catalysts were presulfided with a mixture of 5.0 vol% H<sub>2</sub>S in H<sub>2</sub> at 400 °C for 3 h before the reaction. The reactor was cooled in the H<sub>2</sub>S/H<sub>2</sub> stream to reaction temperature and pressurized with hydrogen. Then the solution containing DBT was fed into the reactor by a liquid pump. H<sub>2</sub>S produced during the reaction was absorbed by bubbling through a commercial basic scintillator solution (Carbosorb). The compositions of liquid product were analyzed by a gas chromatography. Radioactivities of the unreacted <sup>35</sup>S-DBT in liquid product and the formed <sup>35</sup>S-H<sub>2</sub>S in the absorbed solution were measured by a liquid scintillation counter.

Typical operation procedure was same as the case of Mo/Al<sub>2</sub>O<sub>3</sub> in *Chapter 2*: (a) A decalin solution of 1 wt% <sup>32</sup>S-DBT was pumped into the reactor until the conversion of DBT became constant (about 3 h). (b) After that, decalin solution of 1 wt% <sup>35</sup>S-DBT was substituted for that of <sup>32</sup>S-DBT. The reaction with <sup>35</sup>S-DBT was performed until the formation amount of <sup>35</sup>S-H<sub>2</sub>S became constant (about 4 h). (c) Then, the reactant solution was returned again to the decalin solution of 1 wt% <sup>32</sup>S-DBT and reacted for 4-5 h.

### 4.3 Results

#### 4.3.1 Co-Mo/Al<sub>2</sub>O<sub>3</sub>

A solution of 1 wt% <sup>35</sup>S-DBT was reacted on sulfided Co-Mo/Al<sub>2</sub>O<sub>3</sub> at 250 °C and 50 kg/cm<sup>2</sup>. The changes in radioactivities of the unreacted <sup>35</sup>S-DBT and the produced <sup>35</sup>S-H<sub>2</sub>S with the reaction time are shown in Figure 4.1. After <sup>35</sup>S-DBT was substituted for <sup>32</sup>S-DBT, the radioactivities of the unreacted <sup>35</sup>S-DBT in the liquid product increased and approached a steady

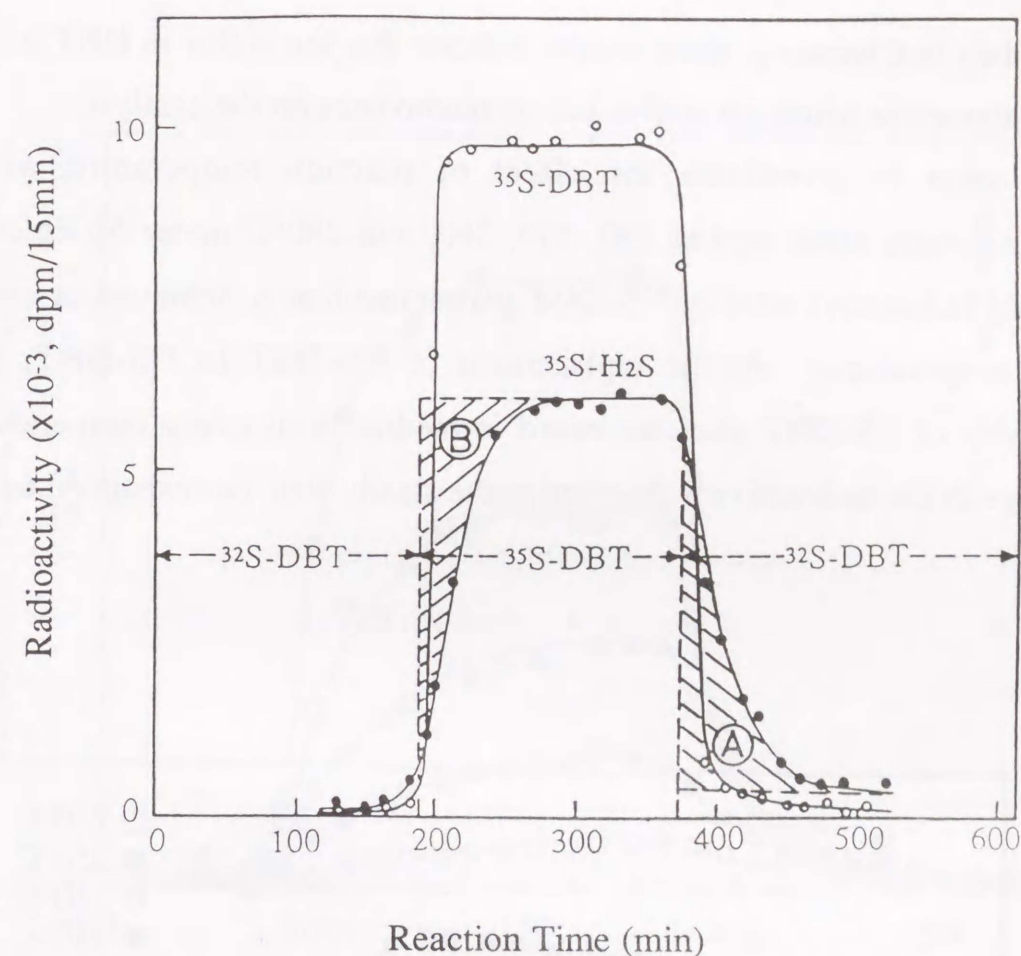


Figure 4.1. Changes in radioactivities of unreacted <sup>35</sup>S-DBT and formed <sup>35</sup>S-H<sub>2</sub>S with reaction time. Co-Mo/Al<sub>2</sub>O<sub>3</sub>, 250 °C, 50 kg/cm<sup>2</sup>,  
○: Unreacted <sup>35</sup>S-DBT; ●: Formed <sup>35</sup>S-H<sub>2</sub>S.

state immediately. Similar to the case of Mo/Al<sub>2</sub>O<sub>3</sub> (MoO<sub>3</sub> 12.5 %) described in *Chapter 2*, in the case of the produced <sup>35</sup>S-H<sub>2</sub>S, however, about 145 min was needed to approach the steady state in released radioactivities. When the solution of <sup>35</sup>S-DBT returned to that of <sup>32</sup>S-DBT at 370 min, the radioactivities of the unreacted <sup>35</sup>S-DBT also decreased immediately from the steady state to the normal state. However, the time delay for the produced <sup>35</sup>S-H<sub>2</sub>S from its steady state to the normal state still was ca. 100 min as shown in Figure 4.1.



As described in *Chapter 2*, these results indicate that the sulfur in DBT is not directly released as hydrogen sulfide but accommodates on the catalyst.

In order to investigate the effect of reaction temperature, same experiments were conducted at 230, 250, 260, and 280°C under 50 kg/cm<sup>2</sup>. The steady radioactive state of <sup>35</sup>S-DBT was immediately achieved at every reaction temperature. At the replacement of <sup>35</sup>S-DBT to <sup>32</sup>S-DBT, the radioactivity of <sup>35</sup>S-DBT also decreased immediately at every temperature. The change in the radioactivity observed at the steady state corresponded to the

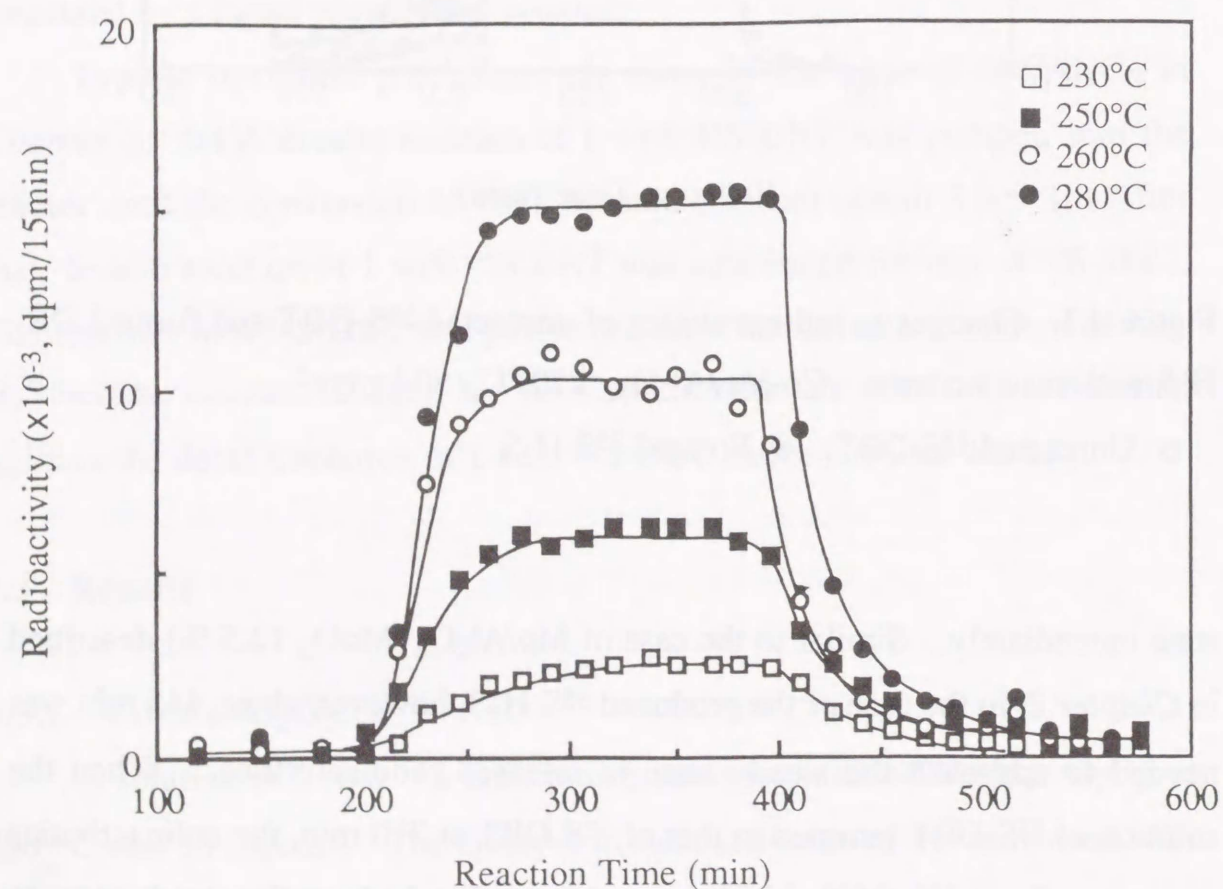


Figure 4.2. Changes in radioactivities of formed <sup>35</sup>S-H<sub>2</sub>S with reaction time at various temperatures. Co-Mo/Al<sub>2</sub>O<sub>3</sub>, 230-280 °C, 50 kg/cm<sup>2</sup>.

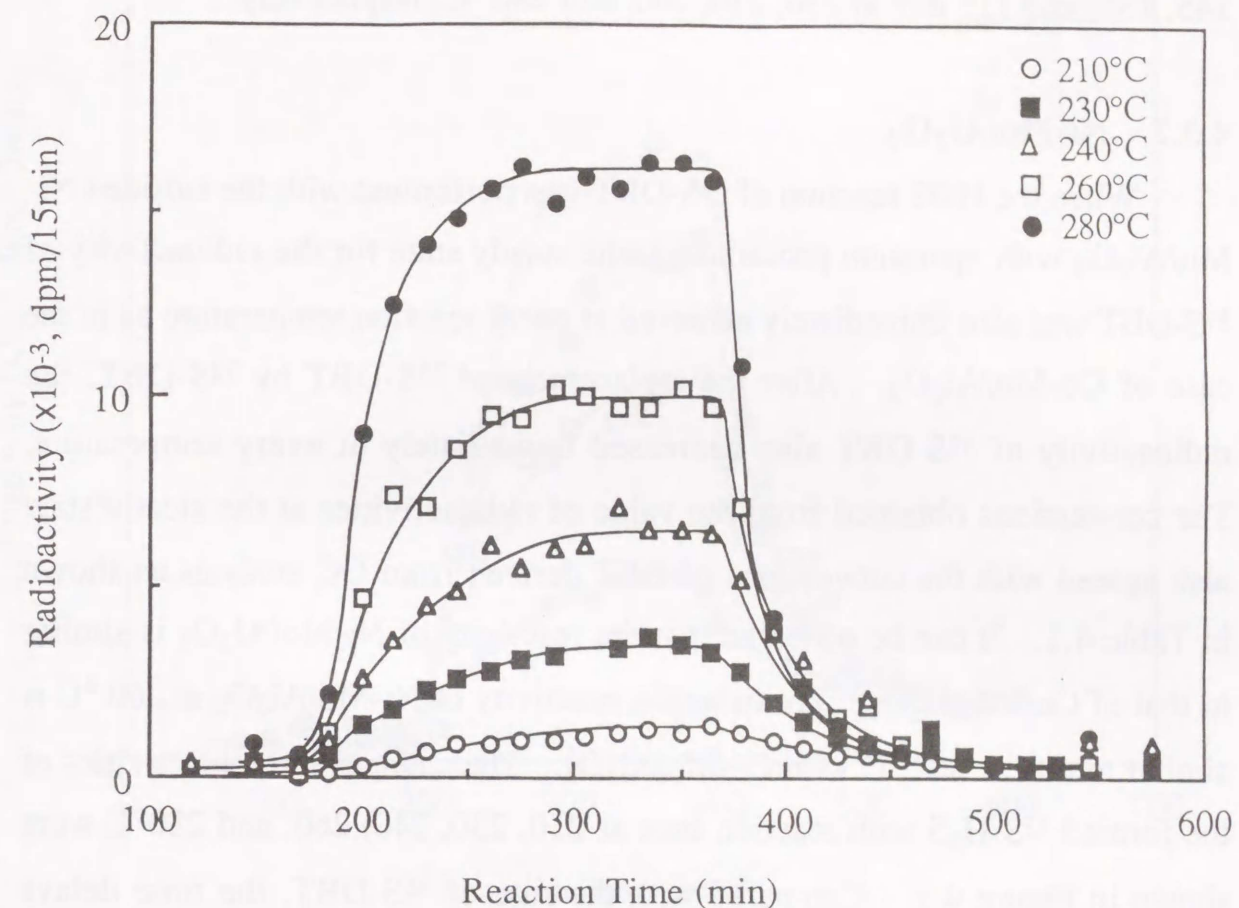


Figure 4.3. Changes in radioactivities of formed <sup>35</sup>S-H<sub>2</sub>S with reaction time at various temperatures. Ni-Mo/Al<sub>2</sub>O<sub>3</sub>, 210-280 °C, 50 kg/cm<sup>2</sup>.

change of a conversion of DBT. Moreover, the conversions derived from gas chromatography analysis agreed with that determined from the radioactivities of the unreacted <sup>35</sup>S-DBT in the liquid product (Table 4.1). Figure 4.2 shows the changes in radioactivity of the produced <sup>35</sup>S-H<sub>2</sub>S with reaction time at 230, 250, 260 and 280 °C. Contrary to the case of <sup>35</sup>S-DBT, the time delays for <sup>35</sup>S-H<sub>2</sub>S released to approach a steady state in radioactivities were significantly affected by the reaction temperature. The time delays observed for <sup>35</sup>S-H<sub>2</sub>S



became shorter with the increase in the reaction temperature. They were 160, 145, 130, and 115 min at 230, 250, 260, and 280 °C, respectively.

#### 4.3.2 Ni-Mo/Al<sub>2</sub>O<sub>3</sub>

When the HDS reaction of <sup>35</sup>S-DBT was performed with the sulfided Ni-Mo/Al<sub>2</sub>O<sub>3</sub> with operation procedure 1, the steady state for the radioactivity of <sup>35</sup>S-DBT was also immediately achieved at every reaction temperature as in the case of Co-Mo/Al<sub>2</sub>O<sub>3</sub>. After the replacement of <sup>35</sup>S-DBT by <sup>32</sup>S-DBT, the radioactivity of <sup>35</sup>S-DBT also decreased immediately at every temperature. The conversions obtained from the value of radioactivities at the steady state also agreed with the conversions of DBT derived from GC analysis as shown in Table 4.1. It can be observed that the reactivity of Ni-Mo/Al<sub>2</sub>O<sub>3</sub> is similar to that of Co-Mo/Al<sub>2</sub>O<sub>3</sub>. For example, reactivity of Ni-Mo/Al<sub>2</sub>O<sub>3</sub> at 260 °C is similar to that at 260 °C with Co-Mo/Al<sub>2</sub>O<sub>3</sub>. The changes in radioactivities of the formed <sup>35</sup>S-H<sub>2</sub>S with reaction time at 210, 230, 240, 260, and 280°C were shown in Figure 4.3. Compared with the case of <sup>35</sup>S-DBT, the time delays observed for <sup>35</sup>S-H<sub>2</sub>S were also significantly affected by the reaction temperature. As in the case of Co-Mo/Al<sub>2</sub>O<sub>3</sub>, the time delay for <sup>35</sup>S-H<sub>2</sub>S became longer with decreased reaction temperature.

#### 4.3.3 Mo/Al<sub>2</sub>O<sub>3</sub>.

When the HDS reaction of <sup>35</sup>S-DBT was performed with the sulfided Mo/Al<sub>2</sub>O<sub>3</sub> (MoO<sub>3</sub> 16%), the steady state for the radioactivity of <sup>35</sup>S-DBT was also immediately achieved at every reaction temperature as in the case of Co-Mo/Al<sub>2</sub>O<sub>3</sub>. After the replacement of <sup>35</sup>S-DBT by <sup>32</sup>S-DBT, the radioactivity of <sup>35</sup>S-DBT also decreased immediately at every temperature. The conversions obtained from the radioactivities at the steady state also agreed with the conversions of DBT derived from GC analysis as shown in Table 4.2.

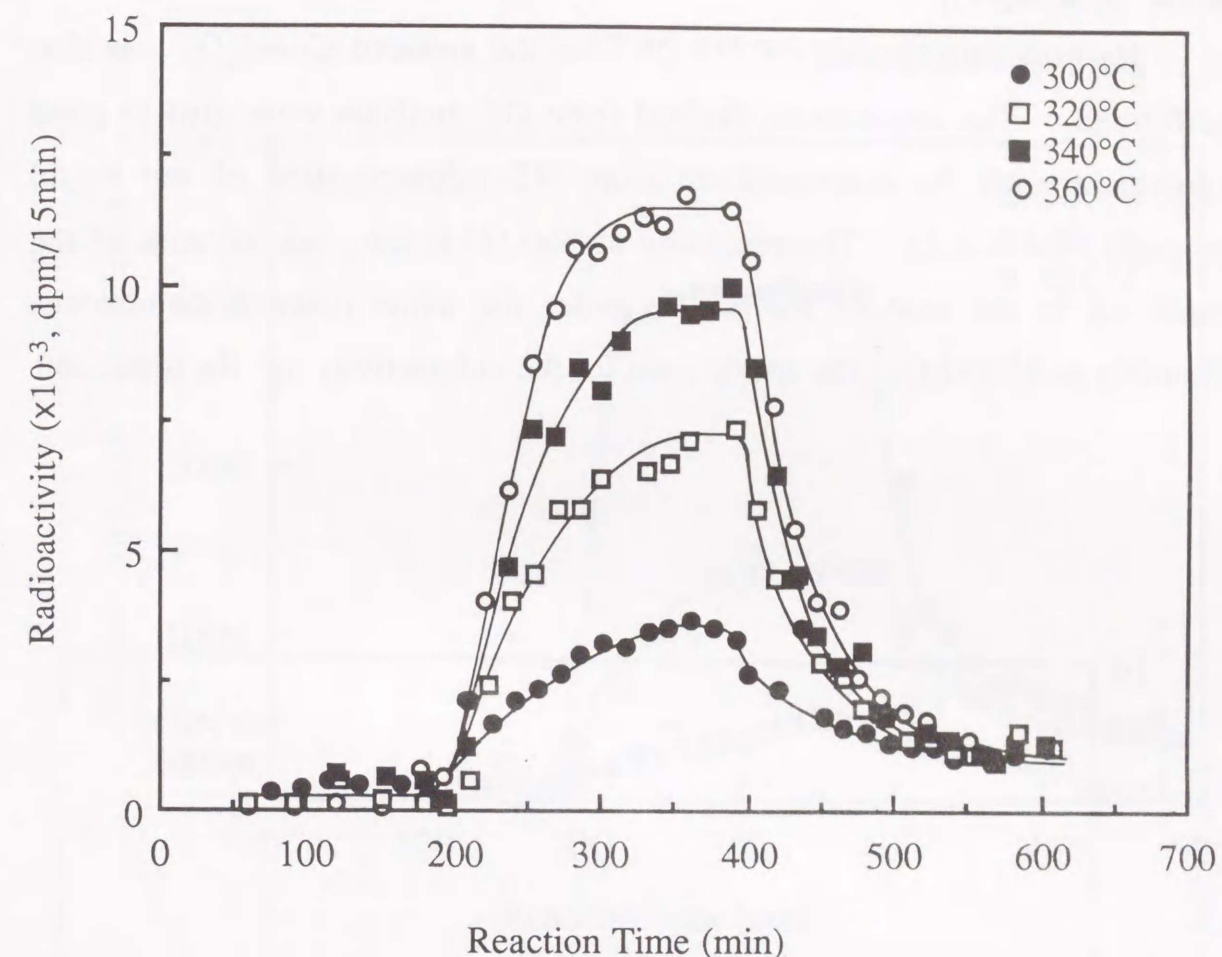


Figure 4.4. Changes in radioactivities of formed <sup>35</sup>S-H<sub>2</sub>S with reaction time at various temperatures. Mo/Al<sub>2</sub>O<sub>3</sub>, 300-360 °C, 50 kg/cm<sup>2</sup>.

It can be observed that the reactivity at 340 °C with Mo/Al<sub>2</sub>O<sub>3</sub> is similar to that with Co-Mo/Al<sub>2</sub>O<sub>3</sub> at 260°C. The changes in radioactivities of the formed <sup>35</sup>S-H<sub>2</sub>S with reaction time at 300, 320, 340, and 360 °C were shown in Figure 4.4. Compared with the case of <sup>35</sup>S-DBT, the time delays observed for <sup>35</sup>S-H<sub>2</sub>S were significantly affected by the reaction temperature. As in the case of Co-Mo/Al<sub>2</sub>O<sub>3</sub>, the time delay for <sup>35</sup>S-H<sub>2</sub>S became longer with decrease in reaction temperature.



#### 4.3.4 Co/Al<sub>2</sub>O<sub>3</sub>.

Hydrodesulfurization of <sup>35</sup>S-DBT on the sulfided Co/Al<sub>2</sub>O<sub>3</sub> was also performed. The conversions derived from GC analysis were also in good agreement with the determination from <sup>35</sup>S-radioactivities of the liquid products (Table 4.2). The reactivity at 360 °C is only one-seventh of the reactivity in the case of Mo/Al<sub>2</sub>O<sub>3</sub> under the same reaction conditions. Similarly to Mo/Al<sub>2</sub>O<sub>3</sub>, the steady state for the radioactivity of the unreacted

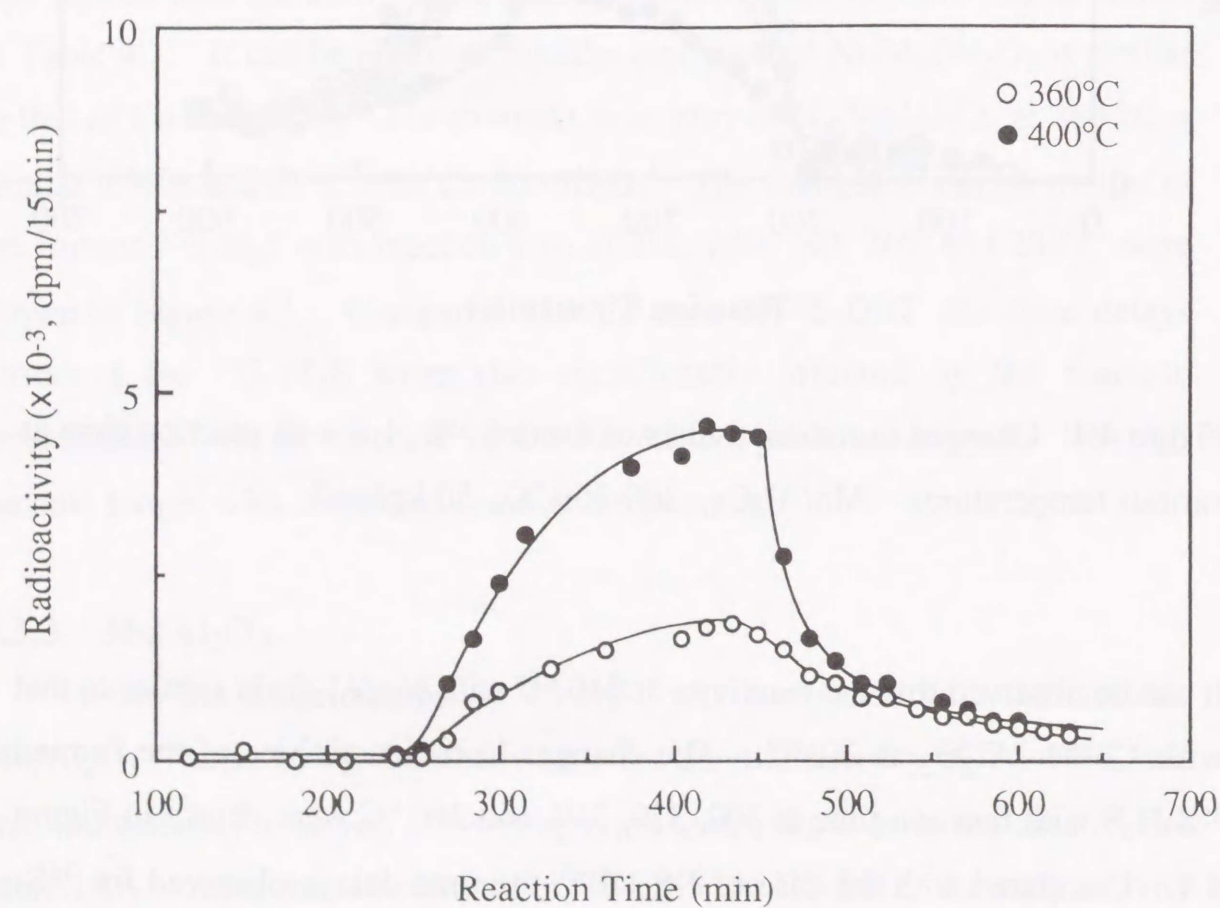


Figure 4.5. Changes in radioactivities of formed <sup>35</sup>S-H<sub>2</sub>S with reaction time at various temperatures. Co/Al<sub>2</sub>O<sub>3</sub>, 360, 400 °C, 50kg/cm<sup>2</sup>.

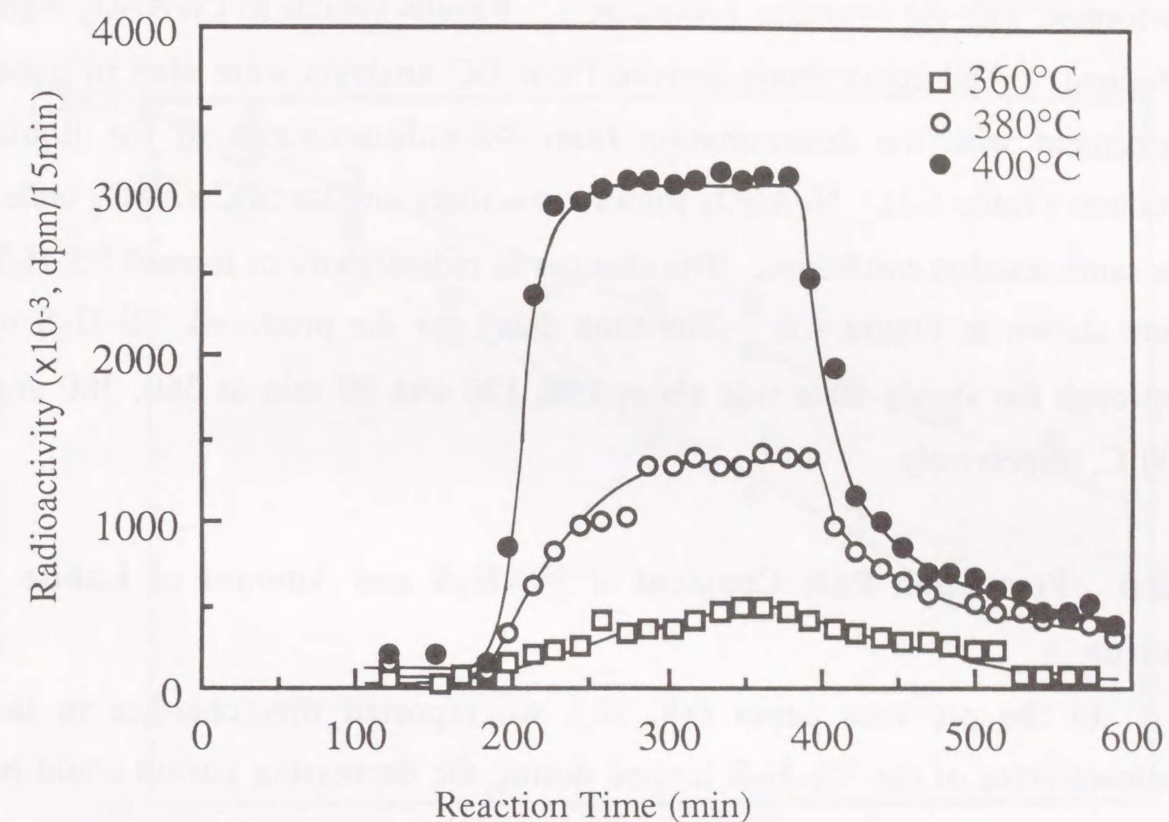


Figure 4.6. Changes in radioactivities of formed <sup>35</sup>S-H<sub>2</sub>S with reaction time at various temperatures. Ni/Al<sub>2</sub>O<sub>3</sub>, 360-400 °C, 50 kg/cm<sup>2</sup>.

<sup>35</sup>S-DBT was always immediately achieved at every temperature, while the time delay for the produced <sup>35</sup>S-H<sub>2</sub>S to approach the steady state was about 160, and 130 min at 360, and 400 °C, respectively (Figure 4.5). The time delay for Co/Al<sub>2</sub>O<sub>3</sub> at 360 °C (Figure 4.5) was longer than that (ca. 115 min) for Mo/Al<sub>2</sub>O<sub>3</sub> at 360 °C (Figure 4.4). This result indicates that the time delay for <sup>35</sup>S-H<sub>2</sub>S elution is not due to the adsorption/desorption of H<sub>2</sub>S on alumina support, but to the sulfur exchange between the sulfur in DBT and sulfur on the catalyst.



### 4.3.5 Ni/Al<sub>2</sub>O<sub>3</sub>

Hydrodesulfurization of <sup>35</sup>S-DBT on the sulfided Ni/Al<sub>2</sub>O<sub>3</sub> was also performed with the operation procedure 1. Results similar to Co/Al<sub>2</sub>O<sub>3</sub> were obtained. The conversions derived from GC analysis were also in good agreement with the determination from <sup>35</sup>S-radioactivities of the liquid products (Table 4.2). Ni/Al<sub>2</sub>O<sub>3</sub> shows a reactivity similar to Co/Al<sub>2</sub>O<sub>3</sub> under the same reaction conditions. The changes in radioactivity of formed <sup>35</sup>S-H<sub>2</sub>S were shown in Figure 4.6. The time delay for the produced <sup>35</sup>S-H<sub>2</sub>S to approach the steady state was about 150, 120 and 90 min at 360, 380 and 400°C, respectively.

### 4.3.6 Formation Rate Constant of <sup>35</sup>S-H<sub>2</sub>S and Amount of Labile Sulfur

In the previous paper (19, 20), we reported that changes in the radioactivities of the <sup>35</sup>S-H<sub>2</sub>S formed during the decreasing period could be expressed as an exponential function of reaction time. The formation rate of <sup>35</sup>S-H<sub>2</sub>S from the catalysts could be treated as a first order reaction. In this work, the first order plots of the formation rate of <sup>35</sup>S-H<sub>2</sub>S from the catalysts were also obtained for all reaction. As the examples, the first order plots of formation rate of <sup>35</sup>S-H<sub>2</sub>S at 260 °C for Co-Mo/Al<sub>2</sub>O<sub>3</sub>, at 260 °C for Ni-Mo/Al<sub>2</sub>O<sub>3</sub> and at 340 °C for Mo/Al<sub>2</sub>O<sub>3</sub> were shown in Figure 4.7. These lines can be revealed as a function of time:

$$\ln y = \ln z - kt \quad (4.1)$$

where  $y$  represents the formation rate of <sup>35</sup>S-H<sub>2</sub>S (dpm/min);  $z$  the formation rate of <sup>35</sup>S-H<sub>2</sub>S at steady state (dpm/min),  $k$  the rate constant of the release of <sup>35</sup>S-H<sub>2</sub>S (min<sup>-1</sup>),  $t$  reaction time (min). The release rate constants of <sup>35</sup>S-H<sub>2</sub>S for all catalysts were listed in Tables 1 and 2. Furthermore, the first order

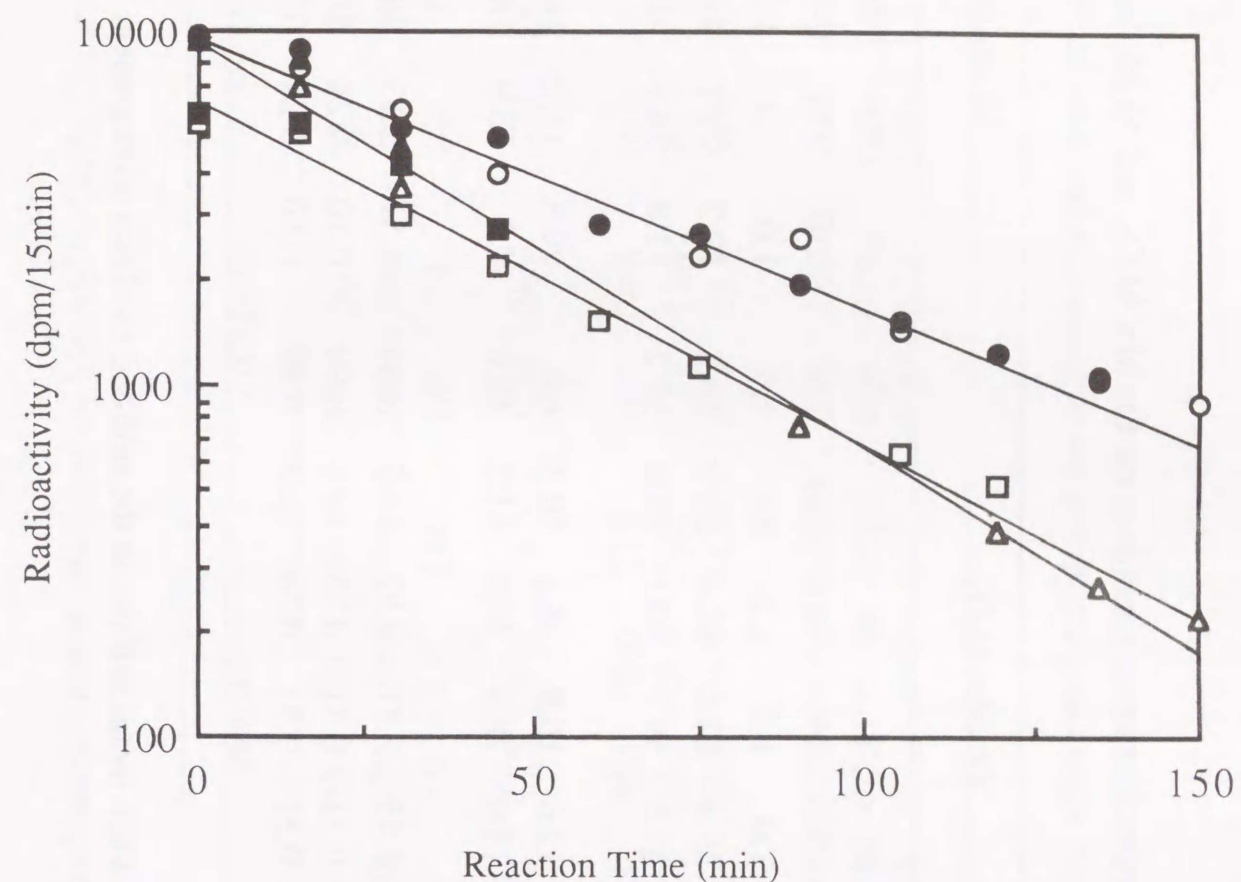


Figure 4.7. First order plots of release rate of <sup>35</sup>S-H<sub>2</sub>S. Mo/Al<sub>2</sub>O<sub>3</sub> (340°C, 50kg/cm<sup>2</sup>): ○ Decreasing period, ● Increasing period. Co-Mo/Al<sub>2</sub>O<sub>3</sub> (260 °C, 50 kg/cm<sup>2</sup>): □ Decreasing period, ■ Increasing period. Ni-Mo/Al<sub>2</sub>O<sub>3</sub> (260 °C, 50 kg/cm<sup>2</sup>): Δ Decreasing period, ▲ Increasing period.

plot of the values, where radioactivity of each increasing period of produced <sup>35</sup>S-H<sub>2</sub>S in Figure 4.1 was subtracted from that at steady state, also showed the linear relationship (Figure 4.7) and two slopes at this temperature were



Table 4.1. Kinetic parameters at various hydrodesulfurization conditions on Co-Mo/Al<sub>2</sub>O<sub>3</sub>, and Ni-Mo/Al<sub>2</sub>O<sub>3</sub>.

Catalyst	Co-Mo/Al <sub>2</sub> O <sub>3</sub>					Ni-Mo/Al <sub>2</sub> O <sub>3</sub>					
Reaction pressure, kg/cm <sup>2</sup>	50	50	50	50	50	10	50	50	50	50	
Reaction temperature, °C	230	250	260	280	280	280	210	230	240	260	280
Concentration of DBT, wt%	1.0	1.0	1.0	1.0	3.0	1.0	1.0	1.0	1.0	1.0	1.0
Conversion from GC analysis, %	23.4	39.4	62.6	92.4	53.9	59.8	12.7	29.1	43.3	64.5	99.5
Conversion from radioactivity of <sup>35</sup> S, %	23.7	37.8	59.7	90.1	53.0	57.2	11.8	28.9	42.1	63.0	97.1
Labile sulfur, S <sub>0</sub> , mg/g.cat.	5.8	12.6	19.9	26.1	30.3	6.6	29.5	11.2	14.7	16.2	18.4
S <sub>0</sub> /S <sub>Total</sub> <sup>a</sup> , %	8.27	18.0	28.4	37.2	43.2	42.0	8.2	13.9	18.2	20.1	22.8
Rate constant of formed H <sub>2</sub> S, k, x10 <sup>-2</sup> , min <sup>-1</sup>	2.26	2.45	2.71	2.92	4.65	3.34	1.57	2.13	2.40	3.26	4.40
S <sub>0</sub> x k, mg/min.g.cat.	0.13	0.31	0.51	0.76	1.41	0.99	0.10	0.24	0.35	0.52	0.81
Rate of DBT HDS, mg/min.g.cat.	0.19	0.32	0.51	0.76	1.32	0.98	0.10	0.24	0.35	0.53	0.81

<sup>a</sup> S<sub>Total</sub> is defined as the amount of total sulfur when metal sulfides in the sulfided catalysts were present as MoS<sub>2</sub>, Co<sub>9</sub>S<sub>8</sub>, and NiS.

Table 4.2. Kinetic parameters at various hydrodesulfurization conditions on Mo/Al<sub>2</sub>O<sub>3</sub>, Co/Al<sub>2</sub>O<sub>3</sub>, and Ni/Al<sub>2</sub>O<sub>3</sub>.

Catalyst	Mo/Al <sub>2</sub> O <sub>3</sub>				Co/Al <sub>2</sub> O <sub>3</sub>		Ni/Al <sub>2</sub> O <sub>3</sub>		
Reaction pressure, kg/cm <sup>2</sup>	50	50	50	50	50	50	50	50	50
Reaction temperature, °C	300	320	340	360	360	400	360	380	400
Concentration of DBT, wt%	1.0	1.0	1.0	1.0	1.0	1.0	1.0	1.0	1.0
Conversion from GC analysis, %	22.1	45.5	59.9	75.3	11.0	28.0	10.4	18.6	32.3
Conversion from radioactivity of <sup>35</sup> S, %	24.0	46.4	58.0	73.9	11.5	28.8	10.6	18.8	31.1
Labile sulfur, S <sub>0</sub> , mg/g.cat.	13.1	21.1	25.9	29.8	7.15	11.4	7.2	9.9	12.8
S <sub>0</sub> /S <sub>Total</sub> <sup>a</sup> , %	18.4	29.6	36.3	41.8	36.2	60.5	55.8	76.7	99.2
Rate constant of formed H <sub>2</sub> S, k, x10 <sup>-2</sup> , min <sup>-1</sup>	1.38	1.76	1.83	1.94	1.26	2.00	1.17	1.54	2.06
S <sub>0</sub> x k, mg/min.g.cat.	0.18	0.37	0.47	0.58	0.09	0.23	0.08	0.15	0.26
Rate of DBT HDS, mg/min.g.cat.	0.18	0.37	0.49	0.62	0.09	0.23	0.09	0.15	0.26

<sup>a</sup> S<sub>Total</sub> is defined as the amount of total sulfur when metal sulfides in the sulfided catalysts were present as MoS<sub>2</sub>, Co<sub>9</sub>S<sub>8</sub>, and NiS.



overlapped each other for Co-Mo/Al<sub>2</sub>O<sub>3</sub>. The same results were also obtained for Ni-Mo/Al<sub>2</sub>O<sub>3</sub>, and Mo/Al<sub>2</sub>O<sub>3</sub> (Figure 4.7). This indicates that the rate of release of <sup>35</sup>S-H<sub>2</sub>S is equal to that of <sup>32</sup>S-H<sub>2</sub>S, and that the isotopic effect between <sup>35</sup>S and <sup>32</sup>S would be negligible.

According to the method described in *Chapter 2*, the area A or B in Figure 4.1 is  $z/k$  (dpm) which can be calculated from the integral ( $t: 0-\infty$ ) of equation 4.1. The amount of labile sulfur on the catalyst ( $S_0$ ) can be presented by  $(z/k)/(^{35}\text{S}_{\text{DBT}}/S_{\text{DBT}})$ , where  $^{35}\text{S}_{\text{DBT}}$  is radioactivities in 1 mol of DBT (dpm/mol) and  $S_{\text{DBT}}$  is the amount of sulfur in 1 mol DBT (g/mol). The amount of labile sulfur for all catalysts under various reaction conditions were obtained and were summarized in Tables 1 and 2

The apparent activation energies of HDS for DBT on all catalysts calculated from the Arrhenius plots of the rates of HDS (Figure 4.8) were about  $20 \pm 1$  kcal/mol for Mo/Al<sub>2</sub>O<sub>3</sub>, Co/Al<sub>2</sub>O<sub>3</sub>, Co-Mo/Al<sub>2</sub>O<sub>3</sub>, Ni/Al<sub>2</sub>O<sub>3</sub>, and Ni-Mo/Al<sub>2</sub>O<sub>3</sub>. This was consistent with the results reported in *Ref. 4*. It implies that the same reaction process occurs either on sulfided Mo/Al<sub>2</sub>O<sub>3</sub>, Co-Mo/Al<sub>2</sub>O<sub>3</sub>, and Ni-Mo/Al<sub>2</sub>O<sub>3</sub>.

#### 4.4 Discussion

Results of EXAFS indicated that molybdenum sulfide in sulfided Mo/Al<sub>2</sub>O<sub>3</sub> is present as MoS<sub>2</sub>-like phase (5, 6). In *Chapter 2*, we estimated quantitatively the amount of sulfur in the sulfided Mo/Al<sub>2</sub>O<sub>3</sub> (MoO<sub>3</sub> 12.5 %) under the practical reaction condition and found that molybdenum sulfide was present in the form of MoS<sub>1.92</sub>. Thus, we could assume that the molybdenum sulfide is still present as the MoS<sub>2</sub> for Mo/Al<sub>2</sub>O<sub>3</sub> (MoO<sub>3</sub> 16.0 %).

For the sulfided Co/Al<sub>2</sub>O<sub>3</sub>, the stable sulfide is Co<sub>9</sub>S<sub>8</sub> (36-39). Results of EXAFS have also indicated existence of Co<sub>9</sub>S<sub>8</sub>-like phase.

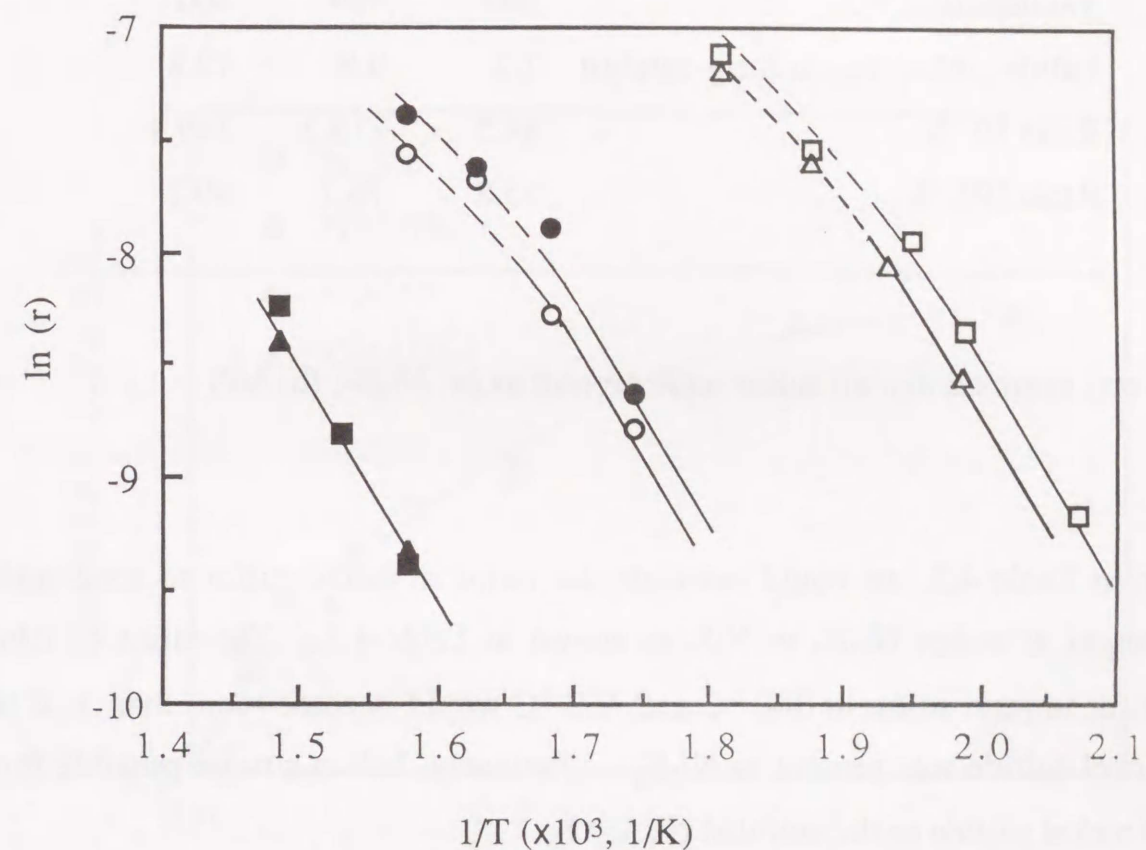


Figure 4.8. Arrhenius plots of the rates of HDS.

- : Mo/Al<sub>2</sub>O<sub>3</sub> (12.5 %);      ●: Mo/Al<sub>2</sub>O<sub>3</sub> (16.0 %)
- : Ni-Mo/Al<sub>2</sub>O<sub>3</sub>;              ■: Ni/Al<sub>2</sub>O<sub>3</sub>
- △: Co-Mo/Al<sub>2</sub>O<sub>3</sub>;             ▲: Co/Al<sub>2</sub>O<sub>3</sub>

For the sulfided Ni/Al<sub>2</sub>O<sub>3</sub>, the forms of nickel sulfide may be relatively complicated. The Ni-S phase diagram is very complex but there are two relatively stable sulfides, i.e., Ni<sub>3</sub>S<sub>2</sub> and NiS (20). The free energies of formation of Ni<sub>3</sub>S<sub>2</sub> and NiS are quite comparable (20). The stability of these sulfides will depend on the temperature and H<sub>2</sub>/H<sub>2</sub>S ratio in the gas phase (21).



Table 4.3. Ratios of labile sulfur to total sulfur on sulfided Ni/Al<sub>2</sub>O<sub>3</sub>.

Temperature, °C	360	380	400
Labile sulfur, mg-sulfur/g-catalyst	7.2	9.9	12.8
Ratio I <sup>a</sup> ), %	84.5	115.2	149.4
Ratio II <sup>b</sup> ), %	55.8	76.7	99.2

It was assumed that all sulfur were present as (a) Ni<sub>3</sub>S<sub>2</sub>; (b) NiS

From Table 4.2, we could calculate the ratios of labile sulfur to total sulfur present as either Ni<sub>3</sub>S<sub>2</sub> or NiS, as shown in Table 4.3. The ratios of labile sulfur to total sulfur at 380 °C and 400 °C would become more than 1, if the nickel sulfide was present as Ni<sub>3</sub>S<sub>2</sub>. Obviously, NiS is a more possible form of nickel sulfide in the sulfided Ni/Al<sub>2</sub>O<sub>3</sub>.

For the sulfided Co-Mo/Al<sub>2</sub>O<sub>3</sub>, and Ni-Mo/Al<sub>2</sub>O<sub>3</sub>, it is very difficult to determine the form of metal sulfide because of the complexity of bimetal system. Results of EXAFS have indicated that molybdenum sulfide is still present in MoS<sub>2</sub>-like phase (6, 7). Therefore, we could assume that cobalt or nickel sulfide and molybdenum sulfide in the sulfided Co-Mo/Al<sub>2</sub>O<sub>3</sub> and Ni-Mo/Al<sub>2</sub>O<sub>3</sub> were still present in the form of Co<sub>9</sub>S<sub>8</sub> or NiS and MoS<sub>2</sub>, respectively.

On the basis of this assumption, it was further assumed that only sulfur present in the Co<sub>9</sub>S<sub>8</sub> or NiS phase in the sulfided Co-Mo/Al<sub>2</sub>O<sub>3</sub> or Ni-Mo/Al<sub>2</sub>O<sub>3</sub> was labile, and that sulfur present in the form of MoS<sub>2</sub> was nonlabile. The ratios of the amount of labile sulfur to total amount of sulfur present in the Co<sub>9</sub>S<sub>8</sub> or NiS phase for Co/Al<sub>2</sub>O<sub>3</sub>, Co-Mo/Al<sub>2</sub>O<sub>3</sub>, Ni/Al<sub>2</sub>O<sub>3</sub> and

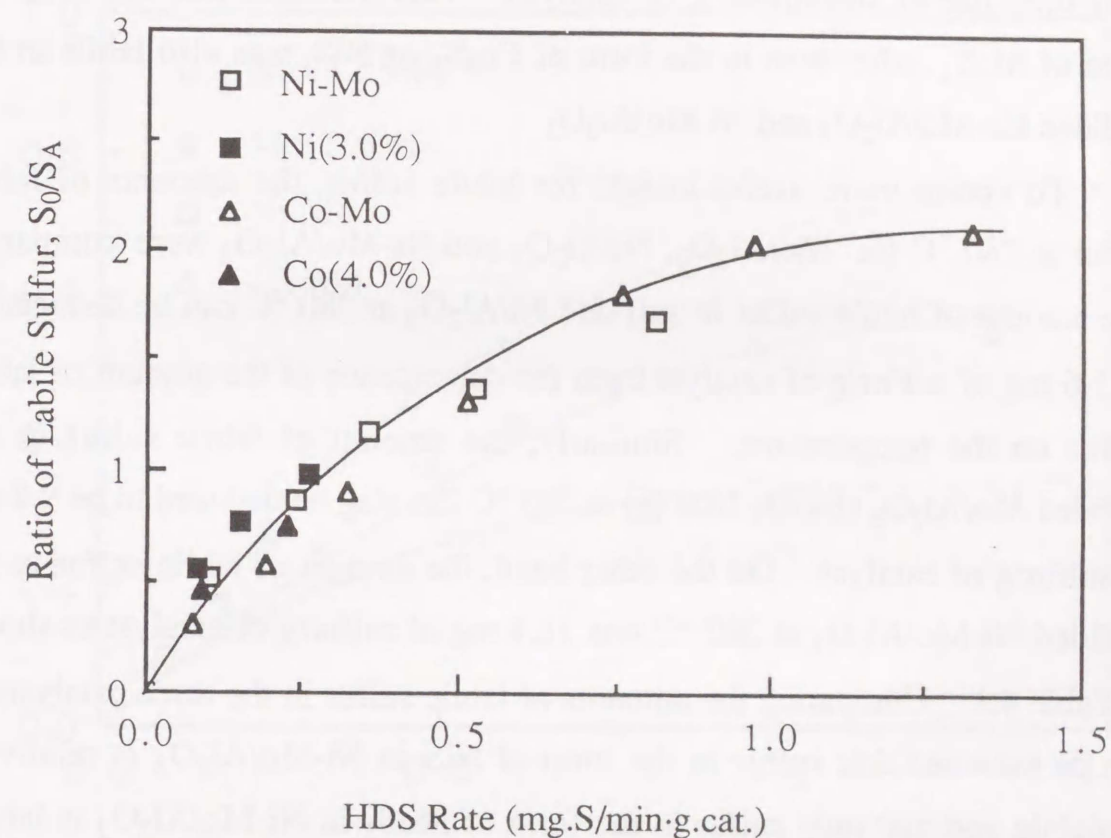


Figure 4.9. Plots of ratio of labile sulfur vs rate of DBT HDS.

Open symbols which belong to Co-Mo/Al<sub>2</sub>O<sub>3</sub> (Δ) and Ni-Mo/Al<sub>2</sub>O<sub>3</sub> (□), it was assumed that the sulfur in MoS<sub>2</sub> phase was not labile but only the sulfur in Co<sub>9</sub>S<sub>8</sub> or NiS phase was labile in the sulfided Ni-Mo/Al<sub>2</sub>O<sub>3</sub> and Co-Mo/Al<sub>2</sub>O<sub>3</sub>. The solid symbols belong to Co/Al<sub>2</sub>O<sub>3</sub> (▲) and Ni/Al<sub>2</sub>O<sub>3</sub> (■). The ratios of labile sulfur on the sulfided catalysts were estimated from S<sub>0</sub>/S<sub>A</sub> (S<sub>A</sub>: total amount of sulfur present in the form of Co<sub>9</sub>S<sub>8</sub> or NiS in the sulfided Co/Al<sub>2</sub>O<sub>3</sub>, Ni/Al<sub>2</sub>O<sub>3</sub>, Co-Mo/Al<sub>2</sub>O<sub>3</sub>, and Ni-Mo/Al<sub>2</sub>O<sub>3</sub>).



Ni-Mo/Al<sub>2</sub>O<sub>3</sub> were plotted against the rate of HDS in Figure 4.9. The ratio of labile sulfur to total sulfur present in the form of NiS or Co<sub>9</sub>S<sub>8</sub> in the For sulfided Co-Mo/Al<sub>2</sub>O<sub>3</sub> or Ni-Mo/Al<sub>2</sub>O<sub>3</sub> became more than one at rate of HDS over 0.29 mg of sulfur/min·g of catalyst. This indicates that sulfur in the form of MoS<sub>2</sub>, other than in the form of Co<sub>9</sub>S<sub>8</sub> or NiS, was also labile in the sulfided Co-Mo/Al<sub>2</sub>O<sub>3</sub> and Ni-Mo/Al<sub>2</sub>O<sub>3</sub>.

To obtain more useful insight for labile sulfur, the amounts of labile sulfur at 280 °C for Mo/Al<sub>2</sub>O<sub>3</sub>, Ni/Al<sub>2</sub>O<sub>3</sub> and Ni-Mo/Al<sub>2</sub>O<sub>3</sub> were compared. The amount of labile sulfur in sulfided Ni/Al<sub>2</sub>O<sub>3</sub> at 280 °C can be deduced to be 1.6 mg of sulfur/g of catalyst from the dependence of the amount of labile sulfur on the temperature. Similarly, the amount of labile sulfur in the sulfided Mo/Al<sub>2</sub>O<sub>3</sub> (MoO<sub>3</sub> 16.0 %) at 280 °C can also be deduced to be 9.8 mg of sulfur/g of catalyst. On the other hand, the amount of labile sulfur in the sulfided Ni-Mo/Al<sub>2</sub>O<sub>3</sub> at 280 °C was 18.4 mg of sulfur/g of catalyst as shown in Table 4.1. Comparing the amounts of labile sulfur in the three catalysts, it can be assumed that sulfur in the form of NiS in Ni-Mo/Al<sub>2</sub>O<sub>3</sub> is relatively nonlabile and that only sulfur in the form of MoS<sub>2</sub> in Ni-Mo/Al<sub>2</sub>O<sub>3</sub> is labile. Similarly, when the same treatment method was applied to the sulfided Mo/Al<sub>2</sub>O<sub>3</sub> (MoO<sub>3</sub> 12.5%) as reported in Chapter 2, Co/Al<sub>2</sub>O<sub>3</sub> and Co-Mo/Al<sub>2</sub>O<sub>3</sub>, the amounts of labile sulfur for three catalysts were 9.1, 2.0, and 19.9 mg of sulfur/g of catalyst at 260°C, respectively. It can be also assumed that sulfur in the form of Co<sub>9</sub>S<sub>8</sub> in Co-Mo/Al<sub>2</sub>O<sub>3</sub> is relatively nonlabile and that only sulfur in the form of MoS<sub>2</sub> in Co-Mo/Al<sub>2</sub>O<sub>3</sub> is labile. On the basis of these assumptions, the ratios of the amount of labile sulfur to total sulfur present in the form of MoS<sub>2</sub> were plotted against the HDS rate as shown in Figure 4.10. The ratios in sulfided Mo/Al<sub>2</sub>O<sub>3</sub> (12.5 %), Co-Mo/Al<sub>2</sub>O<sub>3</sub> and Ni-Mo/Al<sub>2</sub>O<sub>3</sub> increased with an increase in the rate of HDS and approached the steady values for the three catalysts. The maximum values of their ratios

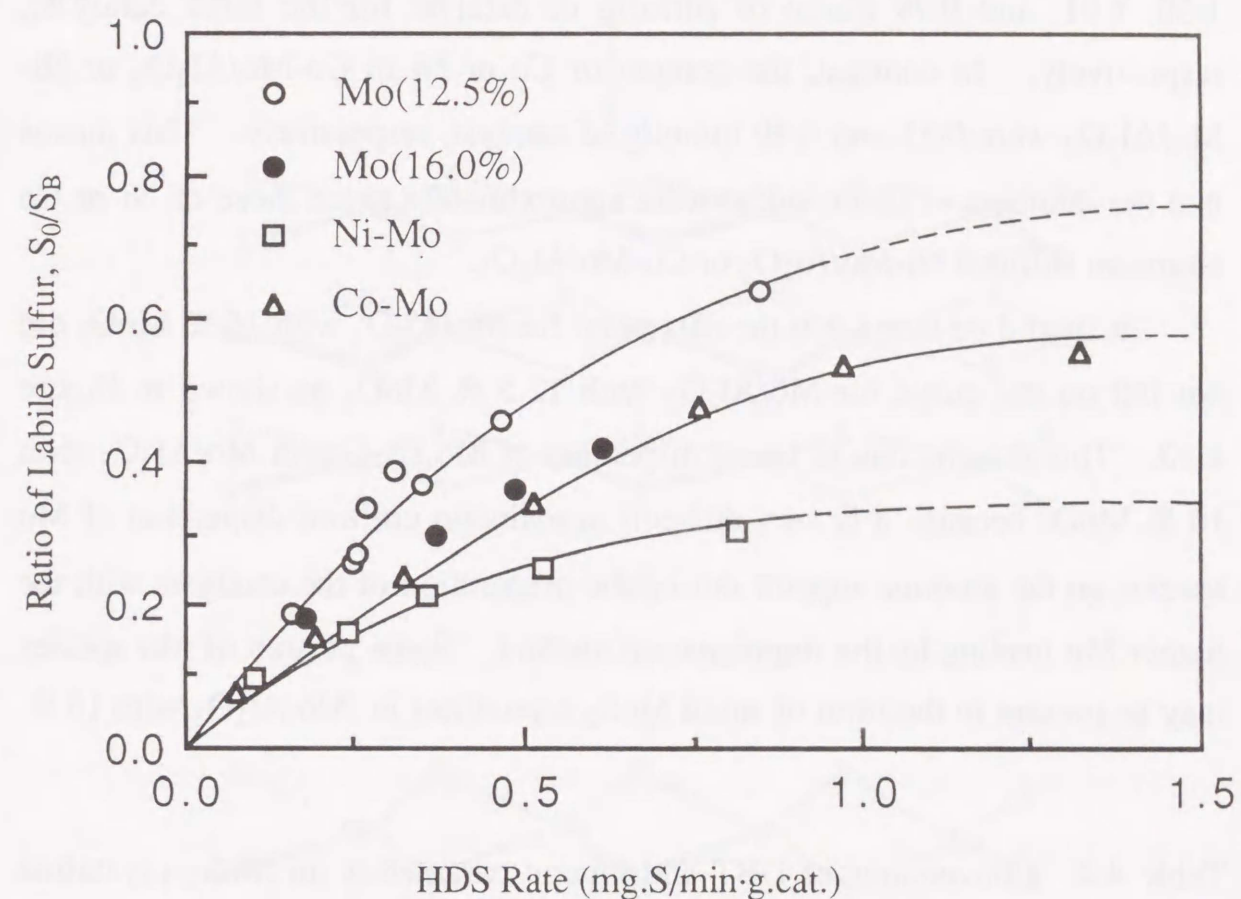


Figure 4.10. Plots of ratio of labile sulfur vs rate of DBT HDS.

○: Mo/Al<sub>2</sub>O<sub>3</sub> (12.5 %); ●: Mo/Al<sub>2</sub>O<sub>3</sub> (16 %); □: Ni-Mo/Al<sub>2</sub>O<sub>3</sub>;

△: Co-Mo/Al<sub>2</sub>O<sub>3</sub>. It was assumed that the sulfur in Co<sub>9</sub>S<sub>8</sub> and NiS phase was not labile but only the sulfur in MoS<sub>2</sub> phase was labile in the sulfided Co-Mo/Al<sub>2</sub>O<sub>3</sub> and Ni-Mo/Al<sub>2</sub>O<sub>3</sub>. The ratios of labile sulfur on the sulfided catalysts were estimated from S<sub>0</sub>/S<sub>B</sub> (S<sub>B</sub>: total amount of sulfur present in the form of MoS<sub>2</sub> in the sulfided Mo/Al<sub>2</sub>O<sub>3</sub>, Co-Mo/Al<sub>2</sub>O<sub>3</sub> and Ni-Mo/Al<sub>2</sub>O<sub>3</sub>).



would be deduced to be ca. 0.75, 0.59, and 0.37 for Mo/Al<sub>2</sub>O<sub>3</sub> (12.5 %), Co-Mo/Al<sub>2</sub>O<sub>3</sub> and Ni-Mo/Al<sub>2</sub>O<sub>3</sub>, respectively. At this time, the amounts of labile sulfur would be about 41.8, 32.3, and 25.2 mg of sulfur/g of catalyst, i.e., 1.30, 1.01, and 0.79 mmol of sulfur/g of catalyst for the three catalysts, respectively. In contrast, the content of Co or Ni in Co-Mo/Al<sub>2</sub>O<sub>3</sub> or Ni-Mo/Al<sub>2</sub>O<sub>3</sub> were 0.51 and 0.39 mmol/g of catalyst, respectively. This means that the numbers of labile sulfur were approximately twice those of Ni or Co atoms on sulfided Ni-Mo/Al<sub>2</sub>O<sub>3</sub> or Co-Mo/Al<sub>2</sub>O<sub>3</sub>.

It should be noted that the data point for Mo/Al<sub>2</sub>O<sub>3</sub> with 16 % MoO<sub>3</sub> did not fall on the curve for Mo/Al<sub>2</sub>O<sub>3</sub> with 12.5 % MoO<sub>3</sub> as shown in Figure 4.10. This may be due to lower dispersion of Mo species in Mo/Al<sub>2</sub>O<sub>3</sub> with 16 % MoO<sub>3</sub> because it is very difficult to maintain uniform dispersion of Mo species on the alumina support during the preparation of the catalysts with the higher Mo loading by the impregnation method. Some portion of Mo species may be present in the form of small MoS<sub>2</sub> crystallites in Mo/Al<sub>2</sub>O<sub>3</sub> with 16 %

Table 4.4. Conversions of DBT and kinetic parameters on MoS<sub>2</sub> crystallite (DBT 1wt%, 50 kg/cm<sup>2</sup>, MoS<sub>2</sub> 0.5 g).

Reaction temperature, °C	400	430
Conversion from radioactivity of <sup>35</sup> S, (%)	14.3	15.4
Conversion from GC analysis, (%)	15.8	19.4
Labile sulfur, S <sub>0</sub> , mg/g of cat.	7.00	6.99
S <sub>0</sub> /S <sub>Total</sub> , %	3.5	3.5
Release rate constant of <sup>35</sup> S-H <sub>2</sub> S, <i>k</i> , ×10 <sup>-2</sup> , min <sup>-1</sup>	1.84	2.27
Rate of DBT HDS, mg/min.g.cat.	0.129	0.158

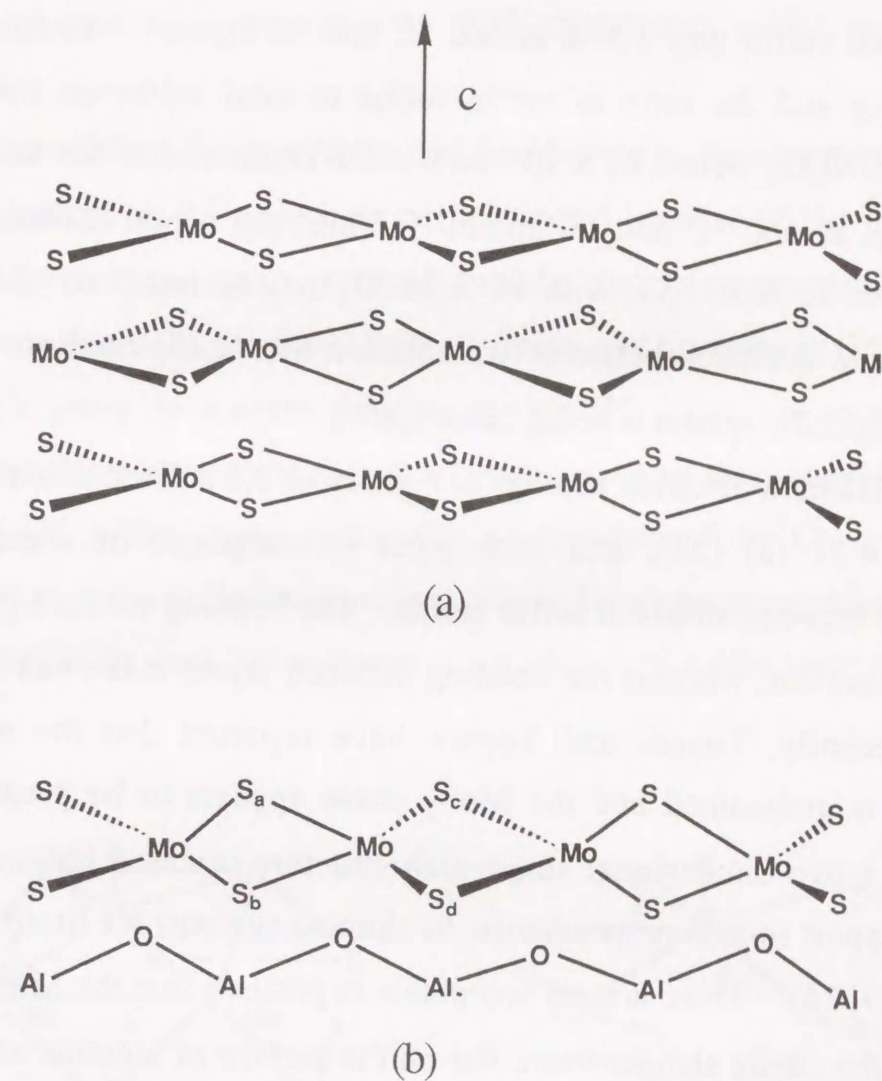


Figure 4.11. Structure of MoS<sub>2</sub>: (a) Crystal structure of molybdenum disulfide; (b) Structure of MoS<sub>2</sub> on sulfided Mo/Al<sub>2</sub>O<sub>3</sub>.



MoO<sub>3</sub>. The HDS activity and the ratio of labile sulfur to total sulfur were very low for the unsupported MoS<sub>2</sub> (see Table 4.4). For instance, the HDS activity was  $1.29 \times 10^{-3}$  mol of DBT/min·mol of Mo and the ratio of labile sulfur to total sulfur was 3.5 % at 400 °C and 50 kg/cm<sup>2</sup>. In contrast, the HDS activity and the ratio of labile sulfur to total sulfur on the 12.5 % sulfided Mo/Al<sub>2</sub>O<sub>3</sub> were  $1.87 \times 10^{-2}$  mol of DBT/min·mol of Mo and 45.5 %, respectively, at 360 °C and 50 kg/cm<sup>2</sup>. Thus, the actual content of well-dispersed Mo in Mo/Al<sub>2</sub>O<sub>3</sub> with 16 % MoO<sub>3</sub> may be less than 16 %. This may cause the deviation between two sulfided Mo/Al<sub>2</sub>O<sub>3</sub> catalysts in Figure 4.10. The specific reason is being investigated.

Molybdenum disulfide belongs to a group of the layered structure shown in Figure 4.11 (a) (23), and each layer is composed of sheets of Mo sandwiched between sheets of sulfur atoms. The bonding within a given layer is mainly covalent, whereas the bonding between layers is the van der Waals type. Recently, Topsøe and Topsøe have reported that the monolayer dispersion is maintained and the MoS<sub>2</sub> phase appears to be predominantly present as a two-dimensional single-slab structure oriented flat-wise on the alumina support (*c*-axis perpendicular to alumina surface) for Mo/Al<sub>2</sub>O<sub>3</sub> up to 12 % Mo (9, 24). Thus, it is an acceptable hypothesis that the MoS<sub>2</sub> phase is present as the single slab structure flat on the surface of alumina as shown in Figure 4.11 (b). However, since the locations of sulfurs on the surface of alumina were different from each other, the labile capacities of sulfurs would also be different. The sulfur between molybdenum layer and alumina surface (S<sub>b</sub>) may be the most difficult to move, and the sulfur over molybdenum layer (S<sub>a</sub>) may be the most mobile. The sulfur in other sites (S<sub>c</sub> or S<sub>d</sub>), which forms a triangle with Mo parallel to alumina surface, may have the intermediate mobile capacity. This explains why the amount of labile sulfur changes depending on the reaction conditions (see Figures 2.3-2.4 and Table

2.1 in Chapter 2). If the sulfur between molybdenum and alumina surface, S<sub>b</sub>, was nonlabile, the amount of labile sulfur in the sulfided Mo/Al<sub>2</sub>O<sub>3</sub> would be 75 % of the total sulfur. This is good agreement with results that the maximum amount of labile sulfur is 75 % of the total sulfur, as shown in Figure 4.10.

For the sulfided Co-Mo/Al<sub>2</sub>O<sub>3</sub> and Ni-Mo/Al<sub>2</sub>O<sub>3</sub>, the structure of MoS<sub>2</sub>-like phase located in the edge may be rearranged because of the presence of Co or Ni atoms, and a square pyramidal model may be an acceptable model. This idea was originally proposed by Ratnasamy and Sivasanker (25) and later by Topsøe's group in a more detailed model (26, 27). In recent works, Louwers and Prins have given a further evidence about this model by the use of EXAFS (7). The square pyramidal coordination of the Co or Ni atoms resembles that of the millerite structure. Co or Ni atoms are connected to the MoS<sub>2</sub> crystallite by four sulfur atoms. An additional sulfur atom is attached

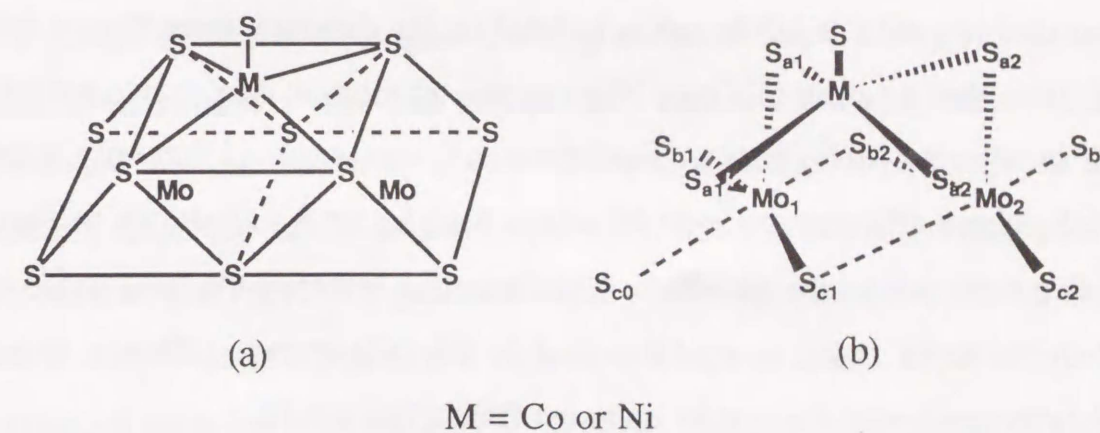


Figure 4.12. Structure of sulfided Co (Ni)-Mo/Al<sub>2</sub>O<sub>3</sub>: (a) Square pyramidal structure; (b) Deformed tetrahedral structure of MoS<sub>2</sub> and structure of Mo-S-Co (Ni).



in front of the Ni atom as shown in Figure 4.12 (a). Even in this model, one could still consider that the structure of  $\text{MoS}_2$  is a deformed tetrahedral structure and only the locations of other two weak Mo-S bond within the layers are changed, as shown in Figure 4.12 (b). The  $\text{Mo}_1\text{-S}_{c0}$  or  $\text{Mo}_2\text{-S}_{c1}$ , and  $\text{Mo}_1\text{-S}_{b2}$  or  $\text{Mo}_2\text{-S}_{b3}$  bonds were considered as two other weak bonds assigned to the van der Waals type in this structure. As mentioned above, the sulfur in the Co-Mo/ $\text{Al}_2\text{O}_3$  or Ni-Mo/ $\text{Al}_2\text{O}_3$  is the most labile among sulfided Co/ $\text{Al}_2\text{O}_3$  or Ni/ $\text{Al}_2\text{O}_3$ , Mo/ $\text{Al}_2\text{O}_3$ , and Co-Mo/ $\text{Al}_2\text{O}_3$  or Ni-Mo/ $\text{Al}_2\text{O}_3$ . This is consistent with the bond energies of metal sulfide calculated by Nørskov et al. (28) and Topsøe et al. (29). They proposed that the bond energies of metal sulfide varied as follows: nickel or cobalt sulfide > molybdenum sulfide > CoMoS or NiMoS. Taking into account that the bond energy of Co-S or Ni-S is higher than that of CoMoS or NiMoS, it is reasonable that the sulfur attached to only Co or Ni atom is more difficult to move. On the other hand, the atomic ratios of Co/Mo and Ni/Mo were 0.59 and 0.37 for Co-Mo/ $\text{Al}_2\text{O}_3$  and Ni-Mo/ $\text{Al}_2\text{O}_3$ , respectively. These values are in very good agreement with the maximum ratios of labile sulfur to total sulfur obtained from Figure 4.10. It indicates that an atom of Co or Ni promotes an atom of Mo or two atoms of sulfur in adjacent  $\text{MoS}_2$  phase. Furthermore, it was assumed that only sulfurs in  $\text{MoS}_2$  phase adjacent to Co or Ni atoms, i.e.,  $\text{S}_{a1}$  or  $\text{S}_{a2}$  as shown in Figure 4.12 (b), were labile, the numbers of labile sulfur in Mo-S-Co (Ni) phase can be deduced to be twice as much as that of Co (Ni) atoms. This is in very good agreement with the results obtained from Figure 4.10.

The HDS activity of sulfided Mo-based catalysts would be relative with the existence of sulfur vacancies (uncoordinated sites). The SH groups also played an important role in the HDS reaction (30, 31). Regarding to the evidence for the presence of SH groups, studies of deuterium exchange (32), chemical titration by silver ions (33) and Raman spectroscopy (34) have

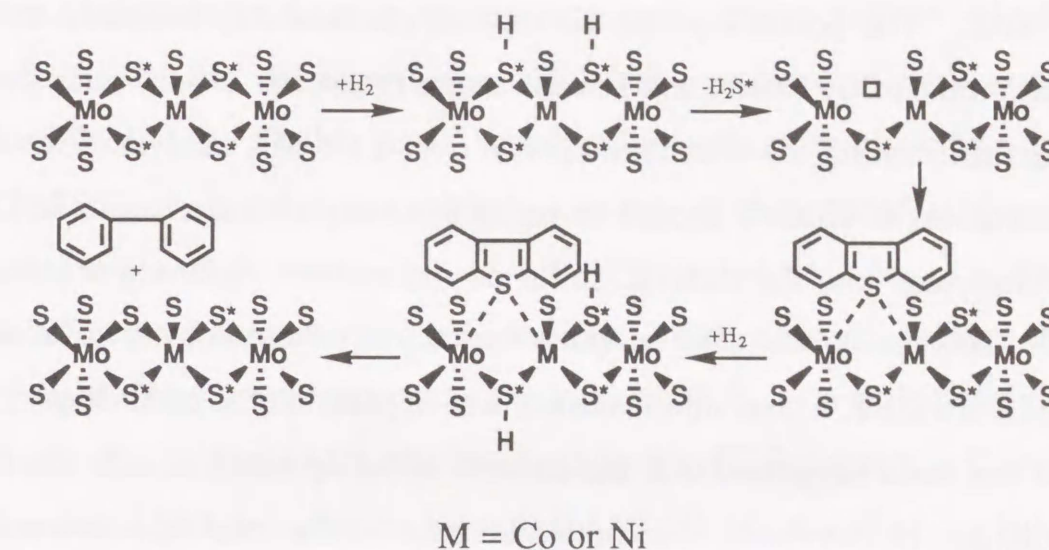


Figure 4.13. Scheme of the mechanism of hydrodesulfurization of DBT on sulfided Co (Ni)- $\text{Mo}/\text{Al}_2\text{O}_3$ .

provided such evidence. More recently, Topsøe and Topsøe postulated that SH groups existed at the edges of  $\text{MoS}_2$ , and found by FT-IR study on sulfided Mo-based catalysts that SH groups and vacancies could interconvert and coexisted in close proximity (24). As mentioned above,  $\text{H}_2\text{S}$  was not formed directly from the sulfur in DBT, but from the sulfur on the catalyst. The absence of DBT did not generate  $\text{H}_2\text{S}$ , while the incorporation of sulfur in DBT onto catalyst generated  $\text{H}_2\text{S}$  (see Chapter 3 or Chapter 5). If the vacancies were the sites for the coordination with the heteroatoms of reactants, the mechanism of DBT HDS would be illustrated more simply as shown in Figure 4.13. It has been also assumed that only sulfur bonded to both Co (or Ni) and Mo in the form of  $\text{MoS}_2$  is labile in the scheme. When  $^{35}\text{S}$  in DBT occupied the vacancy and the carbon-sulfur bonds were cleaved,  $^{35}\text{S}$  would remain on the catalyst as Mo-S species. The generation of  $\text{H}_2\text{S}$  will form a



new vacancy on the catalyst. Thus, a shift of vacancy on the catalyst surface would occur. The possibility that the vacancy position may be easily shifted has been proposed by Ruetten and Ludena in the molecular orbital calculations of the desulfurization reaction of thiophene over a Co-Mo catalyst (35). For this mechanism of HDS, it should be noted that only after the sulfur in DBT was incorporated into the catalyst, sulfur on the catalyst surface was released as  $H_2S$ . This means that after an anion vacancy is occupied by a sulfur atom removed from DBT, a new anion vacancy will appear on the catalyst surface.

It has been suggested that the amount of labile sulfur equals the total sulfur that can be converted to vacancies under a certain reaction condition for a catalyst. Although this amount corresponds closely to the reactivity of the catalyst, it is definitely not equal to the number of active sites. The reactivity of a catalyst will also depend upon the conversion rate between labile sulfur and the vacancy - regeneration rate of active sites, as well as the amount of labile sulfur. Thus, the regeneration rate of active sites as well as the amount of labile sulfur, varies with reaction conditions. Furthermore, the variation in the regeneration rate of active sites is more than in the amount of labile sulfur. This could explain the correspondence between the amounts of labile sulfur and the HDS rates shown in Figure 4.10, where the reactivity of a catalyst could vary significantly although the amount of labile sulfur for the catalyst was approximately constant.

#### 4.5 Conclusions

The hydrodesulfurization of  $^{35}S$ -labeled dibenzothiophene ( $^{35}S$ -DBT) were carried out on the sulfided Co-Mo/ $Al_2O_3$ , Ni-Mo/ $Al_2O_3$ , Mo/ $Al_2O_3$ , Co/ $Al_2O_3$ , and Ni/ $Al_2O_3$ , and the following conclusions were drawn. The similar apparent activation energies ( $20 \pm 1$  kcal/mol) of HDS reaction for DBT

on all sulfided catalysts were estimated from the rate of HDS reaction. It implies that the same reaction process may occur on the sulfided Mo/ $Al_2O_3$ , Co-Mo/ $Al_2O_3$  and Ni-Mo/ $Al_2O_3$ . When the amounts of labile sulfur in sulfided Mo/ $Al_2O_3$ , Co-Mo/ $Al_2O_3$  and Ni-Mo/ $Al_2O_3$  were plotted against the rate of HDS, these increased with an increase in the rate of HDS and the maximum values of labile sulfur were 41.8, 32.3 and 25.2 mg of sulfur/g of catalyst for the three catalysts, respectively. When it was assumed that all sulfur in Mo/ $Al_2O_3$  were present in the form of  $MoS_2$ , it was deduced that ca. 75 % of sulfur in Mo/ $Al_2O_3$  was involved in the HDS reaction. Comparing the amounts of labile sulfur in the sulfided Mo/ $Al_2O_3$ , Co/ $Al_2O_3$  or Ni/ $Al_2O_3$  and Co-Mo/ $Al_2O_3$  or Ni-Mo/ $Al_2O_3$ , it was suggested that the sulfur in the  $Co_9S_8$  or NiS phase on the or Co-Mo/ $Al_2O_3$  or Ni-Mo/ $Al_2O_3$  was nonlabile and only sulfur bonded to both Co (Ni) and Mo in the form of  $MoS_2$  was involved in the HDS reaction. The maximum amounts of labile sulfur on Co-Mo/ $Al_2O_3$  and Ni-Mo/ $Al_2O_3$ , 32.3 and 25.2 mg of sulfur/g of catalyst, correspond to about 59 % and 37 % of sulfur present in the form of  $MoS_2$ . The atomic ratios of Co/Mo and Ni/Mo in used Co-Mo/ $Al_2O_3$  and Ni-Mo/ $Al_2O_3$  are 0.59 and 0.37. The results suggest that the addition of Co or Ni promotes the same amount of Mo species as that of Co or Ni species in the sulfided Co-Mo/ $Al_2O_3$  or Ni-Mo/ $Al_2O_3$  and makes sulfur in this portion of Mo species more labile.



## Reference

1. Ishihara, A., Tajima, H., and Kabe, T., *Chem. Lett.*, 669 (1992).
2. Kabe, T., Ishihara, A., and Tajima, H., *Ind. Eng. Chem. Res.*, **31**, 1577 (1992).
3. Kabe, T., Ishihara, A., Zhang, Q., Tsutsui, H., and Tajima, H., *J. Jpn., Petrol. Inst.*, **36**(6), 467 (1993).
4. Kabe, T., Ishihara, A., and Zhang, Q., *Appl. Catal.*, **A97**, L1 (1993).
5. Bouwens, S. M. A. M., Prins, R., de Beer, V. H. J., and Koningsberger, D. C., *J. Phys. Chem.*, **94**, 3711 (1990).
6. Bouwens, S. M. A. M., van Veen, J. A. R., Koningsberger, D. C., de Beer, V. H. J., and Prins, R., *J. Phys. Chem.*, **95**, 123 (1991).
7. Louwers, S. P. A., and Prins, R., *J. Catal.*, **133**, 94 (1992).
8. Topsøe, H., Clausen, B. S., Topsøe, N.-Y., and Pedersen, E., *Ind. Eng. Chem. Fundam.* **25**, 25 (1986).
9. Topsøe, N.-Y., and Topsøe, H., *J. Catal.*, **139**, 631 (1993).
10. Chianelli, R. R., *Catal. Rev. Sci. Eng.*, **26**, 361 (1984).
11. Topsøe, H., Candia, R., Topsøe, N.-Y., and Clansen, B. S., *Bull. Soci. Chim. Belg.*, **93**, 783 (1984).
12. Topsøe, H., Clausen, B. S., Topsøe, N.-Y., and Pedersen, E., *Ind. Eng. Chem. Fundam.*, **25**, 725 (1984).
13. Wivel, C., Candia, R., Clausen, B. S., Mørup, S., and Topsøe, H., *J. Catal.*, **68**, 453 (1981).
14. Göbölös, S., Wu, Q., and Delmon, B., *Appl., Catal.*, **13**, 89 (1984).
15. Karroua, M., Matralis, H., Grange, P., and Delmon, B., *J. Catal.*, **139**, 371 (1993).
16. Delmon, B., in "Catalysis in Petroleum Refining 1989" (Trimm, D. L., Akaha, S., Absi-Halabi, M., and Bishara, A., Eds.), p. 1, Elsevier, Amsterdam, 1990.
17. Karroua, M., Grange, P., and Delmon, B., *Appl. Catal.*, **50**, L5 (1993).
18. Kabe, T., Qian, W., Ogawa, S., and Ishihara, A., *J. Catal.*, **143**, 239 (1993).
19. Qian, W., Ishihara, A., Shinji, O., and Kabe, T., *J. Phys. Chem.*, **98**, 907 (1994).
20. Kabe, T., Qian, W., and Ishihara, A., *J. Phys. Chem.*, **98**, 912 (1994).
21. Alcock, C. B., "Principles of Pyrometallurgy", Academic Press, London/New York, 1976.
22. Burch, R., and Collins, A., *J. Catal.*, **97**, 385 (1986).
23. Williams, R. H., and Mcevoy, A. J., *J. Phys., D: Appl. Phys.*, **4**, 456 (1971).
24. Topsøe, N.-Y., and Topsøe, H., *J. Catal.*, **139**, 641 (1993).
25. Ratnasamy, P., and Sivasanker, S., *Catal. Rev. Sci. Eng.*, **22**, 401 (1980).
26. Clausen, B. S., Lengeler, B., Candia, R., Als-Nielsen, J., and Topsøe, H., *Bull. Soc. Chim. Belg.*, **90**, 1249 (1981).
27. Topsøe, H., Clausen, B. S., Topsøe, N.-Y., Pedersen, E., Niemann, W., Müller, A. BöggeH., and Lengeler, B., *J. Chem. Soc. Faraday Trans. I*, **83**, 2157 (1987).
28. Nørskov, J. K., Clausen, B. S., and Topsøe, H., *Catal. Lett.*, **13**, 1 (1992).
29. Topsøe, H., Clausen, B. S., Topsøe, N.-Y., Hyldtoft, J., and Nørskov, J. K., *Prepr. Am. Chem. Soc. Div. Pet. Chem.*, **38** (3), 638 (1993).
30. Topsøe, H., in "Proceedings of the NATO Advanced Study Institute on Surface Properties and Catalysis by Non-Metals: Oxides, Sulfides and



- Other Transition Metal Compounds, 1982*" (Bonnelle, J. P., Delmon, B., and Derouane, E., Eds.), p. 329, Reidel, Dordrecht, 1983.
31. Muralidhar, G., Massoth, F. E., and Shabtai, J., *J. Catal.*, **85**, 44 (1984).
  32. Massoth, F. E., *J. Catal.* **36**, 164 (1975).
  33. Maternova, J., *Appl. Catal.*, **3**, 3 (1982).
  34. Payen, E., Kasztelan, S., and Grimblot, J., *J. Mol. Struct.*, **174**, 71 (1988).
  35. Ruetter, F., and Ludena, E. V., *J. Catal.*, **67**, 266 (1981).
  36. de Beer, V. H. J., van Sint Fiet, T. H. M., van der Steen, G. H. A. M., Zwaga, A. C., and Schuit, G. C. A., *J. Catal.*, **35**, 297 (1974).
  37. Delannay, F., Haeussler, E., and Delmon, B., *J. Catal.*, **66**, 469 (1980).
  38. Kasztrlan, S., Grimblot, J., and Bonnelle, J. P., *J. Phys. Chem.*, **91**, 1503 (1987).
  39. Topsøe, H., and Clausen, B. S., *Appl. Catal.*, **25**, 273 (1986).

## Chapter Five

**Behavior of Sulfur on  $^{35}\text{S}$ -Labeled Co-Mo/Al<sub>2</sub>O<sub>3</sub> in hydrodesulfurization of Sulfur Compounds, and in a Mixed Gas of H<sub>2</sub>S/H<sub>2</sub>**



Chapter Five  
**Behavior of Sulfur on  $^{35}\text{S}$ -Labeled Co-Mo/ $\text{Al}_2\text{O}_3$  in  
hydrodesulfurization of Sulfur Compounds, and in a  
Mixed Gas of  $\text{H}_2\text{S}/\text{H}_2$**

**Abstract**

A commercial Co-Mo/ $\text{Al}_2\text{O}_3$  catalyst was labeled by  $^{35}\text{S}$  during HDS of  $^{35}\text{S}$ -labeled dibenzothiophene. Then the HDS reaction of various sulfur-containing compounds or the exchange reaction with a mixed gas of  $\text{H}_2\text{S}$  and  $\text{H}_2$  was carried out on this catalyst. Similar to the Mo/ $\text{Al}_2\text{O}_3$  catalyst in *Chapter 3*,  $\text{H}_2\text{S}$  could not form from the labile sulfur without the supply of sulfur even though in the reduction atmosphere of high pressure of  $\text{H}_2$ . The release rate of  $^{35}\text{S}\text{-H}_2\text{S}$  from  $^{35}\text{S}$ -labeled catalyst could approximately be treated with the first order equation after introducing the sulfur compounds. When the partial pressure of  $\text{H}_2\text{S}$  during HDS of sulfur compounds is similar to the case of introducing  $\text{H}_2\text{S}$ , the release rate of  $^{35}\text{S}\text{-H}_2\text{S}$  from the catalyst were also the same for two cases. This indicates that the formation process of  $^{35}\text{S}\text{-H}_2\text{S}$  from the catalyst during HDS reaction is the same with the case of exchange reaction with  $\text{H}_2\text{S}$ . Moreover, the release rate constants of  $^{35}\text{S}\text{-H}_2\text{S}$  trend toward to a constant value above  $0.36 \text{ kg/cm}^2$  of the partial pressure of  $\text{H}_2\text{S}$ . This indicates that the adsorption of  $\text{H}_2\text{S}$  onto the active sites approached a saturated state in present reaction conditions. The release of  $\text{H}_2\text{S}$  from the catalyst may be the determining-rate step of this reaction.



## 5.1 Introduction

In *Chapter 3*, we reported that, when the HDS reactions of thiophene etc. were carried out on  $^{35}\text{S}$ -labeled  $\text{Mo}/\text{Al}_2\text{O}_3$ , the release rate of  $^{35}\text{S}\text{-H}_2\text{S}$  from the catalyst was independent of the kinds of sulfur compounds but dependent upon the amount of  $^{32}\text{S}$  incorporated into the catalyst (1). This implied that the release rate of  $\text{H}_2\text{S}$  from the catalyst may vary with the atmosphere of reactant and the release process of  $\text{H}_2\text{S}$  from the catalyst may be same for all reaction of various sulfur compounds. In this chapter, we are interested in whether there are also same characteristics for Co or Ni-promoted catalysts. Considering the similarity between Co-Mo/ $\text{Al}_2\text{O}_3$  and Ni-Mo/ $\text{Al}_2\text{O}_3$  as described in *Chapter 4*, a commercial Co-Mo/ $\text{Al}_2\text{O}_3$  catalyst was labeled by  $^{35}\text{S}$  during HDS of  $^{35}\text{S}$ -labeled dibenzothiophene in this work. Then various sulfur-containing compounds were introduced to the catalyst, and the behavior of labile sulfur was estimated by quantitatively evaluating the release process of  $^{35}\text{S}\text{-H}_2\text{S}$  from  $^{35}\text{S}$ -labeled catalyst. Furthermore, a series of mixed gases of  $\text{H}_2\text{S}$  and  $\text{H}_2$  containing different content of  $\text{H}_2\text{S}$  were also introduced to  $^{35}\text{S}$ -labeled catalyst to investigate the behavior of sulfur on the catalyst in  $\text{H}_2\text{S}$  atmosphere. We expected to gain more information concerning the exchange reaction of sulfur on the catalyst with that in sulfur compounds and the formation mechanism of  $\text{H}_2\text{S}$  from the labile sulfur on the catalyst.

## 5.2 Experimental

### 5.2.1 Materials

Benzothiophene (BP), thiophene (T) and decalin were obtained from Kishida Co. Ltd. Dibenzothiophene ( $^{32}\text{S}$ -DBT) and  $^{35}\text{S}$  labeled dibenzo-

thiophene ( $^{35}\text{S}$ -DBT) were synthesized according to the method reported in previous paper (2). The concentrations of sulfur compounds in decalin were 1.0 wt%. The concentrations of  $\text{H}_2\text{S}$  in  $\text{H}_2$  were 0.12-3.4 vol%.

A commercial Co-Mo/ $\text{Al}_2\text{O}_3$  (Ketjen fine 124,  $\text{MoO}_3$ : 12.3 wt%, CoO: 3.8 wt%, Surface area:  $274\text{ m}^2/\text{g}$ ) was used and presulfided with 5 vol%  $\text{H}_2\text{S}/\text{H}_2$  gas mixture by heating to  $200\text{ }^\circ\text{C}$  at a rate of  $5^\circ\text{C}/\text{min}$  and to  $400\text{ }^\circ\text{C}$  at a rate of  $2\text{ }^\circ\text{C}/\text{min}$ , and then maintained at  $400\text{ }^\circ\text{C}$  for 3 h.

### 5.2.2 Apparatus and Procedure

The details of the apparatus employed were described in *Chapter 2*. The reactions were carried out by a fixed-bed flow reactor under the conditions of  $50\text{ kg}/\text{cm}^2$ ,  $200\text{-}260\text{ }^\circ\text{C}$  and WHSV  $28\text{ h}^{-1}$ . Products were analyzed by a gas chromatography with an FID detector. The produced  $\text{H}_2\text{S}$  was absorbed by bubbling through a commercial basic scintillation solution (Carbosorb). The radioactivities of produced  $^{35}\text{S}\text{-H}_2\text{S}$  and unreacted  $^{35}\text{S}\text{-DBT}$  were measured by a liquid scintillation counter.

Two typical operation procedures were the same as the case of using Mo/ $\text{Al}_2\text{O}_3$  in *Chapter 3*:

Operation procedure 1: (a) A decalin solution of 1 wt%  $^{32}\text{S}\text{-DBT}$  was pumped into the reactor until the conversion of DBT became constant (about 3h). (b) After that, a decalin solution of 1 wt%  $^{35}\text{S}\text{-DBT}$  was substituted for that of 1 wt%  $^{32}\text{S}\text{-DBT}$ . The reaction with  $^{35}\text{S}\text{-DBT}$  was performed until the amount of  $^{35}\text{S}\text{-H}_2\text{S}$  released from the exit of the reactor became constant. (c) Then, the reactant solution was substituted again with the decalin solution of 1 wt%  $^{32}\text{S}\text{-DBT}$  and was reacted for 4-5 h.

Operation Procedure 2: Operation steps (a) and (b) in this procedure were same as those in operation procedure 1. (c) The reactant solution of  $^{35}\text{S}\text{-DBT}$  was replaced by the decalin solvent. The reaction was continued for ca.



4 h. (d) After that, the decalin solution of sulfur compound or a mixed gas of  $\text{H}_2\text{S}$  and  $\text{H}_2$  was introduced and reacted for ca. 4h.

In operation procedure 2, the labile sulfur on the catalyst was labeled by  $^{35}\text{S}$  in the step (b). The reaction system was purged with  $\text{H}_2$  in the step (c). Then, the decalin solution of sulfur compounds, or the mixed gas of  $\text{H}_2\text{S}$  and  $\text{H}_2$  was introduced onto the catalyst in the step (d). The behavior of labile sulfur on the catalyst was estimated by tracing the change in radioactivity of formed  $^{35}\text{S}\text{-H}_2\text{S}$ . The total pressure was maintained at  $50 \text{ kg/cm}^2$  and the reaction temperature was  $260^\circ\text{C}$  from the step (a) to (c). To investigate the effects of reaction temperature and the partial pressure of  $\text{H}_2\text{S}$  in gas on the release rate of  $^{35}\text{S}\text{-H}_2\text{S}$ , the temperatures were regulated from  $200^\circ\text{C}$  to  $260^\circ\text{C}$  and the concentrations of  $\text{H}_2\text{S}$  in  $\text{H}_2$  were changed from 0.12 vol% to 3.4 vol% in the step (d).

### 5.3 Results

#### 5.3.1 Label of Labile Sulfur on Catalyst during HDS of $^{35}\text{S}\text{-DBT}$ .

Figure 1 displays the change in radioactivity with reaction time at  $260^\circ\text{C}$ ,  $50 \text{ kg/cm}^2$  and  $\text{WHSV } 28 \text{ h}^{-1}$  according to operation procedure 1. After  $^{35}\text{S}\text{-DBT}$  was substituted for  $^{32}\text{S}\text{-DBT}$ , the radioactivities of the unreacted  $^{35}\text{S}\text{-DBT}$  increased and approached a steady state immediately. In the case of the produced  $^{35}\text{S}\text{-H}_2\text{S}$ , however, about 130 min was needed to approach the steady state. When the solution of  $^{35}\text{S}\text{-DBT}$  returned to that of  $^{32}\text{S}\text{-DBT}$  at 380 min, the radioactivities of the unreacted  $^{35}\text{S}\text{-DBT}$  also decreased immediately, but the time delay for the produced  $^{35}\text{S}\text{-H}_2\text{S}$  from its steady state to normal state was ca 130 min. This indicates that the sulfur in DBT is not directly released as hydrogen sulfide but accommodates on the catalyst as mentioned in *Chapter*

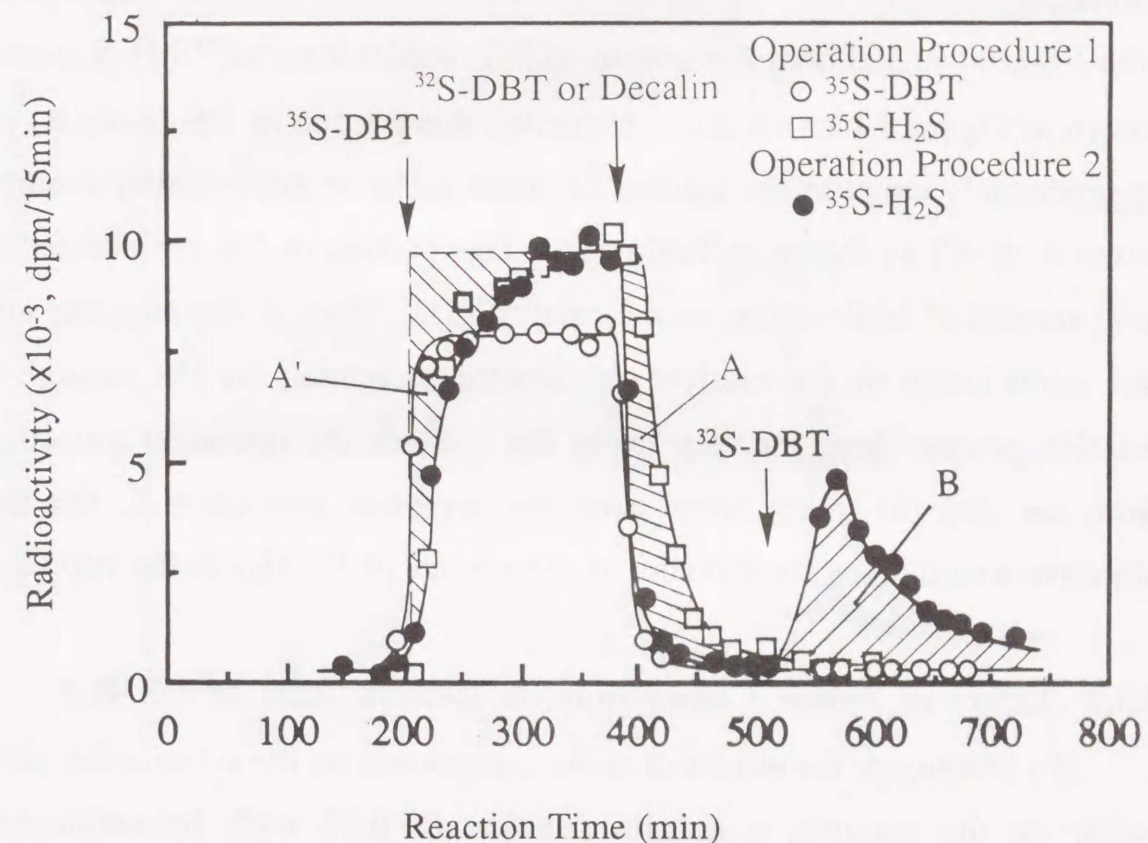


Figure 5.1. Changes in radioactivities of unreacted  $^{35}\text{S}\text{-DBT}$  and formed  $^{35}\text{S}\text{-H}_2\text{S}$  with reaction time.  $\text{Co-Mo/Al}_2\text{O}_3$ ,  $50 \text{ kg/cm}^2$ ,  $260^\circ\text{C}$ .

4. On the other hand, when  $^{35}\text{S}\text{-DBT}$  solution was replaced by a decalin solvent according to operation procedure 2, the radioactivity of formed  $^{35}\text{S}\text{-H}_2\text{S}$  decreased immediately (Figure 5.1). Compared with the results according to operation procedure 1, obviously, a portion of  $^{35}\text{S}$ , which is represented by the area A in Figure 5.1, remained on the catalyst when the solution of  $^{35}\text{S}\text{-DBT}$  was replaced with a decalin solvent. Even though the catalyst was reduced in an atmosphere of hydrogen for ca 3 h,  $^{35}\text{S}\text{-H}_2\text{S}$  was



hardly produced. This indicates that the sulfur remaining on the catalyst does not release without the supply of sulfur by HDS of DBT as in the case of  $\text{Mo}/\text{Al}_2\text{O}_3$  (Chapter 3). However, when the reactant solution was replaced with  $^{32}\text{S}$ -DBT at 505 min, this portion of  $^{35}\text{S}$  could release as  $^{35}\text{S}\text{-H}_2\text{S}$  again as shown in Figure 5.1 (Area B). Moreover this portion of  $^{35}\text{S}$  (Area B) was approximately equal to the amount of labile sulfur at this reaction condition (Area A or A') as shown in Table 5.1. This portion of  $^{35}\text{S}$  represented the total amount of labile sulfur on the catalyst (2). Thus, it was suggested that the labile sulfur on the catalyst was labeled completely by  $^{35}\text{S}$  through the reaction process from the step (a) to (b). Since the operation procedures from the step (a) to (c) were same for operation procedure 2, the main objective would focus attention on the release rate of  $^{35}\text{S}\text{-H}_2\text{S}$  in the step (d).

### 5.3.2 Effect of Sulfur Compounds on Release Rate of $^{35}\text{S}\text{-H}_2\text{S}$ .

To investigate the effects of sulfur compounds on the substitution rate of sulfur on the catalyst, a decalin solution of 0.73 wt% benzothiophene containing the same molar concentration of sulfur as that of DBT was used in the step (d). The change in radioactivity of formed  $^{35}\text{S}\text{-H}_2\text{S}$  with the reaction time was shown in Figure 5.2. The formation curve of  $^{35}\text{S}\text{-H}_2\text{S}$  was the same as the case of DBT until the step (c). When the reactant solution was changed from decalin to the decalin solution of BT, the formation rate of  $^{35}\text{S}\text{-H}_2\text{S}$ , i.e., the rate which  $^{35}\text{S}$  on the catalyst was replaced by  $^{32}\text{S}$  in benzothiophene, was more rapid than that in the case of  $^{32}\text{S}$ -DBT. As the case of  $\text{Mo}/\text{Al}_2\text{O}_3$  in Chapter 3, this could be attributed to the increase of  $^{32}\text{S}$  incorporated from benzothiophene into the catalyst because HDS rate of benzothiophene (conversion = 100 %) was more rapid than that of DBT (conversion = 60.9 %). Similarly, when a decalin solution of 0.46 wt% thiophene containing same sulfur molar concentration as the solution of DBT was also used to

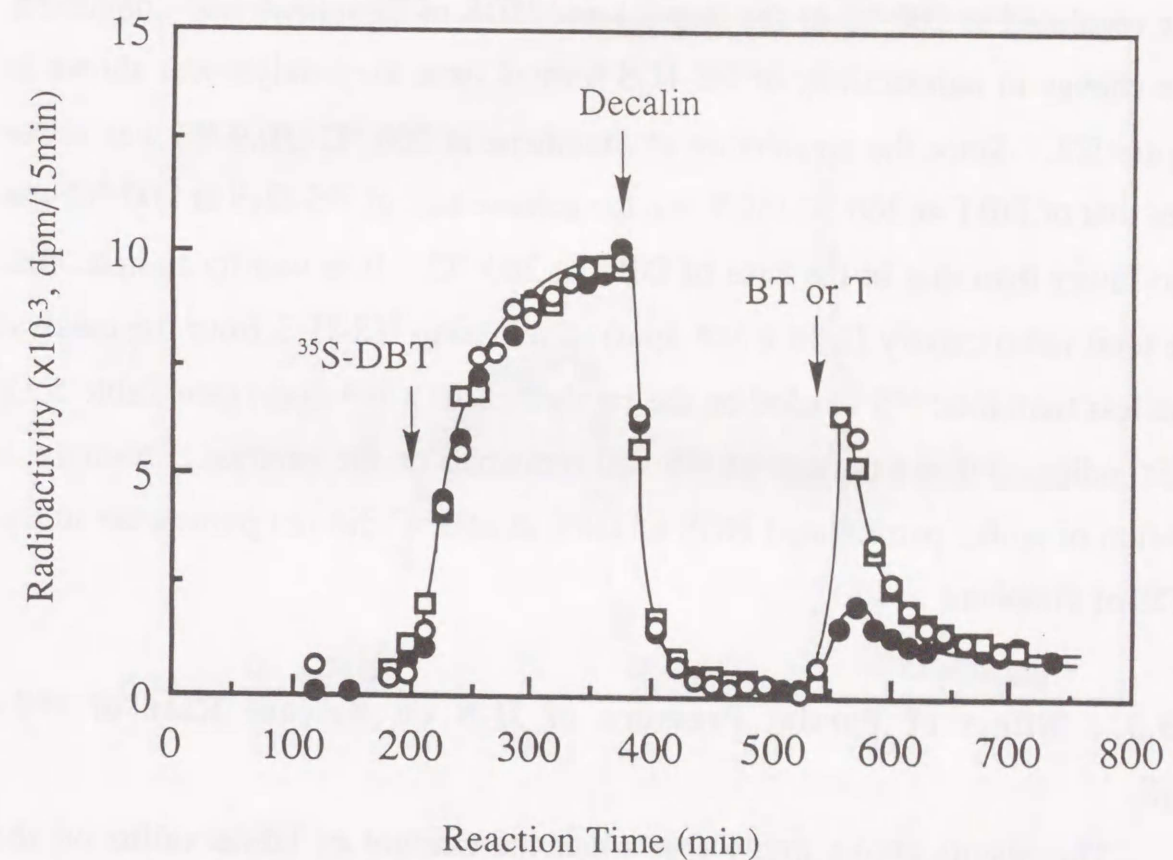


Figure 5.2. Effects of sulfur compounds on the release rate of  $^{35}\text{S}\text{-H}_2\text{S}$ . Co-Mo/ $\text{Al}_2\text{O}_3$ . ○: Thiophene (0.46 wt%, 260°C), ●: Thiophene (0.46%, 200°C), □: Benzothiophene (0.73 wt%, 260 °C), Pressure: 50 kg/cm<sup>2</sup>

conduct the same reaction, a formation curve of  $^{35}\text{S}\text{-H}_2\text{S}$  similar to the case of benzothiophene was obtained, because the conversion of thiophene was also 100 % and the rate of  $^{32}\text{S}$  incorporation was similar as that of benzothiophene. This indicates that the release of  $\text{H}_2\text{S}$  from the catalyst is independent from the kinds of sulfur compounds but only dependent upon the rate of sulfur incorporated into the catalyst.



To investigate the effects of the rate of sulfur incorporated onto the catalyst on the removal rate of  $^{35}\text{S}$  from the catalyst, the reaction temperature was regulated to  $200\text{ }^\circ\text{C}$  in the step (c) and HDS of thiophene was conducted. The change in radioactivity of  $^{35}\text{S}\text{-H}_2\text{S}$  formed from the catalyst was shown in Figure 5.2. Since the conversion of thiophene at  $200\text{ }^\circ\text{C}$  (30.9 %) was lower than that of DBT at  $260\text{ }^\circ\text{C}$  (60.9 %), the release rate of  $^{35}\text{S}\text{-H}_2\text{S}$  at  $200\text{ }^\circ\text{C}$  was also lower than that in the case of DBT at  $260\text{ }^\circ\text{C}$ . It is worthy to note, that the total radioactivity ( $1.58 \times 10^4$  dpm) of releasing  $^{35}\text{S}\text{-H}_2\text{S}$  from the catalyst was less than total  $^{35}\text{S}$  labeled on the catalyst ( $2.76 \times 10^4$  dpm) (see Table 5.1). This indicated that a portion of  $^{35}\text{S}$  still remained on the catalyst. Namely, a portion of sulfur participated HDS of DBT at  $260\text{ }^\circ\text{C}$  did not participate in the HDS of thiophene at  $200\text{ }^\circ\text{C}$ .

### 5.3.3 Effect of Partial Pressure of $\text{H}_2\text{S}$ on Release Rate of $^{35}\text{S}\text{-H}_2\text{S}$ .

The results above imply that when the amount of labile sulfur on the catalyst is a constant, the release rate of  $\text{H}_2\text{S}$  from labile sulfur on the catalyst seems to depend on the atmosphere of reactant during the HDS reaction. Thus, the behavior of sulfur on the catalyst in atmosphere of  $\text{H}_2\text{S}$  was investigated. A mixed gas of  $\text{H}_2\text{S}$  and  $\text{H}_2$  was substituted for the atmosphere of  $\text{H}_2$  in the step (d).

When the catalyst was labeled by  $^{35}\text{S}$  during HDS of  $^{35}\text{S}\text{-DBT}$  at  $50\text{ kg/cm}^2$  and  $260\text{ }^\circ\text{C}$ , then it was purged with  $\text{H}_2$  and the temperature was regulated to  $200\text{ }^\circ\text{C}$ . When replacing  $\text{H}_2$  with a gas of 3.4 vol%  $^{35}\text{S}\text{-H}_2\text{S}$  in  $\text{H}_2$  at  $50\text{ kg/cm}^2$  the change in radioactivities of formed  $^{35}\text{S}\text{-H}_2\text{S}$  with the reaction time was shown in Figure 5.3. It should be noted that decalin solvent still flowed through the catalyst in the step (d) in order to maintain a consistence of the reaction conditions. Although  $^{35}\text{S}\text{-H}_2\text{S}$  was hardly produced when only  $\text{H}_2$

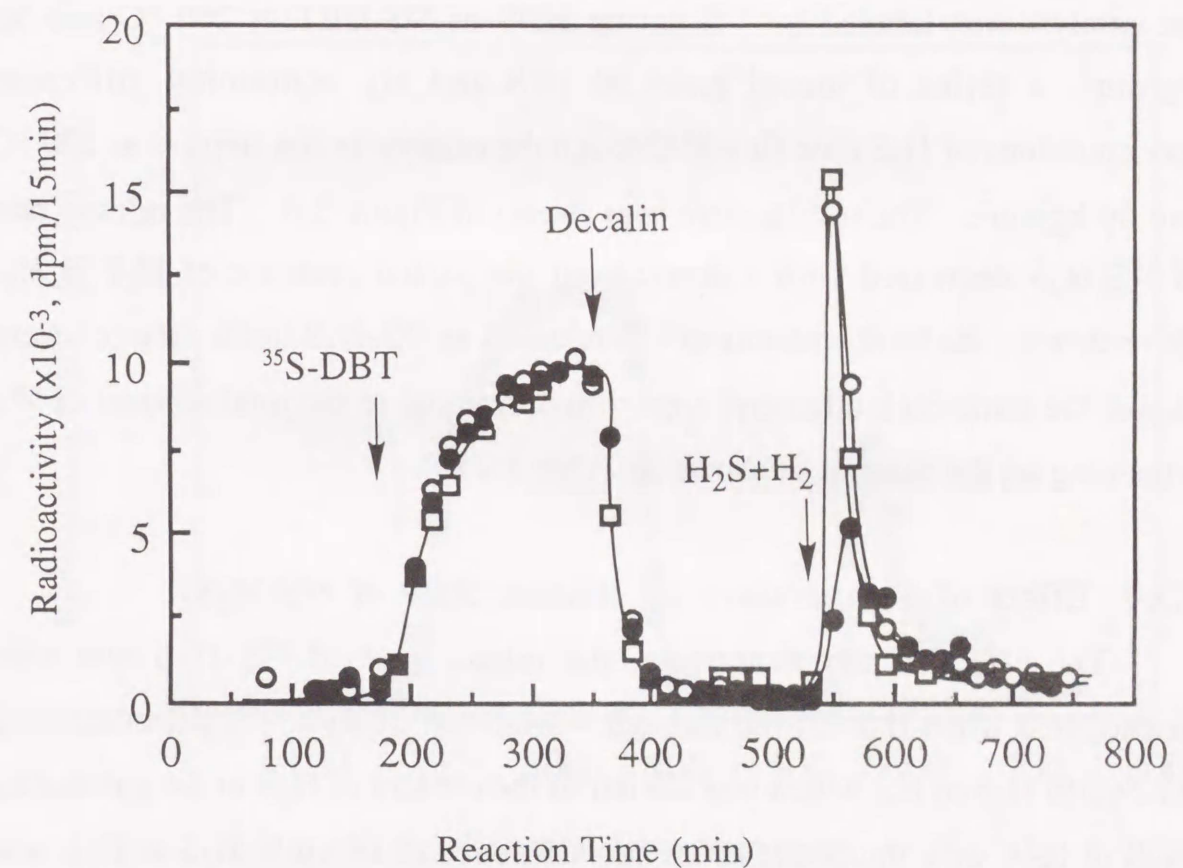


Figure 5.3. Effects of concentrations of  $\text{H}_2\text{S}$  in  $\text{H}_2$  on the release rate of  $^{35}\text{S}\text{-H}_2\text{S}$  in the exchange reaction.

□: 3.4 %  $\text{H}_2\text{S}$ , ○: 0.72 %  $\text{H}_2\text{S}$ , ●: 0.12 %  $\text{H}_2\text{S}$ .

Co-Mo/ $\text{Al}_2\text{O}_3$ , Pressure:  $50\text{ kg/cm}^2$ , Temperature:  $200\text{ }^\circ\text{C}$

flowed throughout the catalyst,  $^{35}\text{S}$  remaining on the catalyst released as  $^{35}\text{S}\text{-H}_2\text{S}$  again after introducing  $\text{H}_2\text{S}$  and the release rate of  $^{35}\text{S}\text{-H}_2\text{S}$  from the catalyst was more rapid than that in the case of sulfur compounds. Moreover, the total amount of  $^{35}\text{S}$  released in the step (d) was approximately equal to one remaining on the catalyst as shown in Table 5.1. This indicates that labile



sulfur can elute as H<sub>2</sub>S from the catalyst with the dissociation of H<sub>2</sub>S adsorbed on the catalyst. In order to survey the effect of the partial pressure of H<sub>2</sub>S, the catalyst was labeled by <sup>35</sup>S during HDS of <sup>35</sup>S-DBT at 260 °C and 50 kg/cm<sup>2</sup>, a series of mixed gases of H<sub>2</sub>S and H<sub>2</sub> containing different concentrations of H<sub>2</sub>S then flowed through the catalyst in the step (d) at 200 °C and 50 kg/cm<sup>2</sup>. The results were also shown in Figure 5.3. The release rate of <sup>35</sup>S-H<sub>2</sub>S decreased with a decrease in the partial pressure of H<sub>2</sub>S in H<sub>2</sub>. Nevertheless, the total amounts of <sup>35</sup>S released as <sup>35</sup>S-H<sub>2</sub>S in the step (d) were almost the same each other and approximately equal to the total amount of <sup>35</sup>S remaining on the catalyst as shown in Table 5.1.

#### 5.3.4 Effect of Temperature on Release Rate of <sup>35</sup>S-H<sub>2</sub>S.

The effect of temperature on the release rate of <sup>35</sup>S-H<sub>2</sub>S was also investigated when H<sub>2</sub>S flowed through <sup>35</sup>S-labeled catalyst. A gas containing 0.12 vol% H<sub>2</sub>S in H<sub>2</sub>, which was similar to the content of H<sub>2</sub>S in the gas during HDS of 0.46 wt% thiophene as mentioned above (0.14 vol% H<sub>2</sub>S in H<sub>2</sub>), was used in operation step (d) of operation procedure 2 at 260 °C and 50 kg/cm<sup>2</sup>. The change in radioactivity of formed <sup>35</sup>S-H<sub>2</sub>S with the reaction time was shown in Figure 5.4. The formation curve of <sup>35</sup>S-H<sub>2</sub>S was very similar to that in the case where 0.46 wt% thiophene was used as shown in Figure 5.2. This implies that the formation process of H<sub>2</sub>S from the catalyst seems to be the same either for the HDS reaction of sulfur compounds or for the exchange reaction with H<sub>2</sub>S. When the temperature was regulated in operation step (c), the changes in radioactivities of formed <sup>35</sup>S-H<sub>2</sub>S at 200°C and 230°C were also shown in Figure 5.4. The release rate of <sup>35</sup>S-H<sub>2</sub>S merely varied with temperature in a small degree. This may be because the desorption process of H<sub>2</sub>S formed from the labile sulfur on the catalyst was the limiting-rate step of this exchange reaction.

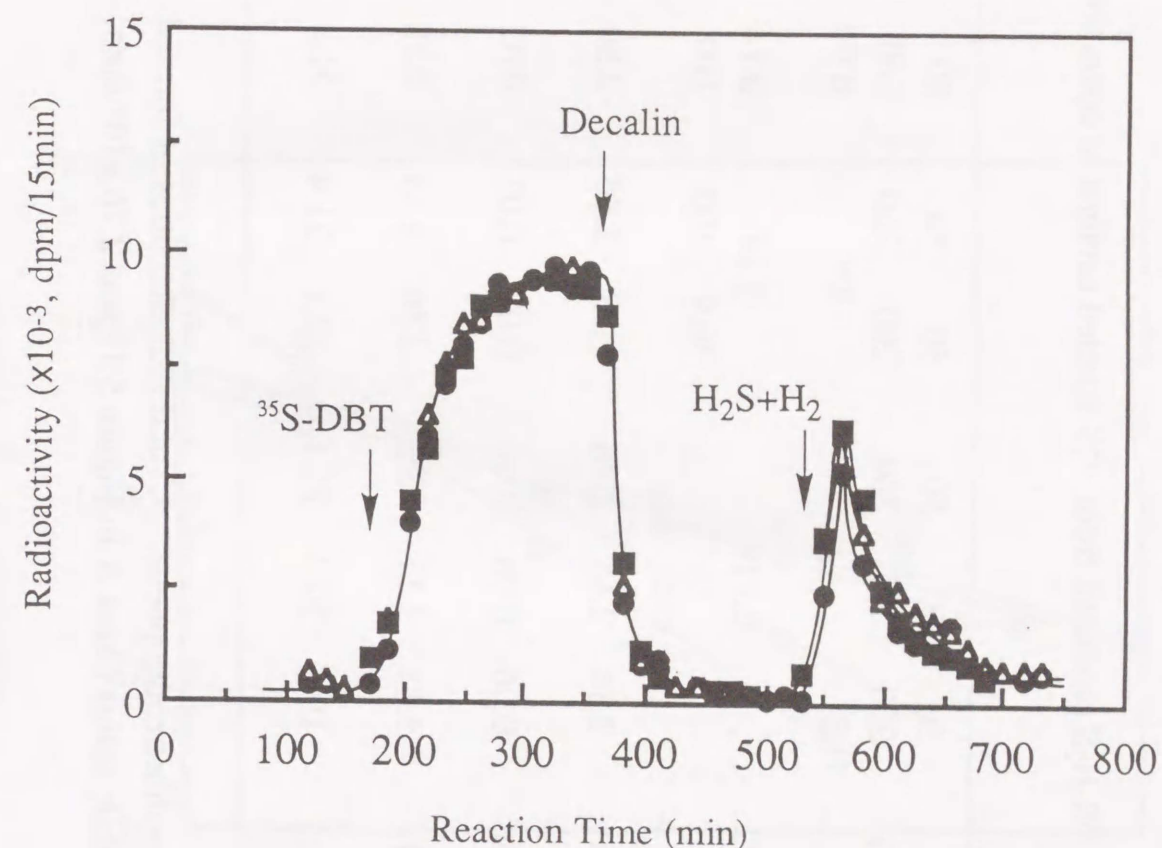


Figure 5.4. Effects of temperatures on the release rate of <sup>35</sup>S-H<sub>2</sub>S

●: 200 °C, △: 230 °C, ■: 260 °C,  
Co-Mo/Al<sub>2</sub>O<sub>3</sub>, Pressure: 50 kg/cm<sup>2</sup>, H<sub>2</sub>S: 0.12 %

#### 5.3.5 Release Rate Constant of <sup>35</sup>S-H<sub>2</sub>S

In Refs. 2 and 3, we postulated that, when the solution of <sup>32</sup>S-DBT was substituted for that of <sup>35</sup>S-DBT, the release rate of <sup>35</sup>S-H<sub>2</sub>S from the catalyst conformed to a first order equation. For the reactions in this work, we tried to treat the change in radioactivity of eluted <sup>35</sup>S-H<sub>2</sub>S as a first order reaction. The first order plot of the radioactivity of produced <sup>35</sup>S-H<sub>2</sub>S also indicated the



Table 5.1. Kinetic parameters and radioactivities of  $^{35}\text{S}\text{-H}_2\text{S}$  produced from  $^{35}\text{S}$ -labeled catalyst in operation step (d).

Pressure, $\text{kg}/\text{cm}^2$	50	50	50	50	50	50	50	50	50
Temperature, $^\circ\text{C}$	200	200	200	230	260	200	260	260	260
Concentration of reactant			$\text{H}_2\text{S}$			$\text{T}^{\text{a}}$		$\text{BT}^{\text{b}}$	$\text{DBT}^{\text{c}}$
in Gas, vol %	3.42	0.72		0.119		0.14		0.14	0.14
Conversion, %						30.9	100	100	60.9
Total radioactivity <sup>d</sup> , $\times 10^4$ , dpm	2.75	2.81	2.54	2.65	2.76	1.58	2.80	2.80	2.80
Partial pressure of $\text{H}_2\text{S}$ in Gas, $\text{kg}/\text{cm}^2$	1.71	0.36	0.06	0.06	0.06	0.02	0.07	0.07	0.04
Rate constant, $k$ , $\times 10^{-2}$ , $\text{dpm}/\text{min}/\text{g}$ of cat.	7.49	6.14	3.01	3.11	3.22	2.36	3.23	3.18	2.60
Labile sulfur, $\text{mg}$ of $\text{S}/\text{g}$ of cat.	21.0	21.5	19.4	20.3	21.1	12.1	21.4	21.4	21.4

<sup>a</sup> T = thiophene. <sup>b</sup> BT = benzothiophene. <sup>c</sup> DBT = dibenzothiophene. <sup>d</sup> Total radioactivities of formed  $^{35}\text{S}\text{-H}_2\text{S}$  in the step (d). <sup>e</sup> Total radioactivities of labile sulfur (Area A in Figure 5.1) was  $2.76 \times 10^4$  dpm.

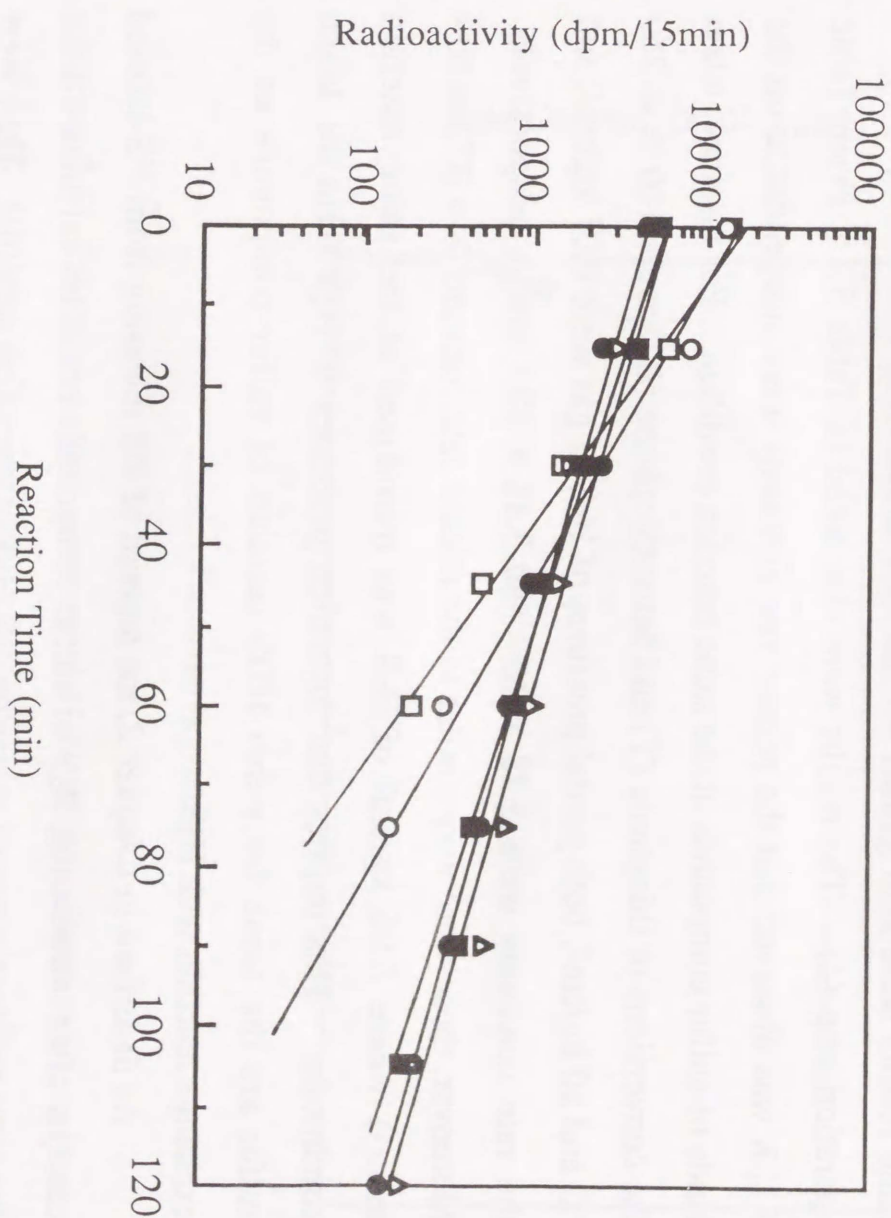


Figure 5.5. First-order plots of the release rate of  $^{35}\text{S}\text{-H}_2\text{S}$ . Symbols and reaction condition see Figures 3 and 4.

linear relationship as shown in Figure 5.5. These curves can be expressed as a function of time:

$$\ln y = \ln z - kt \quad \text{or} \quad y = z e^{-kt} \quad (5.1)$$



where  $y$  denotes the release rate of  $^{35}\text{S-H}_2\text{S}$  at time  $t$  (dpm/min);  $z$  a constant (dpm/min);  $k$  the release rate constant of  $^{35}\text{S-H}_2\text{S}$  ( $\text{min}^{-1}$ );  $t$  the reaction time (min). The release rate constant of elution of  $^{35}\text{S}$  from the catalyst were determined from the slope of linear relationship and listed in Table 5.1. The same results were also gained for the case introducing sulfur compounds in operation step (d). The results were also listed in Table 5.1. From Table 5.1, it was observed that the release rate constants were independence on the kinds of sulfur compounds at the same reaction condition. For instance, when the conversions of thiophene (T) and benzothiophene (BT) were 100 % at 260 °C and 50  $\text{kg/cm}^2$ , both partial pressures of  $\text{H}_2\text{S}$  in gas were 0.07  $\text{kg/cm}^2$ , and the rate constants were  $3.23 \times 10^{-2}$  and  $3.18 \times 10^{-2} \text{ min}^{-1}$ , respectively. Moreover, these were very similar to the release rate constant ( $k = 3.22 \times 10^{-2} \text{ min}^{-1}$ ) where 0.06  $\text{kg/cm}^2$  of  $\text{H}_2\text{S}$  was introduced at the same reaction conditions. This implies that formation processes of  $\text{H}_2\text{S}$  from the labile sulfur are the same for either HDS reaction of sulfur compounds or the exchange reaction with  $\text{H}_2\text{S}$ .

As described in *Chapter 2*, the amount of  $^{35}\text{S}$  releasing from  $^{35}\text{S}$ -labeled catalyst after introducing  $\text{H}_2\text{S}$  or sulfur compounds could be calculated from the total radioactivities of releasing  $^{35}\text{S-H}_2\text{S}$  in operation step (d). They were listed in Table 5.1. These amounts represented the amount of labile sulfur under these reaction conditions. Except for the results in the case of thiophene at 200 °C, the amounts of labile sulfur at various reaction conditions were similar each other. This may be because all partial pressures of  $\text{H}_2\text{S}$  in gas except for the case of thiophene at 200 °C were the same or more than the partial pressure of  $\text{H}_2\text{S}$  when the catalyst was labeled with  $^{35}\text{S}$ . This implies that the amount of labile sulfur only depends on the extent of  $\text{H}_2\text{S}$  in gas.

When the release rate constants of  $^{35}\text{S-H}_2\text{S}$  were plotted against the partial pressures of  $\text{H}_2\text{S}$ , an adsorption curve of the Langmuir type was

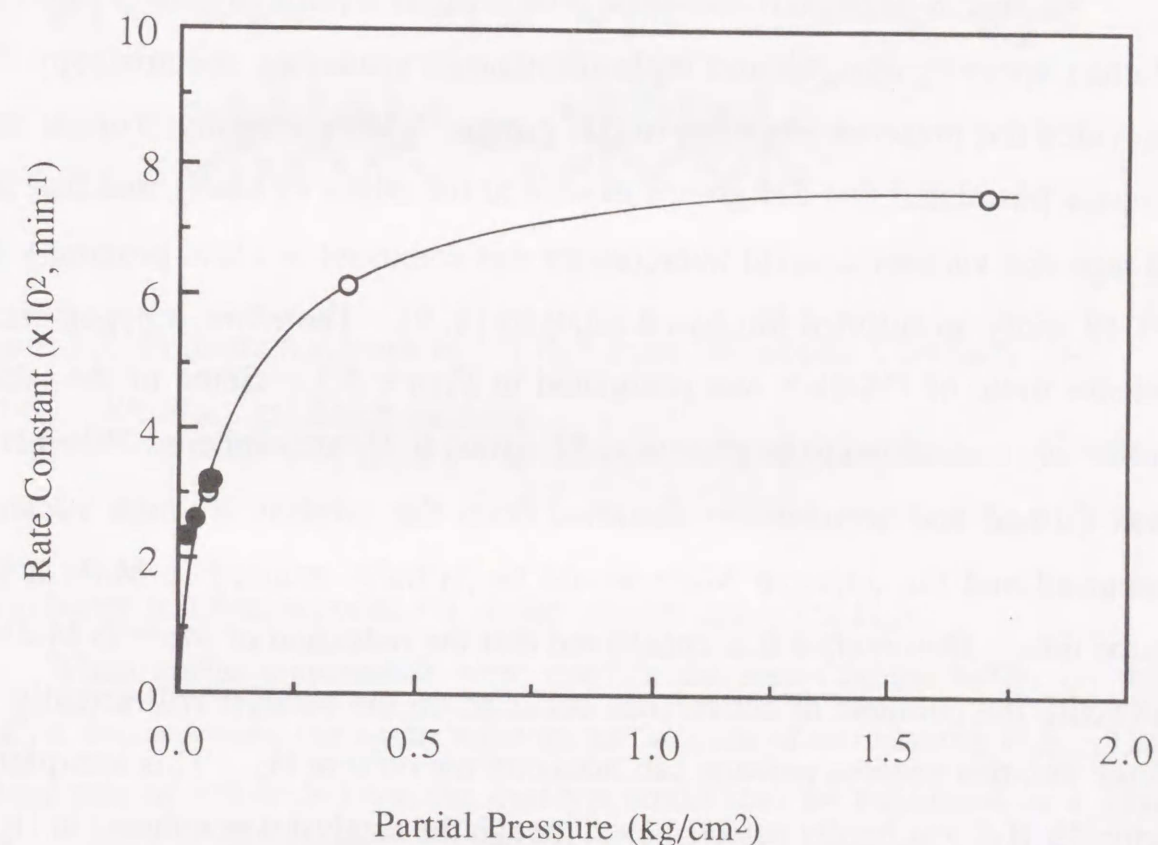


Figure 5.6. Effect of partial pressure of  $\text{H}_2\text{S}$  on the release rate constant of  $^{35}\text{S-H}_2\text{S}$ . Co-Mo/ $\text{Al}_2\text{O}_3$ , Pressure: 50  $\text{kg/cm}^2$ .

obtained as shown in Figure 5.6. The release rate constants of  $^{35}\text{S-H}_2\text{S}$  almost trend toward a constant value above 0.36  $\text{kg/cm}^2$  of partial pressure of  $\text{H}_2\text{S}$ . This means that the adsorption of  $\text{H}_2\text{S}$  on the catalyst approached a saturated state under present reaction conditions. The release of  $^{35}\text{S-H}_2\text{S}$  from the catalyst could be considered to be the determining-rate step for the exchange reaction.



## 5.4 Discussion

Studies of deuterium exchange (4), chemical titration by silver ions (5), Raman spectroscopy (6) and inelastic neutron scattering spectroscopy (7) provided the presence evidence of SH groups. More recently, Topsøe and Topsøe postulated that SH groups existed at the edges of  $\text{MoS}_2$ , and that SH groups and vacancies could interconvert and coexisted in close proximity by FT-IR study on sulfided Mo-based catalysts (8, 9). Therefore, a hypothetical release route of  $^{35}\text{S}\text{-H}_2\text{S}$  was postulated in Figure 5.7. Some of the labile sulfur was considered to be present as SH group in  $\text{H}_2$  atmosphere. When  $\text{H}_2\text{S}$  was formed and sequentially desorbed from the catalyst, an anion vacancy occurred and the adjacent  $\text{Mo}^{4+}$  would be partially reduced to  $\text{Mo}^{3+}$  at the same time. However, if it is considered that the reduction of  $\text{Mo}^{4+}$  to  $\text{Mo}^{3+}$  is difficult, the numbers of active sites occurred on the catalyst will actually be finite and this process perhaps can not continue only in  $\text{H}_2$ . This interpreted why  $^{35}\text{S}\text{-H}_2\text{S}$  was hardly detected even though the catalyst was reduced in  $\text{H}_2$  in the step (c). On the other hand, adsorbed  $\text{H}_2\text{S}$  dissociated and formed new SH groups with adjacent labile sulfur due to the mobility of hydrogen atom after introducing  $\text{H}_2\text{S}$ . The old anion vacancy disappears and the formation process of new anion vacancy was maintained after the desorption of  $\text{H}_2\text{S}$  formed from the labile sulfur. Thus,  $^{35}\text{S}$  remaining on the catalyst was replaced gradually by  $^{32}\text{S}$  and released as  $^{35}\text{S}\text{-H}_2\text{S}$  with the introduction of  $\text{H}_2\text{S}$ . McGarvey and Kasztelan postulated that at temperatures normally used in hydroprocessing reactions (less than  $420^\circ\text{C}$ ) almost only  $\text{Mo}^{4+}$  was present on the surface and there were very low concentrations of  $\text{Mo}^{<4+}$  ions which played an important catalytic role (10). This was consistent with our mechanism. Because the adsorption of  $\text{H}_2\text{S}$  on the catalyst was in saturated state, it would be suggested that the desorption of  $^{35}\text{S}\text{-H}_2\text{S}$  from the catalyst would be the determining-rate

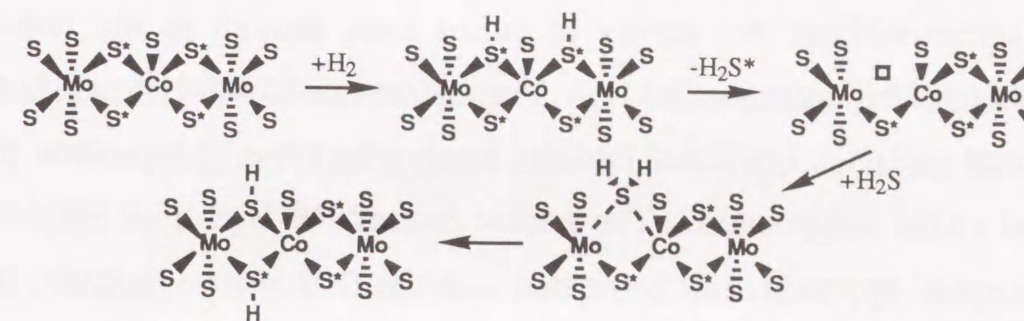


Figure 5.7. Formation scheme of  $^{35}\text{S}\text{-H}_2\text{S}$  from  $^{35}\text{S}$ -labeled  $\text{Co-Mo}/\text{Al}_2\text{O}_3$ .  
S:  $^{32}\text{S}$ , S\*:  $^{35}\text{S}$ , □: Anion vacancy.

of exchange reaction between  $^{35}\text{S}$  on the catalyst and  $^{32}\text{S}$  in  $\text{H}_2\text{S}$ .

When sulfur compounds were used in the step (d), the sulfur on the catalyst demonstrated the same behavior as the case of introducing  $\text{H}_2\text{S}$ . The release rate of  $^{35}\text{S}\text{-H}_2\text{S}$  from the catalyst could also be expressed as a first order equation. This implies that the formation process of  $^{35}\text{S}\text{-H}_2\text{S}$  from the catalyst was the same as that in the case where only  $\text{H}_2\text{S}$  was used. This further supported the scheme proposed previously in *Chapter 4*, i.e., some of labile sulfur can easily form SH group in  $\text{H}_2$ , subsequently, the release of  $\text{H}_2\text{S}$  formed the anion vacancies. Thus, the adsorption capacity of sulfur compounds on the catalyst and the cleavage easiness of C-S bonds caused the difference of HDS conversion for various sulfur compounds.

## 5.5 Conclusions

The present study provided further information about the behavior of sulfur on the catalyst during the HDS reaction or exchange reaction with  $\text{H}_2\text{S}$ .



Similar to the Mo/Al<sub>2</sub>O<sub>3</sub> catalyst in *Chapter 3*, H<sub>2</sub>S could not form from the labile sulfur without the supply of sulfur even though in the reduction atmosphere of high pressure of H<sub>2</sub>. The release rate of <sup>35</sup>S-H<sub>2</sub>S depends the amount of sulfur incorporated into the catalyst and was independent of the kinds of sulfur compounds. The release rate of <sup>35</sup>S-H<sub>2</sub>S from <sup>35</sup>S-labeled catalyst could approximately be treated with the first order equation. When the partial pressure of H<sub>2</sub>S during HDS of sulfur compounds is similar to the case of introducing H<sub>2</sub>S, the release rates of <sup>35</sup>S-H<sub>2</sub>S from the catalyst were similar for two cases. This indicates that the formation process of <sup>35</sup>S-H<sub>2</sub>S from the catalyst during HDS reaction is the same as the case of the exchange reaction with H<sub>2</sub>S. Moreover, the release rate constants of <sup>35</sup>S-H<sub>2</sub>S trend toward to a constant value above 0.36 kg/cm<sup>2</sup> of the partial pressure of H<sub>2</sub>S. This indicated that the adsorption of H<sub>2</sub>S onto the active sites approached a saturated state in present reaction conditions. The desorption of H<sub>2</sub>S from the catalyst may be the determining-rate step of this reaction.

## References

1. Kabe, T., Qian, W., and Ishihara, A., *J. Phys. Chem.*, **98**, 912 (1994).
2. Kabe, T., Qian, W., Ogawa, S., and Ishihara, A., *J. Catal.*, **143**, 239 (1993).
3. Kabe, T., Qian, W., and Ishihara, A., *J. Catal.*, **149**, 171 (1994).
4. Massoth, F. E., *J. Catal.* **36**, 164 (1975).
5. Maternova, J., *Appl. Catal.*, **3**, 3 (1982).
6. Payen, E., Kasztelan, S., and Grimblot, J., *J. Mol. Struct.*, **174**, 71 (1988).
7. Wright, C., J., Sampson, C., Fraser, D., Moyes, R. B., Wells, P. B., and Riekel, C., *J. Chem. Soc., Faraday Trans. 1*, **76**, 1585 (1980).
8. Topsøe, N.-Y., and Topsøe, H., *J. Catal.*, **139**, 631 (1993).
9. Topsøe, N.-Y., and Topsøe, H., *J. Catal.*, **139**, 641 (1993).
10. McGarvey, G., B., and Kasztelan, S., *J. Catal.*, **148**, 149 (1994).



Chapter Six

**Behavior of Sulfur on  $^{35}\text{S}$ -Labeled Co-Mo/ $\text{Al}_2\text{O}_3$  in  
Hydrodesulfurization of 4-Methyldibenzothiophene  
and 4, 6-Dimethyldibenzothiophene**



## Chapter Six

### Behavior of Sulfur on $^{35}\text{S}$ -Labeled Co-Mo/ $\text{Al}_2\text{O}_3$ in Hydrodesulfurization of 4-Methyldibenzothiophene and 4, 6-Dimethyldibenzothiophene

#### Abstract

A commercial Co-Mo/ $\text{Al}_2\text{O}_3$  catalyst was labeled by  $^{35}\text{S}$  during HDS of  $^{35}\text{S}$ -DBT. Then the HDS reaction of 4-methyldibenzothiophene (4-MDBT) and 4, 6-dimethyldibenzothiophene (4, 6-DMDBT) were carried out on this catalyst. The behavior of sulfur on the catalyst was quantified tracing the change in the radioactivity of  $^{35}\text{S}$ - $\text{H}_2\text{S}$  released from  $^{35}\text{S}$ -labeled catalyst during the HDS reaction of methyl-substituted DBTs. Under the same reaction condition, only a portion of labile sulfur participating the HDS reaction of DBT participated the HDS reaction of 4-MDBT and 4, 6-DMDBT and the amount of labile sulfur varied with the kinds of sulfur compounds as follows: DBT > 4-MDBT > 4, 6-DMDBT. Moreover, the reaction rate was approximately proportional to the amount of labile sulfur at lower HDS reaction rate range. This means that the number of active sites was proportional to the amount of labile sulfur at lower HDS rate. Compared with DBT, the number of active sites participating the HDS reaction of methyl-substituted DBTs decreased because of the existence of methyl groups.



## 6.1 Introduction

Since the environment regulations become increasingly strict, much attention has been focused on deep hydrodesulfurization (HDS) of light oil. It is well known that methyl substitution at 4 and 6-position of dibenzothiophene (DBT) remarkably retarded the rate of HDS (1-3). In a direct HDS of middle distillate of Arabian light oil, 6% of 4-methyldibenzothiophene (4-MDBT) and 50% of 4, 6-dimethyldibenzothiophene (4, 6-DMDBT) remained still even though the total conversion of sulfur compounds yielded more than 90% (3). Amorelli et al. also reported a similar result in the characterization of sulfur compounds in deep hydrotreating of middle distillates (4). This result confirms those of Kilanowski et al. (5) and Houalla et al. (6) in model HDS reaction. In order to reach deep desulfurization of light oil (sulfur contents < 0.05wt%), it is necessary to investigate the effect of methyl substituents on HDS of dibenzothiophenes. It was suggested that the retarding effect of the methyl substitution on HDS rates of DBTs was not attributed to the hindrance of adsorption of DBTs on the catalyst but to the steric hindrance in the C-S bond scission of the adsorbed DBTs (7). Obviously, the comprehension on the retarding effect of the methyl substitution was not sufficient. On the other hand, the radioisotope tracer method made it possible to more directly estimate the behavior of sulfur during HDS reaction when the radioactive  $^{35}\text{S}$  labeled dibenzothiophene ( $^{35}\text{S}$ -DBT) were carried out on Mo-based catalysts (8-11). Recently, it was suggested that the reactivity of catalysts was involved in the amount of labile sulfur and regeneration rate of active sites (11).

In this chapter, we will investigate what is behavior of sulfur on the catalyst during HDS reaction of methyl-substituted dibenzothiophenes so that further comprehending the retarding effect of methyl-substituents. Because of the difficulty of synthesis of  $^{35}\text{S}$ -labeled methyl-substituted dibenzo-

thiophene, we attempted to establish a relatively simple method to investigate the behavior of sulfur during HDS reaction of 4-MDBT or 4, 6-DMDBT in the present study. A commercial Co-Mo/ $\text{Al}_2\text{O}_3$  catalyst was labeled by  $^{35}\text{S}$  during HDS of  $^{35}\text{S}$ -DBT, then the HDS reaction of 4-MDBT and 4, 6-DMDBT were carried out on this catalyst. The behavior of sulfur on the catalyst was quantified tracing the change in the radioactivity of  $^{35}\text{S}$ - $\text{H}_2\text{S}$  released from  $^{35}\text{S}$ -labeled catalyst during HDS of methyl-substituted DBT.

## 6.2 Experimental

### 6.2.1 Materials

Decalin was a commercial GR grade from Kishida Co. Ltd. Dibenzothiophene ( $^{32}\text{S}$ -DBT), 4-methyldibenzothiophene and 4, 6-dimethyldibenzothiophene (4, 6-DMDBT) were synthesized by reported methods (7).  $^{35}\text{S}$ -labeled dibenzothiophene ( $^{35}\text{S}$ -DBT,  $1.14 \times 10^6$  dpm/g) was synthesized according to the method reported in previous paper (10). Hydrogen was obtained from Tohei Chemicals. Hydrogen sulfide in hydrogen ( $\text{H}_2\text{S}:\text{H}_2 = 5:95$ ) was from Takachio Chemicals. The catalyst was a commercial Co-Mo/ $\text{Al}_2\text{O}_3$  (Ketjen fine 124,  $\text{MoO}_3$ : 12.3 wt%, CoO: 3.8 wt%, Surface area:  $274 \text{ m}^2/\text{g}$ ). It was supplied as a 1/32 cylindrical extrudate which was crushed and screened to provide 0.42-0.84 mm granules used in this work.

### 6.2.2 Apparatus and Procedure

The HDS reactions were carried out on a high-pressure-flow microreactor. The reactor was 4 mm I.D. stainless steel tube packed with 0.2 g of catalyst particles. After calcined at  $450^\circ\text{C}$  in air overnight, the catalyst was presulfided using a gas mixture of 5 %  $\text{H}_2\text{S}$  in  $\text{H}_2$  flowing at 5 liters/h at  $400^\circ\text{C}$  and atmospheric pressure for 3 h. After sulfiding, the temperature



was lowered to the desired temperature and the reactor was pressurized with hydrogen. Then, the reactant was supplied with a feed pump (Kyowa Seimitsu KHD-16). HDS reaction was carried out under the following reaction conditions: temperature: 260-360 °C; WHSV: 28-70 h<sup>-1</sup>; initial concentrations of DBTs: 0.1-3.0 wt%. Products were analyzed by a gas chromatography with an FID detector (Hitachi-163). The produced H<sub>2</sub>S was absorbed by bubbling through a commercial basic scintillator solution (Carbosorb, Packard Co. Ltd.). The radioactivities of produced <sup>35</sup>S-H<sub>2</sub>S and unreacted <sup>35</sup>S-DBT were measured by a liquid scintillation counter (LSC-II, Aloka Co. Ltd.).

Typical operation procedures were as follows: (a) A decalin solution of 1.0 wt% <sup>32</sup>S-DBT was pumped into the reactor until the conversion of DBT became constant (ca 2.5 h). (b) After that, the reactant solution was switched to a decalin solution of 1.0 wt% <sup>35</sup>S-DBT. The reaction was performed until the amount of <sup>35</sup>S-H<sub>2</sub>S released from the exit of reactor became constant (ca. 2.5 h). (c) The reactant solution of <sup>35</sup>S-DBT was replaced by decalin and the catalyst was purged by H<sub>2</sub> for ca. 2 h and temperature was regulated to a desired one. (d) Finally, a decalin solution of 4-methyldibenzothiophene or 4,6-dimethyldibenzothiophene was substituted for decalin and was reacted for ca. 3.5 h.

The labile sulfur on the catalyst was labeled by <sup>35</sup>S in the step (b). The catalyst was purged by H<sub>2</sub> in the step (c) to remove any adsorbed <sup>35</sup>S species. Then, the decalin solution of sulfur compounds was introduced into the catalyst in the step (d). The behavior of labile sulfur on the catalyst was estimated by tracing the change in radioactivity of formed <sup>35</sup>S-H<sub>2</sub>S. The total pressure was maintained at 50 kg/cm<sup>2</sup> and the reaction temperature was 340 °C from the step (a) to (c) for all reaction except of indicating elsewhere.

### 6.3 Results

#### 6.3.1 Label of Labile Sulfur on Catalyst during HDS of <sup>35</sup>S-DBT.

Figure 6.1 displays the change in radioactivity of formed <sup>35</sup>S-H<sub>2</sub>S with the reaction time at 340 °C, 50 kg/cm<sup>2</sup> and WHSV 70 h<sup>-1</sup>. After the solution of <sup>35</sup>S-DBT was substituted for that of <sup>32</sup>S-DBT, about 70 min was needed to approach the steady state in radioactivities of produced <sup>35</sup>S-H<sub>2</sub>S. However, when <sup>35</sup>S-DBT solution was replaced by decalin solvent, the change in the radioactivity of formed <sup>35</sup>S-H<sub>2</sub>S decreased immediately as shown in Figure 6.1. As reported in *Ref. 10*, this indicated that a portion of <sup>35</sup>S (Area A) remained

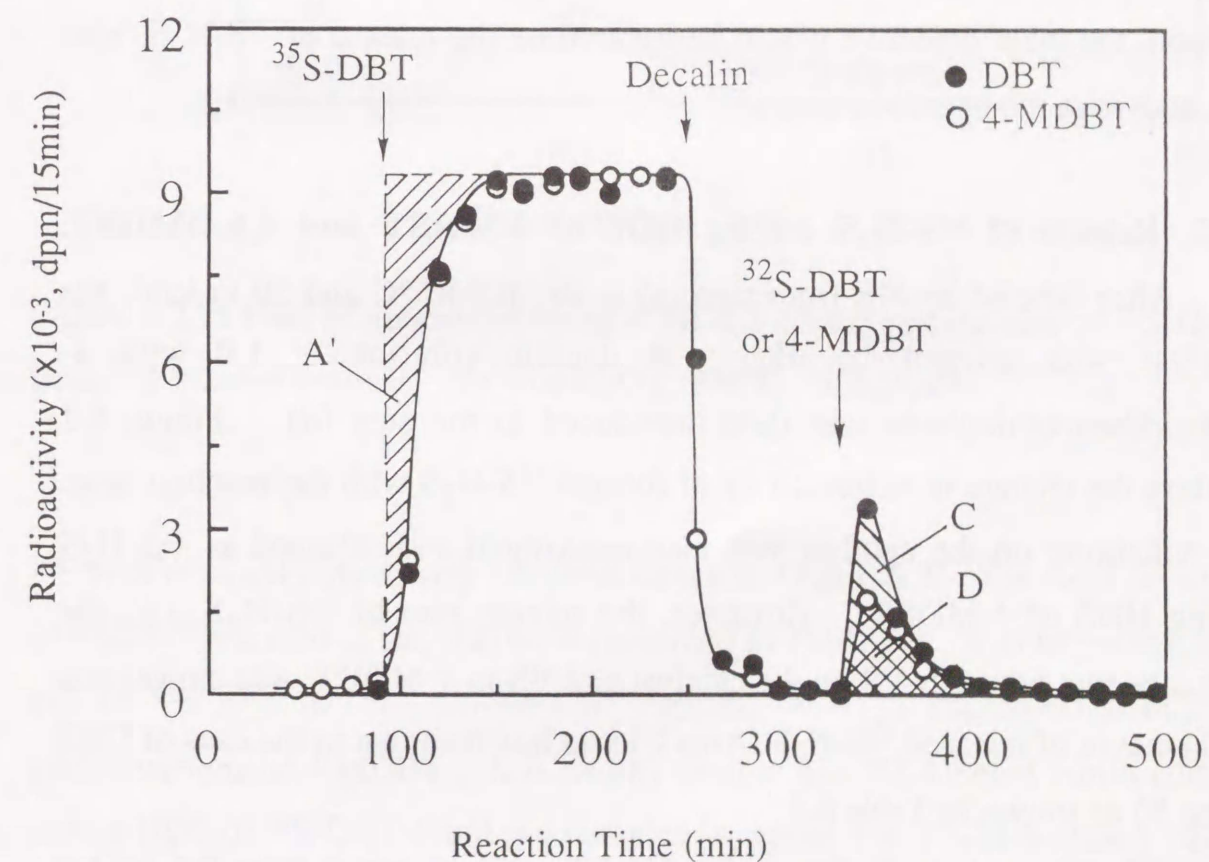


Figure 6.1. Change in radioactivity of formed <sup>35</sup>S-H<sub>2</sub>S with reaction time. Co-Mo/Al<sub>2</sub>O<sub>3</sub>, 340°C, 50kg/cm<sup>2</sup>.



on the catalyst when the solution of  $^{35}\text{S}$ -DBT was replaced with a decalin solvent. Even though the catalyst was reduced in an atmosphere of high pressure of hydrogen for ca. 2 h,  $^{35}\text{S}$ - $\text{H}_2\text{S}$  was hardly produced. On the other hand, when the reactant solution was replaced with  $^{32}\text{S}$ -DBT at 310 min in Figure 6.1, this portion of  $^{35}\text{S}$  could release as  $^{35}\text{S}$ - $\text{H}_2\text{S}$  again as shown in Figure 6.1 (Area B). This portion of  $^{35}\text{S}$ , which was  $1.20 \times 10^4$  dpm and approximately equal to Area A, represented the total amount of labile sulfur on the catalyst. Thus, one can consider that the labile sulfur on the catalyst was completely labeled by  $^{35}\text{S}$  through the reaction process from the step (a) to (c). At the same time, total radioactivity of releasing  $^{35}\text{S}$ - $\text{H}_2\text{S}$  in the step (d) represented the amount of labile sulfur participating HDS in the step (d). Since the operation procedures from the step (a) to (c) were the same for all reaction, the main objective would be focused on the release of  $^{35}\text{S}$ - $\text{H}_2\text{S}$  from the catalyst in the operation step (d).

### 6.3.2 Release of $^{35}\text{S}$ - $\text{H}_2\text{S}$ during HDS of 4-MDBT and 4,6-DMDBT.

After labeled by  $^{35}\text{S}$  from step (a) to (b) at  $340^\circ\text{C}$  and  $50\text{ kg/cm}^2$ , the catalyst was purged by  $\text{H}_2$ . A decalin solution of 1.0 wt% 4-methyldibenzothiophene was then introduced in the step (d). Figure 6.1 displays the change in radioactivity of formed  $^{35}\text{S}$ - $\text{H}_2\text{S}$  with the reaction time.  $^{35}\text{S}$  remaining on the catalyst was also exchanged and released as  $^{35}\text{S}$ - $\text{H}_2\text{S}$  during HDS of 4-MDBT. However, the release rate of  $^{35}\text{S}$ - $\text{H}_2\text{S}$ , i.e., the exchange rate between  $^{35}\text{S}$  on the catalyst and  $^{32}\text{S}$  in 4-MDBT, was slower and total amount of released  $^{35}\text{S}$ - $\text{H}_2\text{S}$  (Area C) was less than that in the case of DBT (Area B) as shown in Table 6.1.

When the concentrations of 4-MDBT were changed from 0.1 to 1.0 wt%, similar results were obtained. Because the conditions were the same from the operation step (a) to (c) for all reactions, changes in radioactivities of

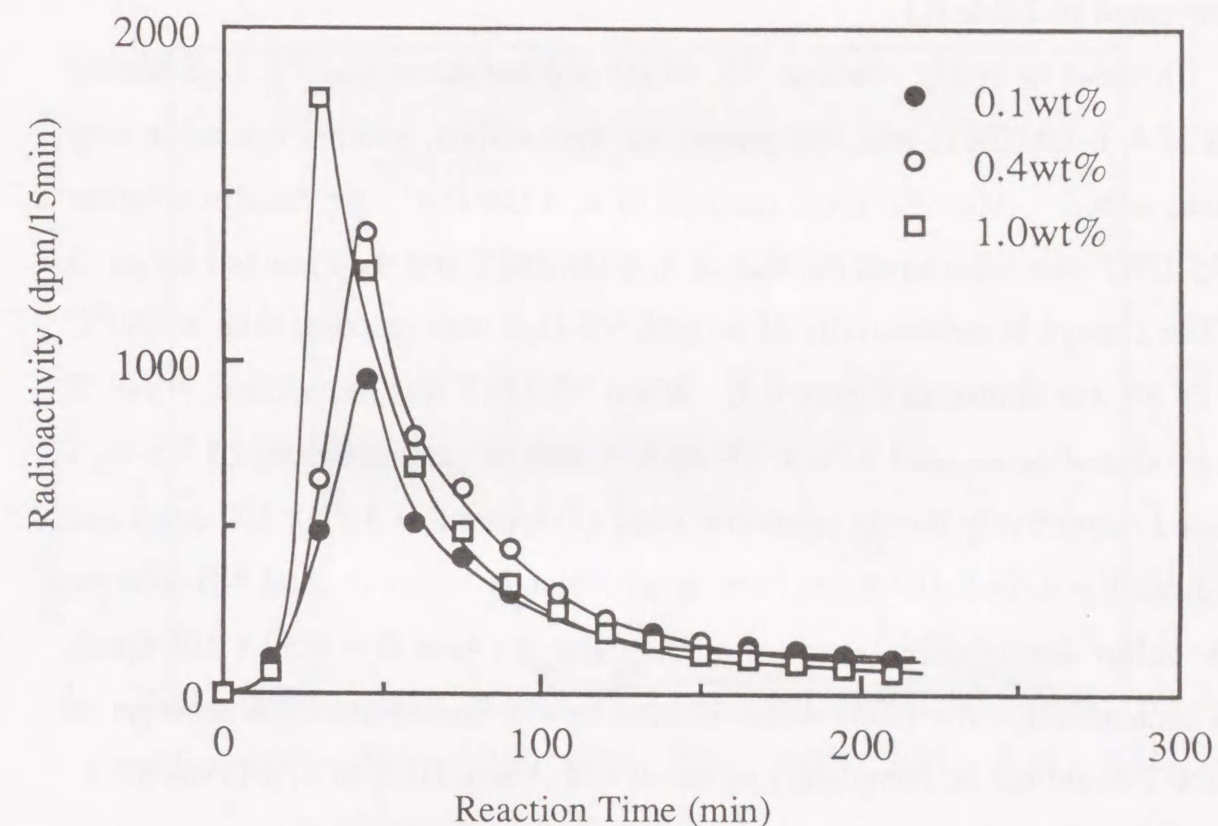


Figure 6.2. Effect of concentration of 4-MDBT on the release rate of  $^{35}\text{S}$ - $\text{H}_2\text{S}$  from  $^{35}\text{S}$ -labeled catalyst. Co-Mo/ $\text{Al}_2\text{O}_3$ ,  $340^\circ\text{C}$ ,  $50\text{ kg/cm}^2$ .

$^{35}\text{S}$ - $\text{H}_2\text{S}$  released only in step (d) were shown in Figure 6.2. The total amount of  $^{35}\text{S}$ - $\text{H}_2\text{S}$  released in step (d) were presented in Table 6.1. Either the release rate of  $^{35}\text{S}$ - $\text{H}_2\text{S}$  or total amounts of released  $^{35}\text{S}$ - $\text{H}_2\text{S}$  decreased with the concentrations of 4-MDBT. It is worthy to note that  $^{35}\text{S}$ -labeled labile sulfur during HDS of  $^{35}\text{S}$ -DBT could not completely released as  $^{35}\text{S}$ - $\text{H}_2\text{S}$  during HDS of 4-MDBT.

Similar results were obtained when 4,6-DMDBT was introduced in step (d).  $^{35}\text{S}$  remaining on the catalyst was also exchanged with  $^{32}\text{S}$  in 4,6-



DMDBT and released as  $^{35}\text{S-H}_2\text{S}$ . The release rate of  $^{35}\text{S-H}_2\text{S}$  and the exchange amount of sulfur were much less than those in the case of 4-MDBT as presented in Table 6.1.

In order to verify whether  $^{35}\text{S}$ , which did not release as  $^{35}\text{S-H}_2\text{S}$  during HDS of 4, 6-DMDBT, was still present on the catalyst, another operation step (e) was added. After the HDS reaction of 4, 6-DMDBT, the decalin solution of  $^{32}\text{S-DBT}$  was substituted for that of 4, 6-DMDBT and then reacted for ca. 3 h. The change in radioactivity of formed  $^{35}\text{S-H}_2\text{S}$  with reaction time at  $280^\circ\text{C}$  and  $28\text{ h}^{-1}$  was shown in Figure 6.3. When  $^{32}\text{S-DBT}$  was introduced,  $^{35}\text{S-H}_2\text{S}$  was produced again, and  $4.76 \times 10^3\text{ dpm}$ , a sum of radioactivities of  $^{35}\text{S-H}_2\text{S}$  released respectively during operation steps (d) (Area E =  $3.12 \times 10^3\text{ dpm}$ ) and (e) (Area F =  $1.64 \times 10^3\text{ dpm}$ ), was approximately equal to total  $^{35}\text{S}$ -labeled labile sulfur during steps (a) to (c) on the catalyst (Area D =  $4.59 \times 10^3\text{ dpm}$ ). This indicated that the labile sulfur labeled by  $^{35}\text{S}$  during the HDS reaction of  $^{35}\text{S-DBT}$  could not be completely replaced with  $^{32}\text{S}$  in HDS of 4, 6-DMDBT.

The effect of temperature was also investigated. When temperature was regulated to a desired one in step (c), then the decalin solutions of 0.4 wt% 4-MDBT and 4, 6-DMDBT were respectively in step (d) and effect of temperature on the extent exchanged were presented in Table 6.1. The extent exchanged increased with the temperatures for both 4-MDBT and 4, 6-DMDBT. Nevertheless, the extents were less than total labile sulfur labeled by  $^{35}\text{S}$  at studied temperatures. These indicate that a portion of labile sulfur participating HDS of DBT does not participate HDS of 4-MDBT or 4, 6-DMDBT.

### 6.3.3 Release Rate of $^{35}\text{S-H}_2\text{S}$ and Amount of Labile Sulfur

As reported in Chapter 5, the release of  $^{35}\text{S-H}_2\text{S}$  can approximately be treated as first order reaction after introducing 4-MDBT or 4, 6-DMDBT.

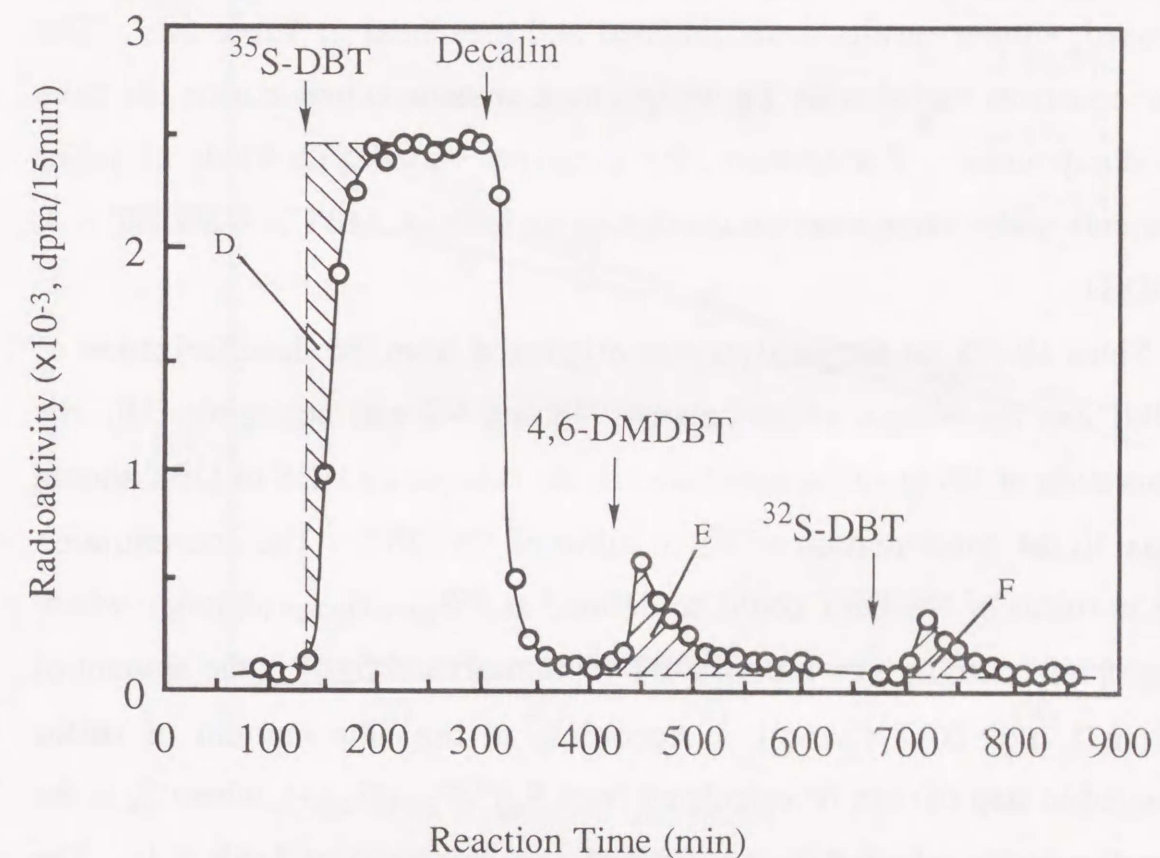


Figure 6.3. Change in radioactivity of formed  $^{35}\text{S-H}_2\text{S}$  with reaction time. Co-Mo/ $\text{Al}_2\text{O}_3$ ,  $280^\circ\text{C}$ ,  $50\text{ kg/cm}^2$ , WHSV:  $28\text{ h}^{-1}$ .

The first order plot of the radioactivity of produced  $^{35}\text{S-H}_2\text{S}$  approximately indicated the linear relationship as shown in Figure 6.4. Thus, the release rate can be expressed as:

$$\ln y = \ln z - kt, \quad y = z e^{-kt} \quad (6.1)$$

where  $y$  denotes the release rate of  $^{35}\text{S-H}_2\text{S}$  at time  $t$  (dpm/min);  $z$  the maximum release rate (dpm/min);  $k$  the release rate constant ( $\text{min}^{-1}$ );  $t$  the



reaction time (min). The release rate constants of elution of  $^{35}\text{S}$  from the catalyst were determined from the slope of linear relationship and listed in Table 6.1. When reaction temperature was changed and DBT or 4, 6-DMDBT were used, similar results were obtained and presented in Table 6.1. The release constants varied with the temperature at same concentration for three sulfur compounds. Furthermore, the constants varied with kinds of sulfur compounds under same reaction conditions as follows: DBT > 4-MDBT > 4, 6-DMDBT.

Since all  $^{35}\text{S}$  on the catalyst was originated from the desulfurization of  $^{35}\text{S}$ -DBT and the isotope effect between  $^{35}\text{S}$  and  $^{32}\text{S}$  was negligible (10), the concentration of  $^{35}\text{S}$  in sulfur introduced to the catalyst by HDS of DBT should be equal to the concentration of  $^{35}\text{S}$  in sulfur of  $^{35}\text{S}$ -DBT. The concentration of  $^{35}\text{S}$  in sulfur of  $^{35}\text{S}$ -DBT could be defined as  $^{35}\text{S}_{\text{DBT}}/\text{S}_{\text{DBT}}$  (dpm/g), where  $^{35}\text{S}_{\text{DBT}}$  is radioactivity in 1 mol of DBT (dpm/mol) and  $\text{S}_{\text{DBT}}$  is the amount of sulfur in 1 mol DBT (g/mol). According to this, the amount of sulfur exchanged in step (d) can be calculated from  $S_a / (^{35}\text{S}_{\text{DBT}}/\text{S}_{\text{DBT}})$ , where  $S_a$  is the total radioactivity released in step (d) and was presented in Table 6.1. The amount of labile sulfur at various reaction conditions was summarized in Table 6.1. It can be observed that the amount of labile sulfur decrease with concentration of sulfur compounds and temperature. Under a certain reaction condition, the amount of labile sulfur on the catalyst varied with the kinds of sulfur compounds as follows: DBT > 4-MDBT > 4, 6-DMDBT.

Comparing the results of DBT, 4-MDBT and 4, 6-DMDBT as shown in Table 6.1, one can obtain further information about effect of methyl substituents. The ratio of amount of labile sulfur in HDS of DBT to that in the case of 4-MDBT was about 3.2 at 260°C and 50kg/cm<sup>2</sup>. This is approximately equal to the ratio of HDS rate in both cases, 3.7. This indicates that the HDS rate was proportional to the amount of labile sulfur. For 4-

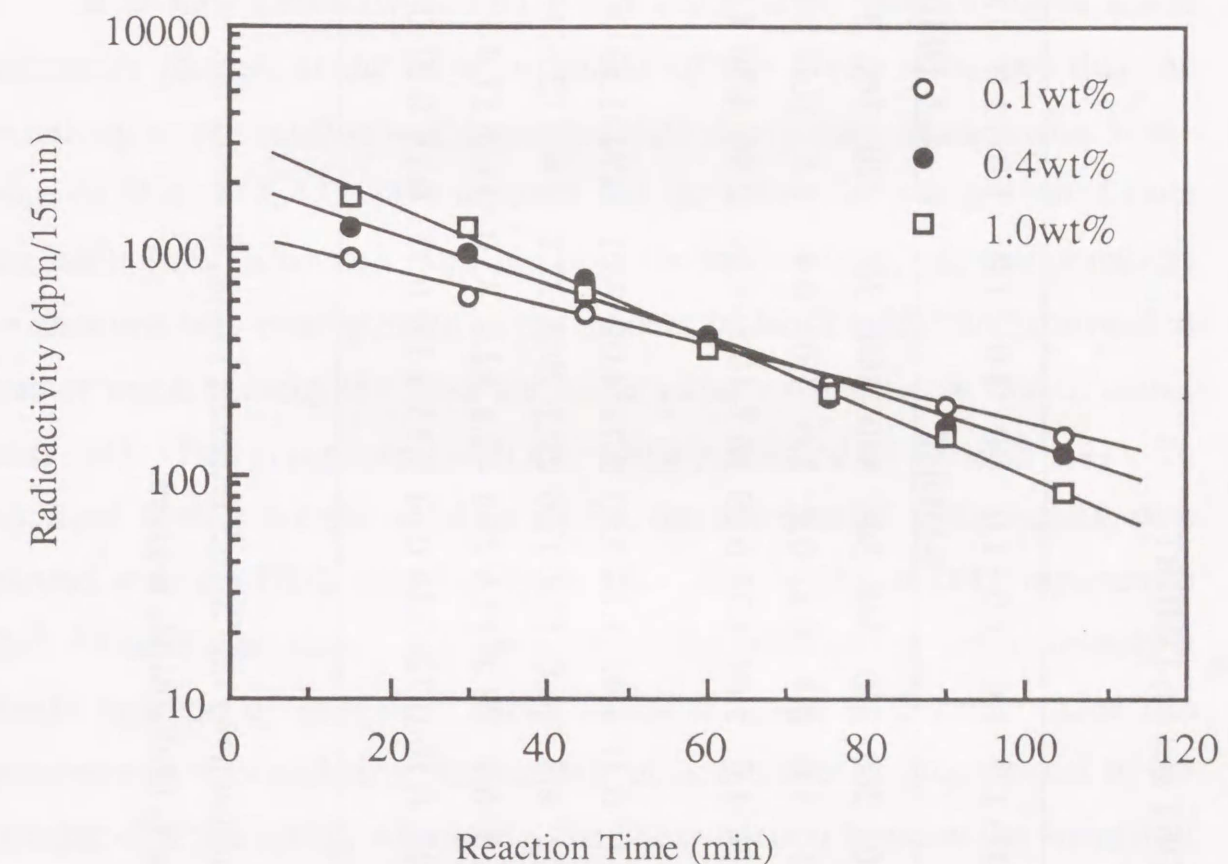


Figure 6.4. First order plots of the release rate of  $^{35}\text{S}$ -H<sub>2</sub>S. Co-Mo/Al<sub>2</sub>O<sub>3</sub>, Temperature: 340 °C, Pressure: 50 kg/cm<sup>2</sup>.

MDBT and 4,6-DMDBT, same result was obtained. For example, two ratios were 2.1 and 2.5 at 320°C and 50kg/cm<sup>2</sup>, respectively. Therefore, it was suggested that the difference of various sulfur compounds in HDS rate originated from to the difference of amount of labile sulfur participating reaction. Taking into account that the active site generated from the labile sulfur, number of active sites participating HDS of 4-MDBT and 4,6-DMDBT would actually decrease because of the existence of methyl substituents.



Table 6.1. Results of HDS Reaction of DBT, 4-MDBT and 4,6-DMDBT.

Concentration of <sup>35</sup> S-DBT <sup>a</sup>	DBT			4-MDBT			4, 6-DMDBT						
	1.0	3.0	3.0	1.0	1.0	1.0	1.0	1.0	1.0	1.0	1.0	1.0	1.0
Reaction temperature, °C	260	340	320	340	260	320	340	340	340	360	320	340	360
Concentration, wt %	1.0	1.0	3.0	3.0	1.0	0.4	0.1	0.4	1.0	1.0	0.4	0.4	1.0
Amount exchanged <sup>b</sup> , x10 <sup>3</sup> dpm	5.1	12.0	11.8	11.9	1.6	5.69	4.73	6.49	10.7	10.8	8.19	2.80	4.30
Rate constant of <sup>35</sup> S-H <sub>2</sub> S, k, x10 <sup>-2</sup> , min.	2.73	5.12	8.86	13.0	0.41	1.92	1.33	2.82	3.71	4.01	3.01	0.74	1.53
Labile Sulfur, S <sub>0</sub> , mg/g.cat.	13.7	32.4	31.8	32.1	4.3	16.0	12.1	17.6	29.2	29.3	22.1	7.6	12.1
S <sub>0</sub> /S <sub>Total</sub> <sup>c</sup> , %	19.8	46.8	45.9	46.3	6.2	23.2	17.5	25.4	42.1	42.1	32.0	11.0	17.4
HDS Rate, mg/min/g.cat.	0.38	1.89	2.85	4.27	0.10	0.32	0.19	0.61	1.15	1.12	0.73	0.13	0.27

<sup>a</sup> When the catalyst was labeled by <sup>35</sup>S. <sup>b</sup> Total radioactivity of <sup>35</sup>S-H<sub>2</sub>S releasing in operation step (d).

<sup>c</sup> The ratio of the labile sulfur to total sulfur on Co<sub>9</sub>S<sub>8</sub>-MoS<sub>2</sub>/Al<sub>2</sub>O<sub>3</sub> is given.

## 6.4 Discussion

It is now generally accepted that MoS<sub>2</sub> slabs contain sulfur anion vacancies located at the edge or corner of the MoS<sub>2</sub> slabs and that the reactivity of the catalyst was correlated with the number of vacancies at the edge of MoS<sub>2</sub> (12, 13). We reported that the active site was generated from the labile sulfur after H<sub>2</sub>S releasing from the labile sulfur, and that reactivity of catalysts was corresponded to the amount of labile sulfur and conversion rate of anion vacancy site from the labile sulfur - regeneration rate of active sites (11). This is consistent with the results postulated by Massoth (14). To obtain further insight of labile sulfur, the amounts of labile sulfur were plotted with the HDS rates in Figure 6.5. The results of DBT reported in *Ref. 10* were also shown in Figure 6.5. The HDS rate is approximately a linear function of amount of labile sulfur at lower HDS rate. One can comprehend if considering the numbers of active sites is proportional to the amount of labile sulfur. Obviously, the linear relation between the amount of labile and HDS rate was no longer tenable at higher HDS rate. This is because the HDS reactivity of a catalyst would also depend upon the conversion rate between labile sulfur and vacancy. As described in *Ref. 11*, the amount of labile sulfur was the total sulfur that could be converted to vacancies under a certain reaction condition for a catalyst. Although amount of labile sulfur involved closely with the reactivity of the catalyst, it was distinctly not equal to the number of active sites. Especially at higher HDS reaction rate, the HDS reaction rate may only depend on the regeneration rate of active sites because the amount of labile sulfur is a limiting value (11). If we consider that the release rate of H<sub>2</sub>S represents qualitatively to the formation rate of active sites from labile sulfur, the relation between the HDS rate and release rate constant of <sup>35</sup>S-H<sub>2</sub>S was also shown in Figure 6.6. At higher HDS rate, the HDS rates



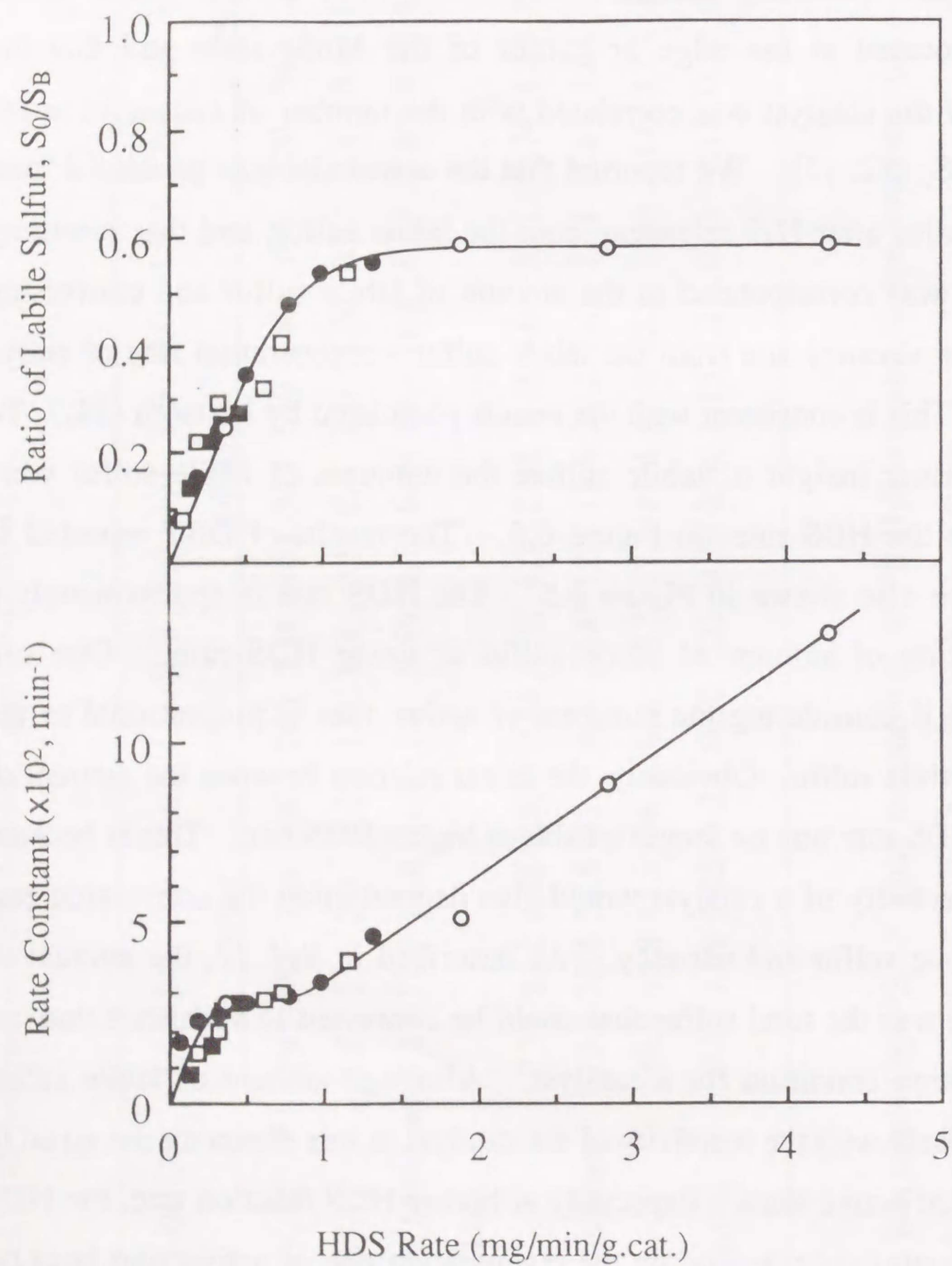


Figure 6.5. Relation among the amount of labile sulfur, the release rate constant of  $H_2S$  and HDS rate.

○: DBT, ■: 4-MDBT, □: 4,6-DMDBT, ●: DBT (from Chapter 4).

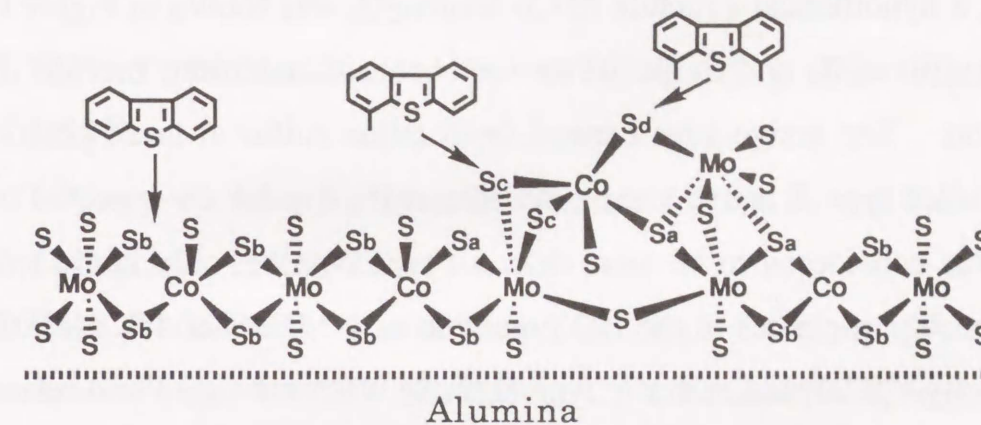


Figure 6.6. Structure of sulfided Co-Mo/ $Al_2O_3$ .

Labile capacity of sulfur:  $S_d > S_c > S_b > S_a$ .

almost increase linearly with the release rate constant of  $H_2S$ . This further supports above interpretation.

Because of the interaction between the sulfur and support, the mobility of labile sulfur was different from each other (10, 14). Topsøe and co-workers (17, 18) reported that two types of CoMoS are observed in alumina supported catalysts: Type I that can be sulfided at the normal sulfiding temperature and type II was sulfided only at high sulfiding temperature (type II being more active than type I in HDS). The difference between type I and II were supposed to be the existence, in the first case, of remaining Mo-O-Al linkages, while type II Co-Mo-S is fully sulfided, which means that the interaction between active phase and support is only the van der Waals type. Recently, Bouwens et al. proposed that arrangement of  $MoS_2$  slabs may occur in practical catalyst and that a portion of  $MoS_2$  present as multistacks. Co atoms with sulfur in the  $MoS_2$  multistacks would form more active Co-S-Mo



phase - type II different from normal Co-S-Mo phase-type I (20). On the basis above, a hypothetical structure of Co-Mo/Al<sub>2</sub>O<sub>3</sub> was shown in Figure 6.6. The labile sulfur at S<sub>c</sub> and S<sub>d</sub> positions were considered more mobile than other position. The active sites created from labile sulfur at these positions may be so-called type II active sites. Because reactivity for the type II Co-S-Mo phase was considered to be more than for type I phase, only labile sulfur in type II phase participates in the HDS reaction of 4-MDBT and 4, 6-MDBT. Therefore, only <sup>35</sup>S-labeled sulfur in type II phase was exchanged and released as <sup>32</sup>S-H<sub>2</sub>S during HDS of 4-MDBT and 4, 6-DMDBT.

### 6.5 Conclusions

The radioisotope tracer method using <sup>35</sup>S-DBT is a useful method to determine the behavior of sulfur during practical HDS reaction of methyl-substituted dibenzothiophenes. Under the same reaction condition, a portion of labile sulfur participating the HDS reaction of DBT did not participate the HDS reaction of 4-MDBT and 4, 6-DMDBT. The amount of labile sulfur varied with the kinds of sulfur compounds as follows: DBT > 4-MDBT > 4, 6-DMDBT. Moreover, the reaction rate was approximately proportional to the amount of labile sulfur at lower HDS reaction rate range. This means that the number of active sites was proportional to the amount of labile sulfur at lower HDS rate. Compared to DBT, the number of active sites participating the HDS reaction of methyl-substituted DBTs decreased because of the existence of methyl groups. Therefore, it was suggested that there are more than two kinds of active sites, and the HDS reaction of 4-MDBT and 4, 6-DMDBT only occurs on the more reactive sites.

### Reference

1. Kabe, T., Ishihara, A., and Tajima, H., *Ind. Eng. Chem. Res.*, **31**, 1577 (1992).
2. Ishihara, A., Itoh, T., Hino, T., Nomura, M., Qi, P., and Kabe, T., *J. Catal.*, **140**, 184 (1993).
3. Kabe, T., Ishihara, A., and Zhang, Q., *Appl. Catal.*, **A: 97**, L1 (1993).
4. Amorelli, A., Amos, Y. D., Halsig, C. P., Kosman, J. J., Jonker, R. J., de Wind, M., and Vrieling, J., *Hydrocarbon Process*, **6**, 93 (1992).
5. Kilanowski, D. R., Teeuwen, H., de Beer, V. H. J., Gates, B. C., Schuit, G. C. A., and Kwart, H., *J. Catal.*, **33**, 129 (1978).
6. Houalla, M., Broderick, D. H., Sapre, A. V., Nag, N. K., de Beer, V. H. J., Gates, B. C., and Kwart, H., *J. Catal.*, **61**, 523 (1980).
7. Ishihara, A., and Kabe, T., *Ind. Eng. Chem., Res.*, **32**, 753 (1993).
8. Qian, W., Ishihara, A., Ogawa, S., and Kabe, T., *J. Phys. Chem.*, **98**, 907 (1994).
9. Kabe, T., Qian, W., and Ishihara, A., *J. Phys. Chem.*, **98**, 912 (1994).
10. Kabe, T., Qian, W., Ogawa, S., and Ishihara, A., *J. Catal.*, **143**, 239 (1993).
11. Kabe, T., Qian, W., and Ishihara, A., *J. Catal.*, **149**, 171 (1994).
12. Topsøe, H., Candia, R., Topsøe, N.-Y., and Clausen, B., S., *Bull., Soc., Chim., Belg.*, **93**, 783 (1984).
13. Massoth, F. E., and Muralidhar, G., "4th International Conference on Chemistry and Uses of Molybdenum" (Barry, H. F. and Mitchell, P. C. H., Eds.), p. 343, Climax, Molybdenum Co., Anne Arbor, MI, 1982.
14. Massoth, F., E., and Zeuthen, P., *J. Catal.*, **145**, 216 (1994).
15. Bouwens, S. M. A. M., Prins, R., de Beer, V. H. J., and Koningsberger, D. C., *J. Phys. Chem.*, **94**, 3711 (1990).



16. Bouwens, S. M. A. M., van Veen, J. A. R., Koningsberger, D. C., de Beer, V. H. J., and Prins, R., *J. Phys. Chem.*, **95**, 123 (1991).
17. Candia, R., Sorensen, O., Villadsen, J., Topsøe, N., Clausen, B. S., and Topsøe, H., *Bull. Soc. Chim. Belg.*, **93**, 763 (1984).
18. Topsøe, H., Clausen, B. S., Topsøe, N., and Pedersen, E., *Ind. Eng. Chem. Fundam.*, **25**, 25 (1986).
19. Topsøe, N.-Y., and Topsøe, H., *J. Catal.*, **139**, 641 (1993).
20. Bouwens, S. M. A. M., van Zon, F. B. M., van Dijk, M. P., van der Kraan, A. M., de Beer, V. H. J., van Veen, J. A. R., and Koningsberger, D. C., *J. Catal.*, **146**, 375 (1994).

## Chapter Seven

## Conclusions



## Chapter Seven Conclusions

This dissertation involved to elucidate hydrodesulfurization (HDS) mechanism on Mo-based catalysts by using  $^{35}\text{S}$  radioisotope tracer. Because sulfur plays an important role in HDS of sulfur-containing compounds, the main attention was in focus on elucidating the behavior of sulfur on the catalyst under the practical industrial conditions, i. e., 10-50 kg/cm<sup>2</sup> and 210-400 °C. Radioisotope tracer technique was used as major approach. More information about the structure of catalyst and mechanism of HDS were obtained by quantifying the amount of labile sulfur on the catalyst.

In *Chapter two*,  $^{35}\text{S}$ -labeled dibenzothiophene ( $^{35}\text{S}$ -DBT) was synthesized and its hydrodesulfurization was carried out on a sulfided Mo/Al<sub>2</sub>O<sub>3</sub> in a fixed-bed pressurized flow reactor. By tracing the changes in radioactivities of unreacted  $^{35}\text{S}$ -DBT and formed  $^{35}\text{S}$ -H<sub>2</sub>S, it was found that the sulfur in dibenzothiophene was not directly released as H<sub>2</sub>S but initially accommodated on the catalyst and that H<sub>2</sub>S was formed from the sulfur on the catalyst. Moreover, some parts of sulfur on the catalyst were labile and its amount varied with the reaction condition, e.g., the reaction temperature and concentration of dibenzothiophene. In addition, to determine the sulfided state of Mo/Al<sub>2</sub>O<sub>3</sub> under the reaction conditions, the catalyst was presulfided with  $^{35}\text{S}$ -DBT. From the calculation of radioactivity balance, it was found that the total sulfur present in the sulfided Mo/Al<sub>2</sub>O<sub>3</sub> corresponded to MoS<sub>1.92</sub> under the reaction condition.

In *Chapter three*, the labile sulfur on the sulfided Mo/Al<sub>2</sub>O<sub>3</sub> was labeled with  $^{35}\text{S}$  during the HDS reaction of  $^{35}\text{S}$ -DBT. Then, several sulfur



compounds such as thiophene, benzothiophene, thiophenol, and dibenzothiophene were introduced to this  $^{35}\text{S}$ -labeled catalyst, the behavior of sulfur on the catalyst was estimated by tracing the radioactivity of  $^{35}\text{S}\text{-H}_2\text{S}$  releasing from the catalyst. Moreover, instead of sulfur compounds, the nitrogen and oxygen-containing compounds were introducing to  $^{35}\text{S}$ -labeled catalyst, the behavior of sulfur on the catalyst during HDO and HDN reactions was elucidated. These results indicated that  $^{35}\text{S}$  remained on the catalyst could not be removed without the supply of sulfur originated from the HDS reaction of sulfur compounds. The removal rate of  $^{35}\text{S}$  from the catalyst depended upon the rate of HDS of those sulfur compounds, that is, amount of sulfur incorporated into the catalyst. This indicates that  $\text{H}_2\text{S}$  is formed from some portion of sulfur on the catalyst other than from that in the sulfur compounds. When hydrodeoxygenation (HDO) reaction of dibenzofuran was carried out on  $^{35}\text{S}$ -labeled catalyst, only some portion of  $^{35}\text{S}$  could be replaced by oxygen atoms and released as  $^{35}\text{S}\text{-H}_2\text{S}$ . In contrast to this,  $^{35}\text{S}$  was hardly replaced by nitrogen atoms when only hydrogenation of nitrogen compounds occurred. Therefore, it was suggested that the hydrogenation reaction could not cause the formation of  $\text{H}_2\text{S}$  and  $\text{H}_2\text{S}$  has not been formed from the labile sulfur on the catalyst until the hydrogenolysis reaction occurred.

In *Chapter four*, the radioisotope tracer method has been used to quantify the behavior of sulfur on sulfided Co and Ni-Mo/ $\text{Al}_2\text{O}_3$ . The apparent activation energies of HDS reaction of DBT were  $20\pm 1$  kcal/mol for all Mo-based catalysts with or no promoted atoms. This implies that the same reaction process may occur on the sulfided Mo-based catalysts. The formation rate constants of  $^{35}\text{S}\text{-H}_2\text{S}$  from the catalysts were determined and the amounts of labile sulfur on the sulfided catalysts were estimated. When the amounts of labile sulfur in sulfided Mo/ $\text{Al}_2\text{O}_3$ , Co-Mo/ $\text{Al}_2\text{O}_3$  and Ni-Mo/ $\text{Al}_2\text{O}_3$  are plotted against the rates of HDS, they increase with increase in the rate of

HDS. The maximum amounts of labile sulfur were 41.8, 32.3, and 25.2 mg of sulfur/g of catalyst for the three catalysts, respectively. When it was assumed that all sulfur in Mo/ $\text{Al}_2\text{O}_3$  was present in the form of  $\text{MoS}_2$ , it was deduced that ca. 75% of sulfur in Mo/ $\text{Al}_2\text{O}_3$  was involved in the HDS reaction. Compared with the amounts of labile sulfur in the sulfided Co/ $\text{Al}_2\text{O}_3$  or Ni/ $\text{Al}_2\text{O}_3$ , Mo/ $\text{Al}_2\text{O}_3$ , and Co-Mo/ $\text{Al}_2\text{O}_3$  or Ni-Mo/ $\text{Al}_2\text{O}_3$ , it was suggested that the sulfur in  $\text{Co}_9\text{S}_8$  or NiS phase on Co-Mo/ $\text{Al}_2\text{O}_3$  or Ni-Mo/ $\text{Al}_2\text{O}_3$  was nonlabile and only sulfur bonded both to Co (Ni) and to Mo in the form of  $\text{MoS}_2$  were related to HDS reaction. The maximum amounts of labile sulfur in Co-Mo/ $\text{Al}_2\text{O}_3$  and Ni-Mo/ $\text{Al}_2\text{O}_3$ , 32.3 and 25.2 mg of sulfur/g of catalyst, correspond to about 59% and 37% of sulfur present in the form of  $\text{MoS}_2$ . The atomic ratios of Co/Mo and Ni/Mo in used Co-Mo/ $\text{Al}_2\text{O}_3$  and Ni-Mo/ $\text{Al}_2\text{O}_3$  are 0.59 and 0.37. The results suggest that the addition of Co or Ni promotes the same amount of Mo species as that of Co or Ni species in the sulfided Co-Mo/ $\text{Al}_2\text{O}_3$  or Ni-Mo/ $\text{Al}_2\text{O}_3$  and makes sulfur in this portion of Mo species more labile.

In *Chapter five*, the sulfur on a sulfided Co-Mo/ $\text{Al}_2\text{O}_3$  catalyst was labeled by  $^{35}\text{S}$  during the hydrodesulfurization (HDS) of  $^{35}\text{S}$ -labeled dibenzothiophene ( $^{35}\text{S}\text{-DBT}$ ). Similar to the case of Mo/ $\text{Al}_2\text{O}_3$  in *Chapter 3*,  $^{35}\text{S}$  remaining on Co-Mo/ $\text{Al}_2\text{O}_3$  catalyst was also hardly released as  $^{35}\text{S}\text{-H}_2\text{S}$  in the reduction atmosphere of high pressure of hydrogen. On the other hand, when a sulfur-containing compound such as thiophene, benzothiophene, and  $\text{H}_2\text{S}$  were introduced onto the catalyst,  $^{35}\text{S}\text{-H}_2\text{S}$  was eluted again. The release of  $^{35}\text{S}\text{-H}_2\text{S}$  from the catalyst could be regarded as the first order reaction. When the partial pressure of  $\text{H}_2\text{S}$  during HDS of sulfur compounds is similar to the case of introducing  $\text{H}_2\text{S}$ , the release rate of  $^{35}\text{S}\text{-H}_2\text{S}$  from the catalyst was the same for two cases. This indicates that the formation process of  $^{35}\text{S}\text{-H}_2\text{S}$  from the catalyst during HDS reaction is the same with the case of exchange



reaction with  $\text{H}_2\text{S}$ . Moreover, the release rate constants of  $^{35}\text{S}\text{-H}_2\text{S}$  trend toward to a constant value above  $0.36 \text{ kg/cm}^2$  of the partial pressure of  $\text{H}_2\text{S}$ . This indicates that the adsorption of  $\text{H}_2\text{S}$  onto the active sites approached a saturated state in present reaction conditions. The desorption of  $\text{H}_2\text{S}$  from the catalyst may be the determining-rate step of this reaction.

In *Chapter six*, the radioisotope tracer method was applied to elucidate the behavior of sulfur on the catalyst during HDS reaction of 4-methyldibenzothiophene (4-MDBT) and 4, 6-dimethyldibenzothiophene (4, 6-DMDBT). After the labile sulfur of  $\text{Co-Mo/Al}_2\text{O}_3$  was labeled with  $^{35}\text{S}$  during the HDS reaction  $^{35}\text{S}\text{-DBT}$ , the HDS reaction of 4-MDBT and 4,6-DMDBT were carried out on this catalyst. The amounts of labile sulfur participating the reaction of 4-MDBT and 4, 6-DMDBT were quantified by tracing the release rate of  $^{35}\text{S}\text{-H}_2\text{S}$  from the  $^{35}\text{S}$ -labeled catalyst. The results indicated that only some of labile sulfur participating the HDS reaction of DBT participated the HDS reaction of 4-MDBT and 4, 6-DMDBT, and the amount of labile sulfur varied with the kinds of sulfur compounds as follows under a certain reaction condition:  $\text{DBT} > 4\text{-MDBT} > 4, 6\text{-DMDBT}$ . Moreover, the reaction rate was approximately proportional to the amount of labile sulfur at lower HDS reaction rate range. This means that the number of active sites was proportional to the amount of labile sulfur at lower HDS rate. Compared with DBT, the number of active sites participating the HDS reaction of methyl-substituted DBTs decreased because of the existence of methyl groups. Therefore, it is suggested that there are more than two kinds of active sites, and the HDS reaction of 4-MDBT and 4, 6-DMDBT only occurs on the more reactive sites.

Finally, it can be concluded that  $^{35}\text{S}$  radioisotope tracer method is a useful tool to investigate the behavior of sulfur on working catalyst during the hydrodesulfurization of sulfur-containing compounds. This method makes us

gain deeper comprehension for the structure of Mo-based catalysts during the reaction and hydrodesulfurization mechanism. Further, these results give a important clue for us to develop a new catalyst for deep hydrodesulfurization of light oil.



Faint, illegible text on the left page, possibly bleed-through from the reverse side of the paper.

### Publications List



## Publications List

1. Kabe, T., Qian, W., Ogawa, S., and Ishihara, A., Mechanism of Hydrodesulfurization of Dibenzothiophene on Co-Mo/Al<sub>2</sub>O<sub>3</sub> and Co/Al<sub>2</sub>O<sub>3</sub> Catalyst by the Use of Radioisotope <sup>35</sup>S Tracer, *J. Catal.*, **143**, 239-248 (1993) (*Chapter 4*).
2. Qian, W., Ishihara, A., Ogawa, S., and Kabe, T., Study of Hydrodesulfurization by the Use of <sup>35</sup>S-Labeled Dibenzothiophene. 1. Hydrodesulfurization Mechanism on Sulfided Mo/Al<sub>2</sub>O<sub>3</sub>, *J. Phys. Chem.*, **98** (3), 907-911 (1994) (*Chapter 2*).
3. Kabe, T., Qian, W., and Ishihara, A., Study of Hydrodesulfurization by the Use of <sup>35</sup>S-Labeled Dibenzothiophene, 2. Behavior of Sulfur in HDS, HDO and HDN on Sulfided Mo/Al<sub>2</sub>O<sub>3</sub> Catalyst, *J. Phys. Chem.*, **98** (3), 912-916 (1994) (*Chapter 3*).
4. Kabe, T., Qian, W., and Ishihara, A., Study of Hydrodesulfurization of Dibenzothiophene on Ni-Mo/Al<sub>2</sub>O<sub>3</sub>, Mo/Al<sub>2</sub>O<sub>3</sub> and Ni/Al<sub>2</sub>O<sub>3</sub> Catalyst by the Use of Radioisotope <sup>35</sup>S Tracer, *J. Catal.*, **149**, 171-180 (1994) (*Chapter 4*).
5. Qian, W., Wang, W., Ishihara, A., Arai, D., and Kabe, T., Release of Radioactive <sup>35</sup>S-H<sub>2</sub>S from <sup>35</sup>S-Labeled Co-Mo/Al<sub>2</sub>O<sub>3</sub> in Mixed Gases of H<sub>2</sub>S and H<sub>2</sub> by Sulfur Exchange, *J. Catal.*, to be submitted (*Chapter 5*).
6. Qian, W., Wang, W., Ishihara, A., and Kabe, T., Hydrodesulfurization of 4-Methyldibenzothiophene and 4, 6-Dimethyldibenzothiophene on Radioactive <sup>35</sup>S-Labeled Co-Mo/Al<sub>2</sub>O<sub>3</sub> Catalyst, *J. Jpn. Pet. Ins.*, to be submitted (*Chapter 6*).



7. Kabe, T., Ishihara, A., Qian, W., Ogawa S., and Sakuno, H., Possibility of Sulfur Spillover on Desulfurization Catalysts Using Radioactive  $^{35}\text{S}$ , *New Aspects of Spillover Effect in Catalysis* (Inui, T. et al. Eds.), p. 341-344, Kyoto, Japan, 1993 (*Chapters 2 and 4*).
8. Kabe, T., Qian, W., Ishihara, A., Wang, W., and Zhang, C., Elucidation of Mechanism of Deep desulfurization of Light Oil, *5th Japan-China Joint Seminar on Research and Technology for Petroleum Refining*, September 20-22, 1994 in Jiujiang, China (*Chapter 6*).
9. Kabe, T., Qian, W., Wang, W., and Ishihara, A., Sulfur Exchange on Hydrodesulfurization Catalyst Co-Mo/ $\text{Al}_2\text{O}_3$  Using  $^{35}\text{S}$  Radioisotope Tracer, *2nd Japan-EC Joint Workshop on the Frontiers of Catalyst Science and Technology for Energy, Environment and Risks Prevention*, April 26-28, 1995 in Lyon-Villeurbanne, France (*Chapters 5 and 6*).

## Acknowledgments



## Acknowledgments

The studies presented in this dissertation are the summaries of the author's work carried out during 1992-1994 at the Division of Chemical and Biological Science and Technology, Graduate School of Technology, Tokyo University of Agriculture and Technology.

The author wishes to express his sincerest gratitude to Professor Toshiaki Kabe, author's supervisor for providing an opportunity to study in the graduate school, further for his invaluable suggestions, discussion, and encouragement.

The author would like to thank Professor Hideo Kameyama, Dr. Atsushi Ishihara, and Mr. Hidekazu Sakuno for their invaluable discussion and encouragement.

The author appreciates all his friends and colleagues in the university who have encouraged about the completion of this work in different way.

Finally, the author would like to give his greatest thanks to his wife, daughter, parents and brothers for continuous encouragement.

Weihua Qian



